© 2020. Published by The Company of Biologists Ltd | Development (2020) 147, dev176750. doi:10.1242/dev.176750

STEM CELLS AND REGENERATION

RESEARCH ARTICLE

Neurogenesis in the inner ear: the zebrafish statoacoustic ganglion provides new neurons from a Neurod/Nestin-positive progenitor pool well into adulthood

Simone Schwarzer, Nandini Asokan, Oliver Bludau, Jeongeun Chae, Veronika Kuscha, Jan Kaslin* and Stefan Hans‡

ABSTRACT

The vertebrate inner ear employs sensory hair cells and neurons to mediate hearing and balance. In mammals, damaged hair cells and neurons are not regenerated. In contrast, hair cells in the inner ear of zebrafish are produced throughout life and regenerate after trauma. However, it is unknown whether new sensory neurons are also formed in the adult zebrafish statoacoustic ganglion (SAG), the sensory ganglion connecting the inner ear to the brain. Using transgenic lines and marker analysis, we identify distinct cell populations and anatomical landmarks in the juvenile and adult SAG. In particular, we analyze a Neurod/Nestin-positive progenitor pool that produces large amounts of new neurons at juvenile stages, which transitions to a quiescent state in the adult SAG. Moreover, BrdU pulse chase experiments reveal the existence of a proliferative but otherwise marker-negative cell population that replenishes the Neurod/Nestin-positive progenitor pool at adult stages. Taken together, our study represents the first comprehensive characterization of the adult zebrafish SAG showing that zebrafish, in sharp contrast to mammals, display continued neurogenesis in the SAG well beyond embryonic and larval stages.

KEY WORDS: Zebrafish, PNS, Inner ear, Neuronal stem cells

INTRODUCTION

The vertebrate inner ear is a complex structure mediating hearing and balance through an arrangement of mechanosensory hair cells, non-sensory supporting cells and bipolar sensory neurons, which all derive from a transient ectodermal thickening, the otic placode (Barald and Kelley, 2004; Ladher, 2017). Hair cells convert vestibular and auditory stimuli into electrical signals that are transmitted via neurons of the eighth cranial ganglion to the brain (Schwander et al., 2010). In mammalian species, hair cells and neurons are only produced during fetal stages. Despite the presence of neurosensory stem cells in the adult mammalian inner ear that are able to proliferate and differentiate *in vitro*, there is no evidence for the ability to replace lost neurosensory cells in mammals *in vivo*, making deafness irreversible (Bermingham et al., 1999; Li et al., 2003; Ma et al., 1998). Currently, more than 5% of the world's population, which corresponds to roughly 466 million people, are affected by hearing impairment or deafness and it is estimated that this number will rise to more than 900 million people by 2050 (http://www.who.int/news-room/fact-sheets/detail/deafness-and-hearing-loss). Hence, there is a pressing need to develop new therapies to restore hearing abilities. One leading cause of hearing loss is the degeneration of inner ear neurons (Liberman, 2017). Previously, it was thought that inner ear neurons are lost only secondarily owing to hair cell degeneration. Emerging data, however, challenge this view and indicate that neuronal loss can occur independent of damage to hair cells, known as primary degeneration, which can develop as a consequence of environmental and genetic means (Furman et al., 2013; Seal et al., 2008).

Genetic mechanisms of otic development, as well as the anatomical and physiological structure of the inner ear, are highly conserved among vertebrates, meaning that zebrafish – as well as other advantages – are an ideal model organism to study deafness and regeneration of the inner ear (Fritzsch and Elliott, 2017). Since the first anatomical characterization of the teleost inner ear was published as early as 1872 by Gustav Retzius (Retzius, 1872), the zebrafish inner ear has been subject to detailed studies, providing comprehensive descriptions for embryonic and larval development (Bever and Fekete, 2002; Haddon and Lewis, 1996). In particular, neuroblasts that give rise to all neurons of the inner ear derive from the anterior and posteromedial part of the otic vesicle (Sapède et al., 2012). Following delamination, neuroblasts undergo transient amplification before they differentiate into mature neurons that spatially separate the pool of transient amplifying cells from the otic vesicle (Vemaraju et al., 2012). Subsequently, neuronal cells start forming the statoacoustic ganglion (SAG) that can be divided into an anterior part, innervating the anterior and lateral cristae as well as the utricular macula, and a posterior part, innervating the posterior crista and the saccular macula (Sapède and Pujades, 2010). Furthermore, a thorough account of adult ear morphology, with a particular emphasis on the stimuli-receiving hair cells in the sensory patches, has been conducted (Bang et al., 2001). In contrast to mammals, zebrafish exhibit continuous formation of new hair cells throughout life (Higgs et al., 2002). Moreover, hair cell regeneration after trauma has been described in the vestibular and auditory parts of the inner ear in zebrafish and also other non-mammalian vertebrate species (Corwin and Cotanche, 1988; Ryals and Rubel, 1988; Schuck and Smith, 2009; Stone and Rubel, 2000). However, it is unknown whether lifelong formation of new neurons accompanies continued hair cell production and regeneration. In contrast to mammals, zebrafish exhibit lifelong brain growth due to widespread adult neurogenesis along the entire length of the neuraxis and display robust regeneration after brain injury (Lindsey et al., 2018). Recent studies have demonstrated the possibility of targeting and reprogramming glial cells of the central nervous system (CNS) into functional neurons with high efficiency *in vitro* and *in vivo* (Torper and Götz, 2017). Similarly, glia cells closely associated with the neurons of the inner ear can be reprogrammed *in vitro* into neuron-like cells that display a

Center for Regenerative Therapies Dresden (CRTD), Cluster of Excellence, Center for Molecular and Cellular Bioengineering, Technische Universität Dresden, Dresden, Germany.
*Present address: Australian Regenerative Medicine Institute, Monash University Clayton Campus, Clayton, Victoria 3800, Australia.

‡Author for correspondence (stefan.hans@tu-dresden.de)

J.K., 0000-0002-6207-1889; S.H., 0000-0003-0283-0211

Received 15 February 2019; Accepted 25 February 2020

Development (2020) 147, dev176750. doi:10.1242/dev.176750

transcriptome profile resembling that of endogenous inner ear neurons (Noda et al., 2018). However, even if reprogramming of inner ear glia into neurons is successful *in vivo*, the cellular properties of the reprogrammed cells to ensure functional restoration remain unclear. Hence, characterization of species that show continuous formation of new inner ear neurons throughout life may provide important insights.

In this study, we thoroughly characterized the adult zebrafish statoacoustic ganglion (SAG) on an anatomical and cellular level at juvenile and adult stages, and investigated whether zebrafish display continuous neurogenesis within the inner ear beyond larval stages. We found that the SAG is a highly heterogeneous structure containing myelinated Calretinin-positive neurons and a Neurod/Nestin-positive population. Moreover, Sox2-positive cells align in the peripheral and central nervous system transitional zone (PCTZ, also known as Redlich-Obersteiner's-zone). Abundant proliferation of Neurod/Nestin-positive cells is observed at juvenile stages, whereas actively cycling Neurod/Nestin-positive cells are not detectable at adulthood. In contrast, proliferation of marker-negative cells in the vicinity of the Neurod/Nestin-positive cell pool declines from high levels at juvenile stages to a low steady-state level in adulthood. Furthermore, BrdU pulse chase experiments show the existence of a proliferating but otherwise marker-negative cell population that replenishes the Neurod/Nestin-positive progenitor pool. In contrast to the juvenile SAG, in which neurogenesis is frequently observed, adult neurogenesis is an extremely rare event. In summary, we propose the lifelong existence of a Neurod/Nestin-positive neuronal progenitor cell pool as a source of newborn neurons in the SAG of juvenile and adult zebrafish.

RESULTS

Anatomy of the SAG in adult zebrafish

The zebrafish inner ear has been subject to detailed studies (Bever and Fekete, 2002; Haddon and Lewis, 1996; Waterman and Bell, 1984). Here, we focus on the SAG connecting the different sensory patches to the brain. We performed Haematoxylin and Eosin (H&E) and antibody staining on serial cross-sections spanning the complete inner ear of wild-type and *pou4f3*:GFP transgenic animals expressing GFP in differentiated hair cells (Xiao et al., 2005). Consistent with 3D reconstructions of the larval SAG (Sapède and Pujades, 2010), we found that the adult zebrafish SAG is not a cable-like structure but a flat (in dorsal-ventral and lateral-medial dimension) and rather broad (in rostral-caudal dimension) sheet-like structure entering the hindbrain underneath the cerebellum (Fig. 1). As previous thin-sheet laser imaging with 3D reconstruction has shown (Santi et al., 2009), the adult SAG is closely associated with the medial wall of the pars superior (dorsal part of the ear) containing the utricular macula as well as the anterior, lateral and posterior crista and the pars inferior (ventral part of the ear) harbouring the saccular and lagenar macula. Morphologically, the SAG can be divided into two parts: an anterior part shaped like an elbow switching from a dorsal-ventral to a medial-lateral axis (Fig. 1C,F; purple arrowheads); and a posterior part forming a rod-like structure aligned along the dorsal-ventral axis (Fig. 1G,J; purple arrowheads). The anterior part innervates the anterior crista (Fig. 1A,D), the lateral crista (Fig. 1B,E) and the utricular macula (Fig. 1C,F), which all belong to the pars superior. The posterior part connects the posterior crista (Fig. 1H,K), also part of the pars superior, and the saccular and lagenar maculae (Fig. 1G,I,J,L), both belonging to the pars inferior, to the brain. The most abundant cells within the adult SAG are neurons expressing the pan-neuronal markers HuC (also known as Elavl3) and/or HuD (Elavl4) (hereafter HuC/D) in their cell bodies and the calcium-binding protein Calretinin in their soma as well as in their processes (Fig. 1M). In addition, HuC/D labels a subgroup of Calretinin-negative neurons mostly found ventromedial to the Calretinin/HuC/D-positive neurons. This pattern was found throughout the entire rostral-caudal length of the SAG. As sections of the elbow-like structure contain the anterior SAG, with a high accumulation of mature neurons as well as the large sensory patch of the utricular macula, and are relatively stable during tissue preparation, we primarily focused on this part for further studies.

The amount and density of HuC/D-positive neurons decreases during growth of the SAG

Loss of neuronal cells during development and maturation of the vertebrate CNS and peripheral nervous system (PNS) is a well-known phenomenon (Cowan et al., 1984; Oppenheim, 1991). To evaluate the growth and the number of sensory neurons in the SAG, we used the neuronal marker HuC/D to quantify all neurons in the entire anterior SAG of juvenile (2 months) and adult (8 months) zebrafish (Fig. 2). In juveniles, HuC/D-positive neurons are found in the medial part of the SAG throughout all sections, whereas in adult zebrafish, HuC/D-positive neurons are found in the medial part of the SAG in the anterior sections but are distributed more lateral in the posterior sections (Fig. 2A, second last section 2 months versus 8 months). The highest number of HuC/D-positive neurons in 2-month-old fish is found in the first half of the anterior part of the SAG, where neurons are densely accumulating in a relatively small region on the ventral side in the medial part of the SAG. In contrast, the highest number of HuC/D-positive neurons in adult fish is usually located in the posterior part of the anterior SAG and neurons are spread more widely across the medial-lateral axis (Fig. 2A). Quantification revealed a significant decrease in the overall number of HuC/D-positive neurons, as well as in the average number of HuC/D-positive neurons per section in the entire SAG (Fig. 2B,C). In addition, the highest number of HuC/D-positive neurons counted on one section also significantly decreases from juvenile to adult stages (Fig. 2D). However, the overall thickness of the anterior SAG significantly increases with age (Fig. 2E). Taken together, these data reveal that, during growth, HuC/D-positive neurons are lost in the anterior SAG, as is shown by a decreased overall number and density of HuC/D-positive neurons, accompanied by an increased thickness of the adult SAG.

neurod:GFP-positive cells proliferate and give rise to new neurons at juvenile stages but cease to proliferate and display only reduced neurogenesis in the adult SAG

In contrast to mammals, zebrafish exhibit widespread adult neurogenesis and lifelong brain growth (Grandel et al., 2006). Similarly, hair cells in the inner ear are continuously generated throughout life (Schuck and Smith, 2009). During early mammalian inner ear development, the proneural transcription factor Neurod is crucial for neuronal differentiation and is required to build a pool of transient-amplifying neuronal progenitor cells (Kim et al., 2001). Using transgenic *neurod*:GFP zebrafish (Obholzer et al., 2008), we investigated whether neuronal progenitors are still present in the SAG at juvenile and adult stages. Using immunohistochemistry for the proliferation marker PCNA and the neuronal marker HuC/D in *neurod*:GFP transgenic animals, we analyzed proliferation in and neurogenesis from the *neurod*:GFP-positive population, using persistence of GFP from the *neurod*:GFP transgene as short-term lineage tracing. Indeed, *neurod*:GFP expression was found in dispersed groups of cells residing at the ventromedial side in the anterior and posterior part of the zebrafish SAG (Fig. 3, Fig. S2). *In situ* hybridizations against *neurod* and *gfp* on consecutive sections

Development (2020) 147, dev176750. doi:10.1242/dev.176750

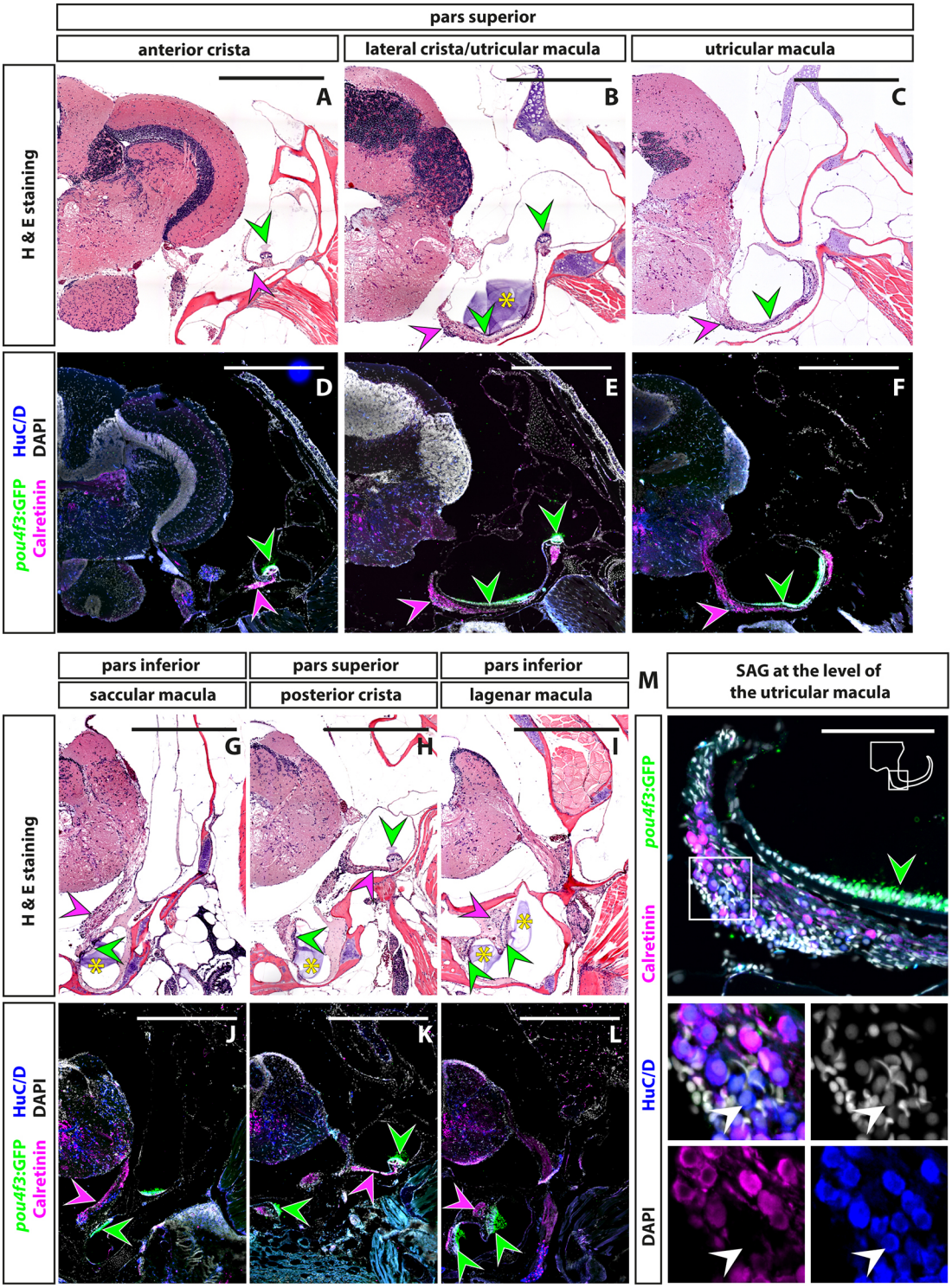

Fig. 1. Anatomy of the statoacoustic ganglion (SAG) in the adult zebrafish. (A-L) H&E staining (A-C,G-I) and immunohistochemistry (D-F,J-L) of cross-sections through the entire inner ear show the innervation of the pars superior, the dorsal part of the inner ear consisting of the anterior (A,D), the lateral (B,E) and the posterior cristae (H,K) and the utricular macula (B,C,E,F) as well as the pars inferior, the ventral part of the inner ear including the saccular macula (G,J) and the lagenar macula (I,L) by the SAG, the eighth cranial nerve. Neurons of the SAG express the neuronal markers HuC/D (labelling neuronal cell bodies) and Calretinin [labelling neuronal cell bodies as well as the axons (purple arrowheads)]. Hair cells in the sensory patches are labelled using *pou4f3*:GFP (green arrowheads). The former position of the three otoliths lapillus (utricular macula), sagitta (saccular macula) and asteriscus (lagenar macula) are visible as light purple residual structures left after decalcification of the otoliths, close to the sensory hair cells in the H&E staining (A-C,G-I; marked with yellow asterisks). (M) Close-up of the medial part of the SAG at the level of the utricular macula; comparison of HuC/D with Calretinin reveals that the latter only labels a subpopulation of neurons in the dorso-lateral part of the SAG (green and white arrowheads point to HuC/D-positive but Calretinin-negative neurons). Bottom panels in M show magnification of boxed area in top panel. Scale bars: 200 µm for A-L; 50 µm for M. Cross-sections show dorsal to the top and lateral to the right. Distance from first section through semicircular canals to the section of interest: anterior cristae (A) 0.5 mm; lateral cristae (B) 1.39 mm; utricular macula (C) 1.66 mm; posterior cristae (G) 2.53 mm; saccular macula (H) 3.15 mm; lagenar macula (I) 3.44 mm.

Development (2020) 147, dev176750. doi:10.1242/dev.176750

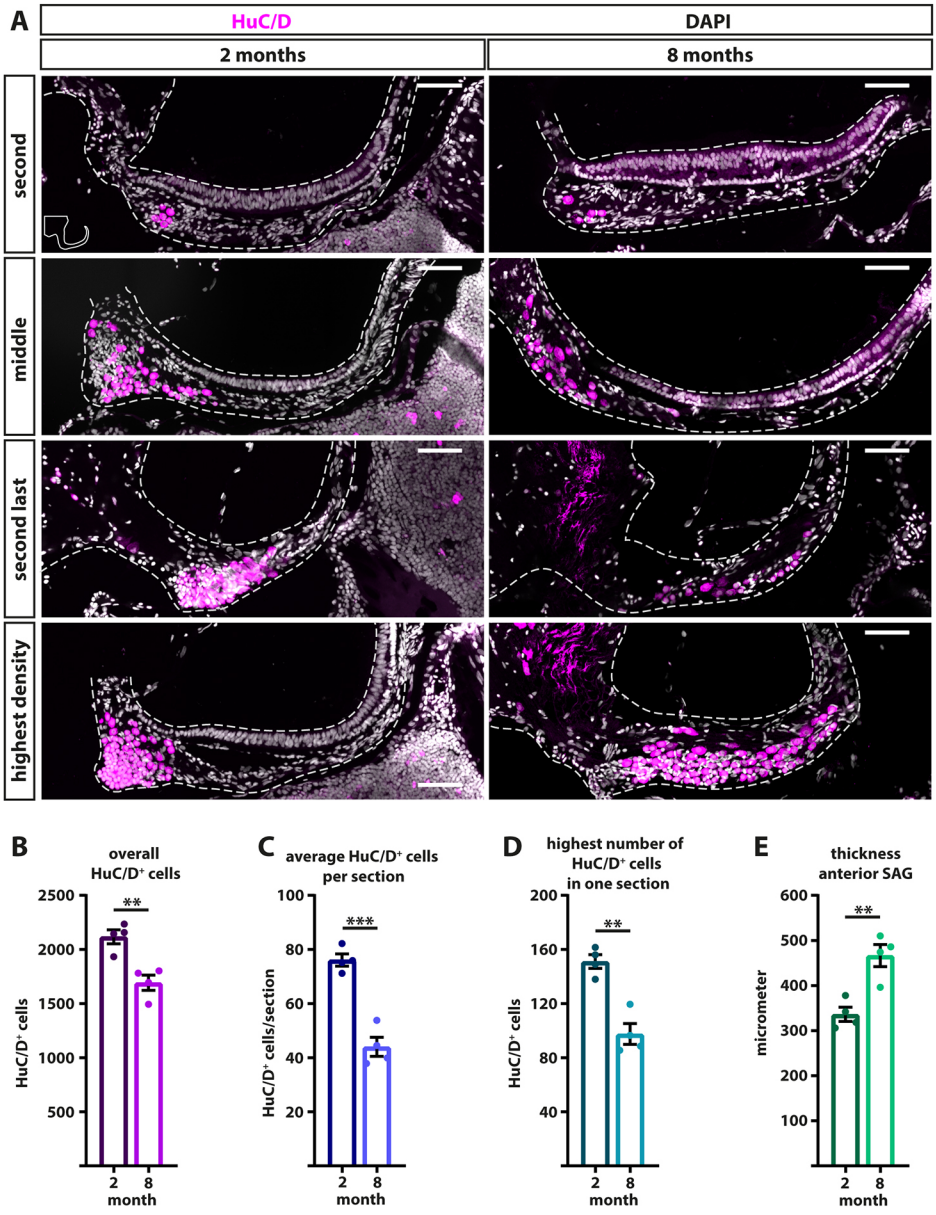

Fig. 2. Number and density of HuC/D-positive neurons decreases during growth of the SAG. (A) Antibody staining against neuronal marker HuC/D in the SAG of 2- and 8-month-old fish. The entire anterior part of the SAG was analyzed, starting with the first section with HuC/D-positive neurons and ending with the last section of the anterior part of the SAG. Shown are the second, middle and second-last section as well as the section with the highest density of HuC/D-positive cells. Note that in 2-month-old fish, the section with the highest density of HuC/D-positive cells is found in the first half of the anterior SAG, whereas at 8 months it is usually found in the last quarter of the anterior SAG. (B-E) Quantification of HuC/D-positive neurons in the entire anterior part of the SAG, showing that the overall number of HuC/D-positive cells (B), the average number of HuC/D-positive cells per section (C) and highest number of HuC/D-positive cells on one section (D) decreases, whereas the overall thickness of the anterior SAG along the anteroposterior axis (E) increases during growth. Scale bars: 50 µm. Cross-sections show dorsal to the top and lateral to the right. For all quantifications: n=4 fish with mean values calculated of all sections of both anterior SAGs; data are presented as mean±s.e.m. Unpaired two-tailed Student's t-test. $^{**}P \leq 0.01$; $^{***}P \leq 0.001$.

of *neurod*:GFP transgenic animals and RT-PCR analysis on dissected SAGs corroborated that the reporter faithfully recapitulates endogenous *neurod* expression (Fig. S1). Simultaneous labelling of GFP, PCNA and HuC/D revealed that *neurod*:GFP-positive cells proliferate (*neurod*:GFP/PCNA-positive) and independently give rise to new neurons (*neurod*:GFP/HuC/D-positive) at juvenile stages (2 and 3 months). We also observed differences in the nuclear shape in these two populations: whereas proliferating *neurod*:GFP-positive cells contain oblong nuclei, newborn neurons display a round-shaped nucleus similar to mature neurons. However, the pool of proliferating *neurod*:GFP-positive cells is absent at adult stages (8 months) and in aged fish (20 months) (Fig. 3A). In contrast, newborn neurons (*neurod*:GFP/HuC/D-positive), although infrequent, are still present in the adult SAG and are mostly found in the first half of the anterior SAG. It is noteworthy that proliferating but *neurod*:GFP-negative cells could be detected within the vicinity of *neurod*:GFP cells at all stages examined (Fig. 3B).

Quantification of overall PCNA-positive cells in the SAG revealed a significant reduction in proliferation from 2 to 3 months and a further decline to a low but steady-state level at adult stages (Fig. 3C). Also, a significant drop in the overall number of *neurod*:GFP-positive cells was observed from 2 to 3 months, with only a further slight decline at adulthood (Fig. 3D). Similarly, the number of proliferating *neurod*:GFP-positive cells decreased significantly during juvenile stages towards complete absence at adulthood (Fig. 3E). Antibody staining with HuC/D revealed that around one-third of *neurod*:GFP-positive cells located at the dorsal side of the *neurod*:GFP-expressing cell pool are also positive for HuC/D. In addition, they show the characteristic round nuclei of sensory neurons, indicating that these cells are early immature neurons, differentiating from the *neurod*:GFP-positive pool into neurons retaining the GFP label (Fig. 3A,F). Neurogenesis significantly decreases from 2 to 3 months and a further reduction can be seen from 3 to 8 months, resulting in only very few *neurod*:GFP/HuC/D-positive cells in the adult SAG (Fig. 3A,F). Interestingly, the number of *neurod*:GFP cells that neither co-express PCNA nor HuC/D (*neurod*:GFP-only cells) is constant during juvenile and adult stages (Fig. 3G). Taken together, the *neurod*:GFP-positive cells constitute a neuronal progenitor pool

Development (2020) 147, dev176750. doi:10.1242/dev.176750

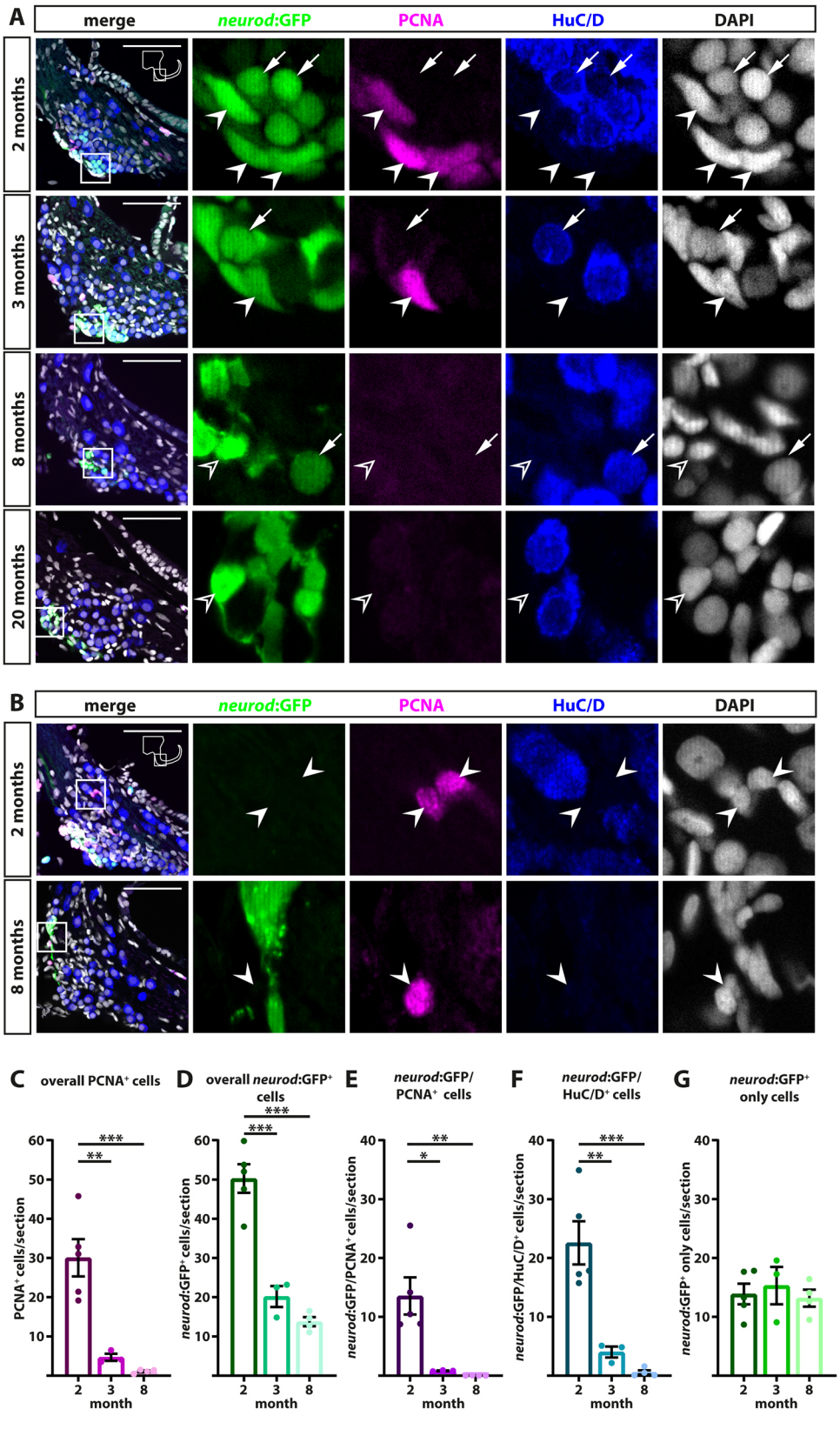

Fig. 3. Proliferation and neurogenesis rapidly decrease at juvenile stages and is severely reduced in the adult zebrafish SAG. (A,B) Antibody staining showing proliferation (PCNA), *neurod*:GFP-positive cells and mature neurons (HuC/D) in the SAG of juvenile (2 and 3 months) and adult (8 and 20 months) *neurod*:GFP zebrafish. (A) At juvenile stages, *neurod*:GFP-positive cells proliferate (*neurod*:GFP/PCNA-positive cells, solid arrowheads) and give rise to new neurons (*neurod*:GFP/HuC/D-positive cells, arrows). In contrast, *neurod*:GFP-positive cells (open arrowheads) are not proliferating in adult fish and *neurod*:GFP/HuC/D-positive cells are rarely found. (B) Proliferating PCNA-positive but *neurod*:GFP-negative cells (arrowheads) can be found in the vicinity of the *neurod*:GFP-positive population at all stages. Panels on right show magnification of boxed areas in left panels. (C-G) Quantification of antibody staining. The overall number of PCNA-positive cells (C), the overall number of *neurod*:GFP-positive cells (D) and *neurod*:GFP/PCNA-positive cells (E) significantly decrease from 2 to 3 months, leaving only few PCNA-positive cells but no *neurod:GFP*/PCNA-positive cells at 8 months. (F) The number of newborn neurons marked by *neurod*:GFP and HuC/D decreases significantly from 2 to 3 and further from 3 to 8 months. (G) The number of cells in the *neurod*:GFP-positive pool that are neither proliferating nor positive for HuC/D stays constant over time. Scale bars: 50 µm. Cross-sections show dorsal to the top and lateral to the right. For quantifications: 2 months, n=3; 3 months, n=3; adult, n=4 (n=fish; 1 SAG/fish; 12 sections/SAG); data are presented as mean±s.e.m. Ordinary one-way ANOVA with Tukey's multiple comparison test. *P≤0.05; **P≤0.01; ***P≤0.001.

that proliferates at juvenile stages but becomes quiescent with respect to proliferation at adulthood. At the same time, neurogenesis from this *neurod*:GFP-positive progenitor pool also rapidly decreases at juvenile stages but – independent from proliferation – does not cease at adult stages.

neurod:GFP-positive cells are proliferating and give rise to new neurons at juvenile stages

Because Neurod is expressed only transiently (Andermann et al., 2002; Kim et al., 2001), the observation of newborn neurons is based on short-term lineage tracing due to persistence of GFP. To

Development (2020) 147, dev176750. doi:10.1242/dev.176750

corroborate our findings, we performed a pulse chase experiment using bromodeoxyuridine (BrdU), a thymidine analogue that is incorporated during the S-phase of the cell cycle and hence labels active cycling cells (Kiernan et al., 2005). To this aim, 3-month-old *neurod*:GFP transgenic animals were exposed to BrdU for 24 h and kept for chase times of 0, 7, 15 and 28 days, after which they were analyzed (Fig. 4A). Consistent with our proliferation analysis at juvenile stages (Fig. 3), we found *neurod*:GFP-positive cells incorporating BrdU at 0 days post treatment (dpt) (Fig. 4B). Subsequently, *neurod*:GFP-positive cells that have incorporated BrdU can differentiate into neurons directly after proliferation, as indicated by the presence of a triple positive newborn neuron (*neurod*:GFP/BrdU/HuC/D-positive) at 0 dpt (seen only once in only one individual). Double-positive more-mature neurons that have already lost the *neurod*:GFP label (BrdU/HuC/D-positive) were observed as early as 7 dpt. In addition, some *neurod*:GFP-positive cells that had incorporated BrdU remained in the *neurod*:GFP-positive pool. Quantification of overall BrdU-positive cells in the SAG revealed a significant increase of BrdU-positive cells from 0 to 15 dpt (Fig. 4C). The percentage of *neurod*:GFP cells which incorporated BrdU (BrdU/*neurod*:GFP-positive) significantly dropped from 0 dpt to the other time points (Fig. 4D). However, the percentage of triple-positive newborn neurons (BrdU/*neurod*:GFP/HuC/D-positive) increased over time to ∼4% at 15 dpt,

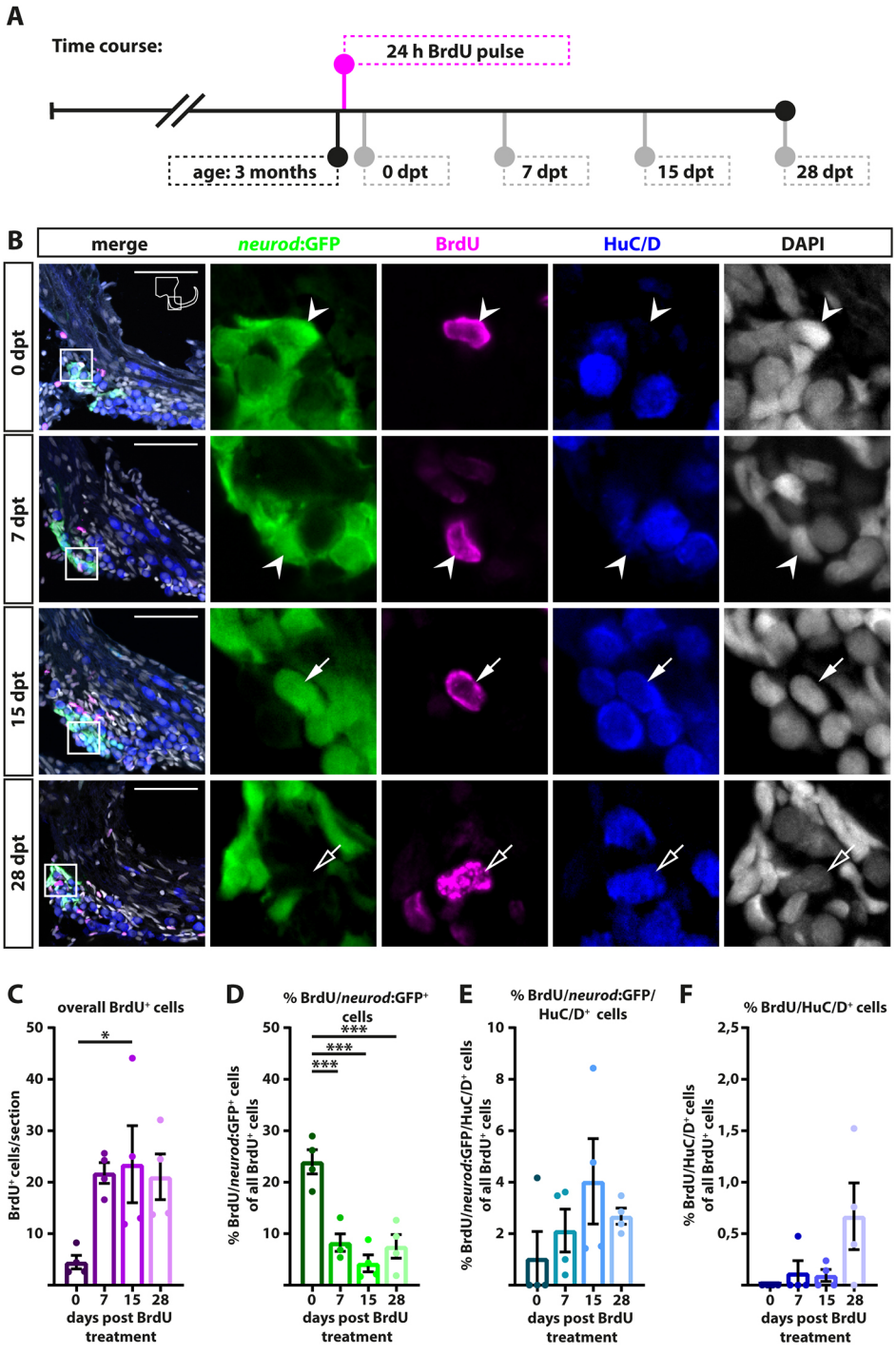

Fig. 4. *neurod*:GFP-positive cells are proliferating and give rise to new neurons at juvenile stages. (A) Time course of the BrdU pulse chase experiment: 3-month-old *Tg(neurod:GFP)* zebrafish were sacrificed at 0, 7, 15 and 28 dpt. (B) Antibody staining shows BrdU/*neurod*:GFP-positive cells (0 and 7 dpt, arrowheads) which differentiate into BrdU/*neurod*:GFP/HuC/D-positive (15 dpt, solid arrows) and BrdU/HuC/D-positive neurons (28 dpt, open arrows). Panels on right show magnification of boxed areas in left panels. (C-F) Quantification of antibody staining. (C) The overall number of BrdU-positive cells increases from 0 dpt to later time points, indicating continued proliferation of precursor cells. (D) Percentage of BrdU/*neurod*:GFP-positive cells of all BrdU-positive cells decreases significantly from 0 dpt to later time points. (E) At 7 dpt, some BrdU/*neurod*:GFP-positive cells have already differentiated into immature BrdU/*neurod*:GFP/HuC/D-positive cells. (F) First newborn BrdU/HuC/D-positive neurons appear as early as 7 dpt and the percentage of BrdU/HuC/D positive neurons increases over time. Scale bars: 50 µm. Cross-sections show dorsal to the top and lateral to the right. For all quantifications $n=4$ (n=fish; 1 SAG/fish; 12 sections/SAG); data are presented as mean±s.e.m. Ordinary one-way ANOVA with Tukey's multiple comparison test. $^{*}P \leq 0.05$; $^{***}P \leq 0.001$.

Development (2020) 147, dev176750. doi:10.1242/dev.176750

revealing the exit of formerly active cycling cells from the *neurod*:GFP-positive progenitor pool to differentiate into neurons (Fig. 4E). Even though the number of newborn neurons (BrdU/HuC/D-positive) was low, we saw an increase in the percentage of BrdU/HuC/D-positive newborn neurons over time (Fig. 4F). In addition, we also calculated the percentage of BrdU double-positive cells in relation to the specific cell type, e.g. *neurod*:GFP-positive progenitor cell, *neurod*:GFP/HuC/D-positive immature neuron and HuC/D-positive mature neuron (Fig. S3A). The number of BrdU/*neurod*:GFP-positive cells per *neurod*:GFP-positive cell does not change significantly during the 28 day trace. Similar to the quantifications shown above, the percentages of BrdU/*neurod*:GFP/HuC/D-positive cells per *neurod*:GFP/HuC/D-positive cell and of BrdU/HuC/D-positive cells per HuC/D-positive cell increases over time. In summary, our data show the continued production of new inner ear neurons at juvenile stages.

A proliferating but marker-negative cell population replenishes the *neurod*:GFP-positive cell pool at adult stages

Our PCNA-based proliferation analysis revealed that *neurod*:GFP-positive cells represent a progenitor pool that shows robust proliferation as well as neurogenesis at juvenile stages but not at adulthood. However, a low but steady-state proliferation outside of the *neurod*:GFP-positive population was detected at adult stages (Fig. 3B). Hence, we repeated the BrdU pulse chase experiment at adult stages to investigate whether non-*neurod*:GFP-positive cells are also able to form new neurons at this later time point (Fig. 5A). Consistent with our proliferation analysis using PCNA (Fig. 3), we found no *neurod*:GFP-positive cell co-localizing with BrdU at 0 dpt (Fig. 5B). In contrast, double-positive cells (*neurod*:GFP/BrdU-positive) were detected at 7 dpt, indicating the presence of a proliferating non-*neurod*:GFP-expressing cell population that can differentiate into *neurod*:GFP-positive cells and thus replenish the pool of *neurod*:GFP-positive cells. Furthermore, triple-positive newborn neurons (*neurod*:GFP/BrdU/HuC/D-positive) as well as more-mature neurons that have already lost the *neurod*:GFP label (BrdU/HuC/D-positive) were present in single individuals with chase times of more than 14 days. Interestingly, again some *neurod*:GFP-positive cells retained the BrdU label at 29 dpt, indicating that not all BrdU-labelled cells developed into mature neurons at this late time point. Quantification of the overall number of BrdU-positive cells (Fig. 5C), as well as the percentage of BrdU-positive-only cells, BrdU/*neurod*:GFP-positive cells and BrdU/HuC/D-positive cells from all BrdU-positive cells (Fig. 5D-G) showed that neurogenesis in the adult SAG is a very rare event. A trend for an increase in the number of BrdU-positive cells from 0 dpt to 7/14/29 dpt can be seen, indicating further proliferation in stem/progenitor cells (Fig. 5C). Importantly, at 0 dpt, all BrdU-positive cells are BrdU-positive-only cells, lacking expression of *neurod*:GFP or HuC/D (Fig. 5D). Consistently, multiple BrdU-positive-only cells remain present at later time points. In contrast, BrdU/*neurod*:GFP-double-positive cells can first be seen at 7 dpt and, moreover, at least one individual per time point displayed BrdU/*neurod*:GFP-double-positive cells in all later time points. Newly formed BrdU/HuC/D-double-positive neurons were only found in one individual at 14 dpt (Fig. 5F). Similarly, quantification of the ratio of BrdU-double-positive cells in relation to their specific cell type displayed the same trends (Fig. S3B). Taken together, our data show that new cells are added to the pool of *neurod*:GFP-positive progenitors from proliferating non-*neurod*:GFP-expressing cells. Moreover, although the number of analyzed animals was not sufficient to reach statistical relevance, adult neurogenesis is an extremely rare event but is present in the adult SAG and new HuC/D-positive neurons are generated.

Nestin expression labels embryonic neuronal progenitors and overlaps with *neurod*:GFP expression at juvenile and adult stages

The cellular composition of neural stem cell niches varies across vertebrate species and even within the very same species. However, neural stem cell niches share common characteristics and possess either a radial glia or neuroepithelial-like identity (Lindsey et al., 2018). We analyzed the cellular composition of the neurogenic niche of the SAG in more detail. One marker associated with neuroepithelial-like stem cell identity is the class IV intermediate filament protein Nestin, which is downregulated when cells differentiate and become post-mitotic (Wiese et al., 2004). During zebrafish development, *nestin* is expressed in proliferative zones of the CNS as well as in the cranial ganglia (Mahler and Driever, 2007). Consistently, analysis of bacterial artificial chromosome (BAC) transgenic *nestin*:GFP animals, in which GFP expression is driven by *nestin* regulatory elements and recapitulates all aspects of the endogenous *nestin* mRNA expression (Kaslin et al., 2009), revealed *nestin*:GFP-positive cells in the region of the *neurod*:GFP-positive niche of the juvenile SAG (Fig. 6A). RT-PCR analysis on dissected SAGs corroborated that the reporter recapitulates endogenous *nestin* expression (Fig. S1). Similar to *neurod*:GFP, co-staining for proliferation (PCNA) and neurons (HuC/D) revealed that *nestin*:GFP-positive cells proliferate (*nestin*:GFP/PCNA-positive cells) and give rise to newborn neurons (*nestin*:GFP/HuC/D-positive cells). To corroborate our hypothesis that *nestin*:GFP and *neurod*:GFP mark the same cell population, we could not simply use animals carrying both transgenes. Hence, we employed a *nestin* reporter line expressing a different fluorophore. In this line, a single open reading frame coding for mCherry and CreER^{T2} separated by a viral T2A peptide sequence is expressed under the control of a *nestin* promoter fragment recapitulating the endogenous cranial *nestin* expression (Fig. S4). Subsequently, we analyzed mCherry expression of *nestin*:mCherry-T2A-CreER^{T2} in combination with the *nestin*:GFP as well as the *neurod*:GFP transgenes. Analysis of double-transgenic fish harbouring *nestin*:GFP and *nestin*:mCherry-T2A-CreER^{T2} proved that both transgenic lines mark the same cell population in the SAG (Fig. S4). Indeed, co-staining for *neurod*:GFP, *nestin*:mCherry-T2A-CreER^{T2} and HuC/D confirmed that *neurod*:GFP and *nestin*:mCherry-T2A-CreER^{T2} are actually co-expressed in most cells in the juvenile and adult SAG (Fig. 6B). However, compared with *neurod*:GFP, expression of *nestin*:mCherry-T2A-CreER^{T2} persists longer in newborn neurons (*nestin*:mCherry-T2A-CreER^{T2}/HuC/D-positive cells) in the juvenile SAG. To estimate the degree of neurogenesis at embryonic/larval stages versus later neurogenesis, we performed long-term lineage tracing of cells recombined during early otic development (Fig. 6C, Fig. S4). This analysis revealed that many, but not all, mature HuC/D-positive neurons populating the adult SAG are derived from the embryonic progeny of the *nestin*:mCherry-T2A-CreER^{T2}-positive cells (Fig. 6D). Quantification of *nestin*:mCherry-T2A-CreER^{T2}-derived HuC/D-positive neurons showed that only ∼57% of all neurons in the adult zebrafish SAG are progeny of *nestin*:mCherry-T2A-CreER^{T2}-positive cells recombined at embryonic/larval stages (Fig. 6E,F). Taken together, expression of the class IV intermediate filament protein Nestin overlaps with *neurod*:GFP expression at juvenile and adult stages and labels neuronal SAG progenitors at embryonic stages.

Development (2020) 147, dev176750. doi:10.1242/dev.176750

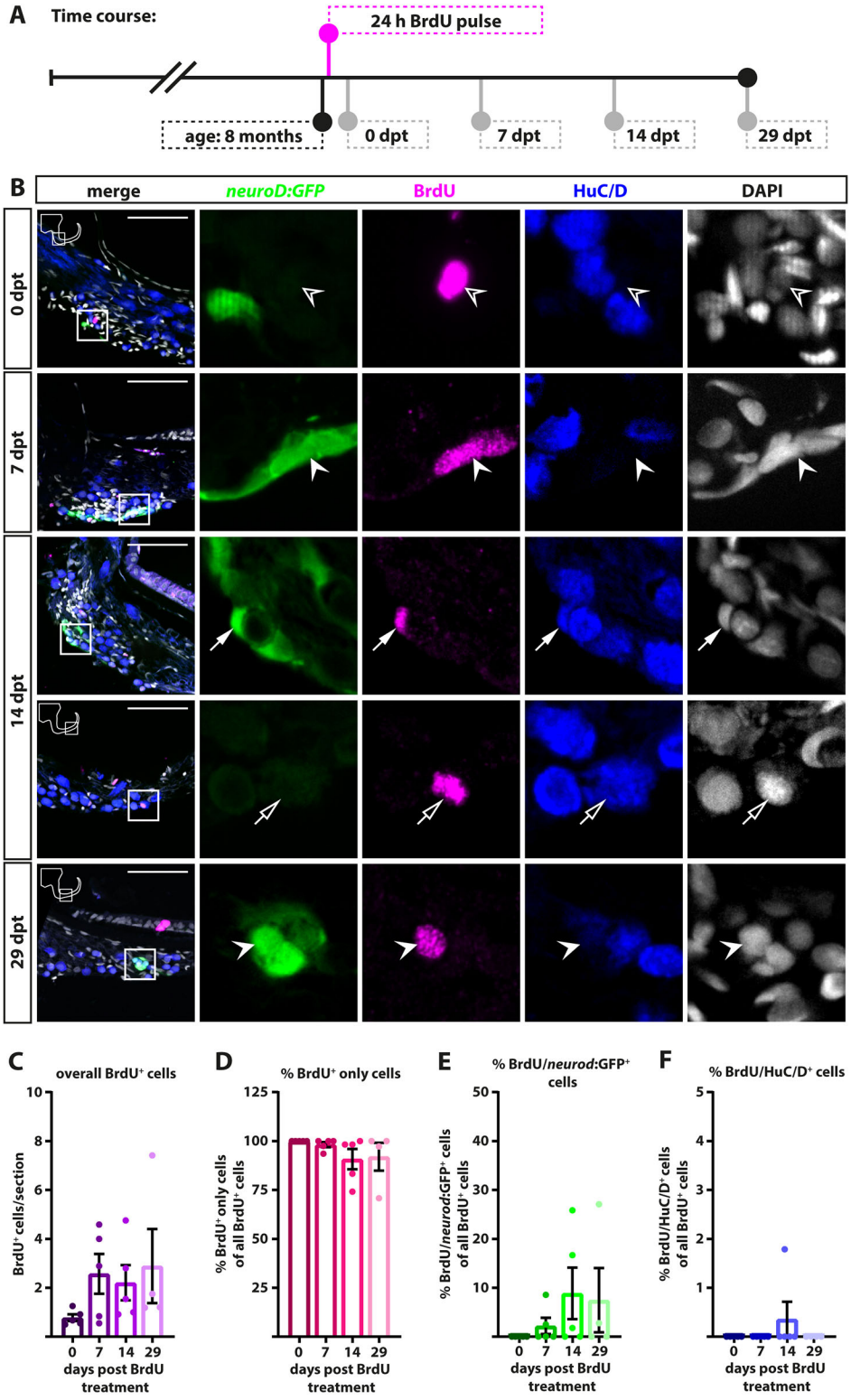

Fig. 5. A proliferating but marker-negative cell population replenishes the *neurod*:GFP-positive cell pool at adult stages. (A) Time course for BrdU pulse chase experiment: 8-month-old *Tg(neurod:GFP)* zebrafish were sacrificed at 0, 7, 14 and 29 dpt. (B) Antibody staining reveals that BrdU-positive cells never co-localize with *neurod*:GFP at 0 dpt (open arrowheads). However, BrdU/*neurod*:GFP-positive cells are present at 7 dpt (solid arrowheads). Newly generated *neurod*:GFP-positive cells can either differentiate into new neurons [BrdU/*neurod*:GFP/HuC/D-positive cells (solid arrows) and BrdU/HuC/D-positive cells (open arrows)], as can be seen as early as 14 dpt, or remain in the pool of *neurod*:GFP-positive cells (solid arrowheads) as can be seen at 29 dpt. Panels on right show magnification of boxed areas in left panels. (C-F) Quantification of overall BrdU-positive cells (C) as well as percentage of BrdU-positive-only cells (D), BrdU/*neurod*:GFP-positive cells (E) and BrdU/HuC/D-positive cells as a fraction of all BrdU-positive cells (F). Scale bars: 50 µm. Cross-sections show dorsal to the top and lateral to the right. For quantifications: 0, 7, 14 days, *n*=5; 29 days, *n*=4 (*n*=fish; 1 SAG/fish; 12 sections/SAG); data are presented as mean±s.e.m. Ordinary one-way ANOVA with Tukey's multiple comparison test.

Distribution of glia and myelination label the PCTZ in the SAG

In the zebrafish telencephalon, radial glia expressing the filamentous proteins glial fibrillary acidic protein (GFAP; also known as Zrf1), S100B and members of the Hairy/enhancer of split 4 (Her4) family serve as neuronal progenitor cells (Chapouton et al., 2011; Ganz et al., 2010; Lam et al., 2009). To analyze the presence and distribution of cells with glial characteristics as well as myelinated cells in the SAG, we used transgenic reporter lines and marker analysis to characterize the expression of the glia markers S100B, GFAP and Her4.3 as well as the myelin markers Claudin K and Mbp. Claudin K expression indicates strong myelination in the medial part entering the brain and low myelination in the lateral part of the juvenile SAG, resulting in a sharp boundary between both myelination levels (Fig. 7A). Similarly, *her4.3*:GFP, as well as endogenous GFAP and S100B all show an identical expression pattern and are expressed in the medial part of the

Development (2020) 147, dev176750. doi:10.1242/dev.176750

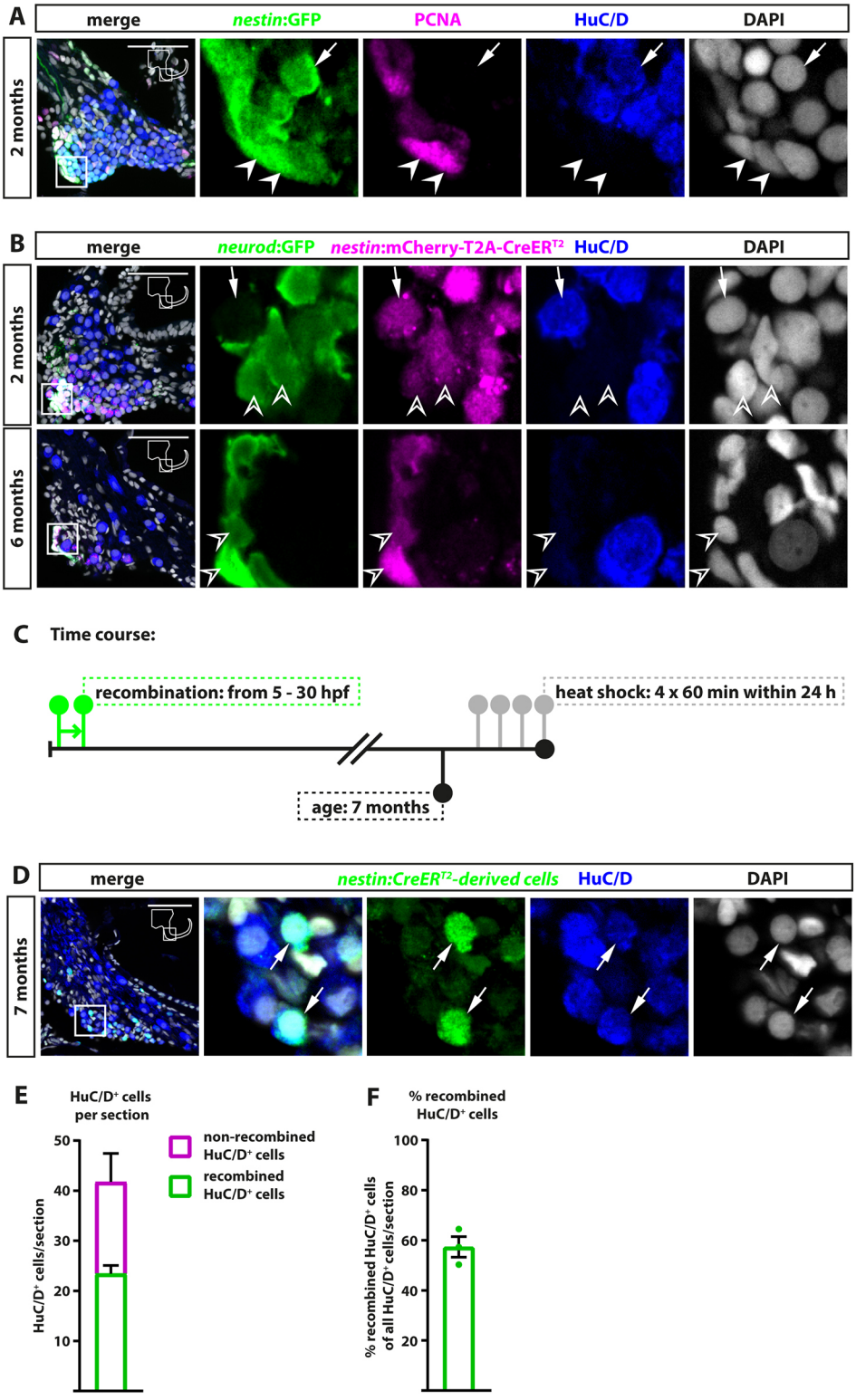

Fig. 6. Nestin expression labels embryonic neuronal progenitors and overlaps with *neurod*:GFP expression at juvenile and adult stages. (A) Antibody staining showing *nestin*:GFP expression in the region of the *neurod*:GFP-positive cells. *nestin*:GFP-positive cells are proliferating (*nestin*:GFP/PCNA-positive cells, solid arrowheads) and differentiate into neurons (*nestin*:GFP/HuC/D-positive cells, arrows) in 2-month-old zebrafish. (B) *nestin*:mCherry-T2A-CreER^{T2} is expressed in the *neurod*:GFP-positive progenitor pool (open arrowheads) in 2- and 6-month-old zebrafish; expression of *nestin*:mCherry-T2A-CreER^{T2} persists longer in newly differentiated neurons than *neurod*:GFP expression (arrows). (C) Time course of *nestin*:mCherry-T2A-CreER^{T2} long-term lineage tracing experiment. Recombination in *Tg(nestin:mCherry-T2A-CreER^{T2}), Tg(hsp70l:loxP-DsRed2-loxP-nlsEGFP)* double-transgenic embryos was induced from 5-30 hpf. At 7 months, zebrafish were heat shocked four times within 24 h to activate the reporter and afterwards analyzed for *nestin*:CreER^{T2}-derived cells. (D) Co-staining of GFP-positive *nestin*:CreER^{T2}-derived cells with HuC/D shows the presence of *nestin*:CreER^{T2}-derived/HuC/D-positive cells (arrows). (E,F) Quantification of GFP-positive (recombined) and GFP-negative (non-recombined) HuC/D-positive cells (E) and percentage of recombined HuC/D-positive cells (F). Panels on right show magnification of boxed areas in left panels. Scale bars: 50 µm. Cross-sections show dorsal to the top and lateral to the right. Quantification: *n*=3 (*n*=fish; 1 SAG/fish; 12 sections/SAG); data are presented as mean±s.e.m.

juvenile and adult SAG, with a sharp border to the more lateral part in which the neuronal HuC/D-positive cell bodies reside (Fig. 7B, Fig. S5). Simultaneous labelling with the myelin marker Mbp revealed co-localization of GFAP-positive cells within the strongly myelinated territory in the adult SAG (Fig. 7C). The change in myelination has been described as the PCTZ, the boundary between the CNS, with oligodendrocyte-mediated myelination, and the PNS, with Schwann cell-mediated myelination (Bojrab et al., 2017; Fraher, 1999; Wang et al., 2013). Because co-localization indicated that glia cells reside within the highly myelinated territory, and hence within the CNS, we also examined the expression of Sox2, which plays pivotal roles in the regulation of neural stem cells (Hagey et al., 2018). Besides strong expression in the sensory patch of the utricular macula, Sox2 can be found in a straight line in the medial part of the SAG (Fig. 8A). Co-staining of GFAP and GFP in *Tg(sox2:GFP)* and *Tg(neurod:GFP)* revealed that *sox2*:

Development (2020) 147, dev176750. doi:10.1242/dev.176750

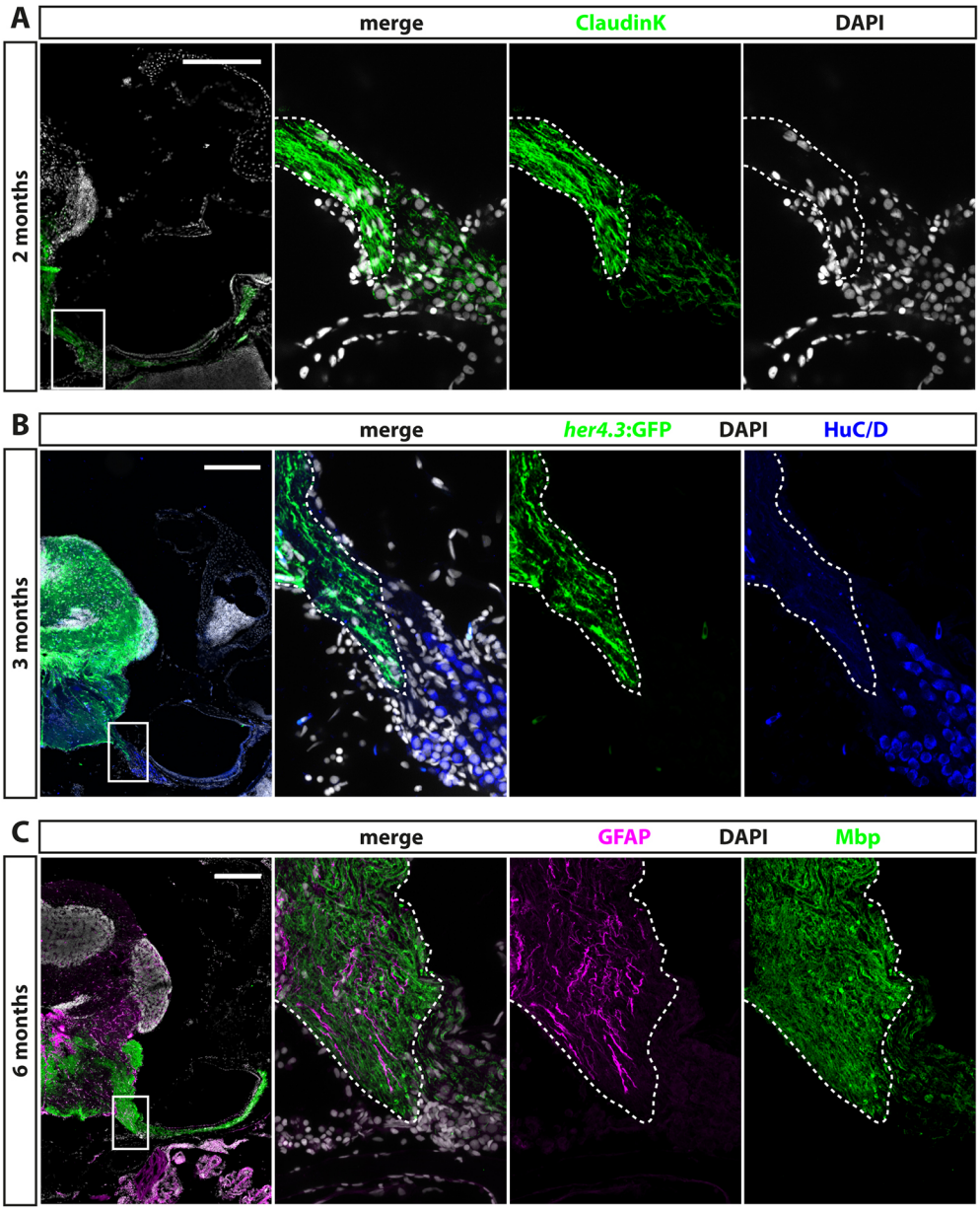

Fig. 7. Expression of glia markers and differences in myelination patterns mark the PCTZ in the SAG. (A) Antibody staining against Claudin K showing the PCTZ (dashed line) as a sharp boundary, visible as a change in the myelination pattern in the SAG in 2-month-old fish. (B) Antibody staining against the glia marker *her4.3*:GFP and HuC/D in 3-month-old zebrafish reveals expression of *her4.3*:GFP in the medial part of the SAG, similar to the myelination expression pattern (dashed line); HuC/D-positive neurons reside lateral from the PCTZ. (C) Co-staining of the glia marker GFAP and the myelination marker Mbp shows a similar expression pattern as reported in A and B, with the PCTZ marked by a change in the myelination pattern and medial expression of the glia marker. Panels on right show magnification of boxed areas in left panels. Scale bars: 200 µm. Cross-sections show dorsal to the top and lateral to the right.

GFP-positive cells are located only a few µm lateral to the GFAP domain (Fig. 8B). In contrast, the *neurod*:GFP-positive cell population is located at the ventral side of the SAG, notably separated (more than 50 µm) from the GFAP domain (Fig. 8C). Therefore, Sox2-positive cells reside along the PCTZ and are clearly outside of the Neurod/Nestin-positive progenitor pool. Interestingly, the density of nuclei medial to the line of Sox2-positive cells is usually very low compared with the area lateral of Sox2-positive cells. This, together with the characteristic elongated shape of the Sox2-positive nuclei, allows identification of the PCTZ, even on the basis of the nuclear DAPI staining.

In summary, we show that cells with glial characteristics, expressing GFAP, S100B and *her4.3*:GFP, as well as cells expressing the neural stem cell marker Sox2, are not present in or near the Neurod/Nestin-positive progenitor pool. However, together with the distribution of myelin markers Claudin K and Mbp, they mark the PCTZ in the medial part of the SAG, which is highly similar to the mammalian system (Fraher and Delanty, 1987; Hu et al., 2014).

DISCUSSION

In zebrafish, hair cells in the inner ear are produced throughout life (Higgs et al., 2002). To investigate whether continued hair cell formation is accompanied by neurogenesis, we thoroughly characterized the cellular composition of and neurogenesis in the SAG beyond larval stages. We found that the SAG can be morphologically divided into an anterior and a posterior part in cross-sections: these parts do, however, display the same cellular composition (Fig. 9A). We have identified a neurogenic niche at the ventromedial side consisting of Neurod- and Nestin-double-positive cells. Importantly, the neurogenic niche in the adult SAG is not a continuous band of cells but is rather composed of dispersed islets along the anteroposterior axis. The cell bodies of the neurons are located at the dorsolateral side of the neurogenic niche, with newborn neurons being in close proximity to the neurogenic niche (Fig. 9B). The lateral part of the SAG contains mostly the dendrites of mature neurons innervating hair cells in the respective sensory patches. In contrast, the medial part contains the axons of the mature

Development (2020) 147, dev176750. doi:10.1242/dev.176750

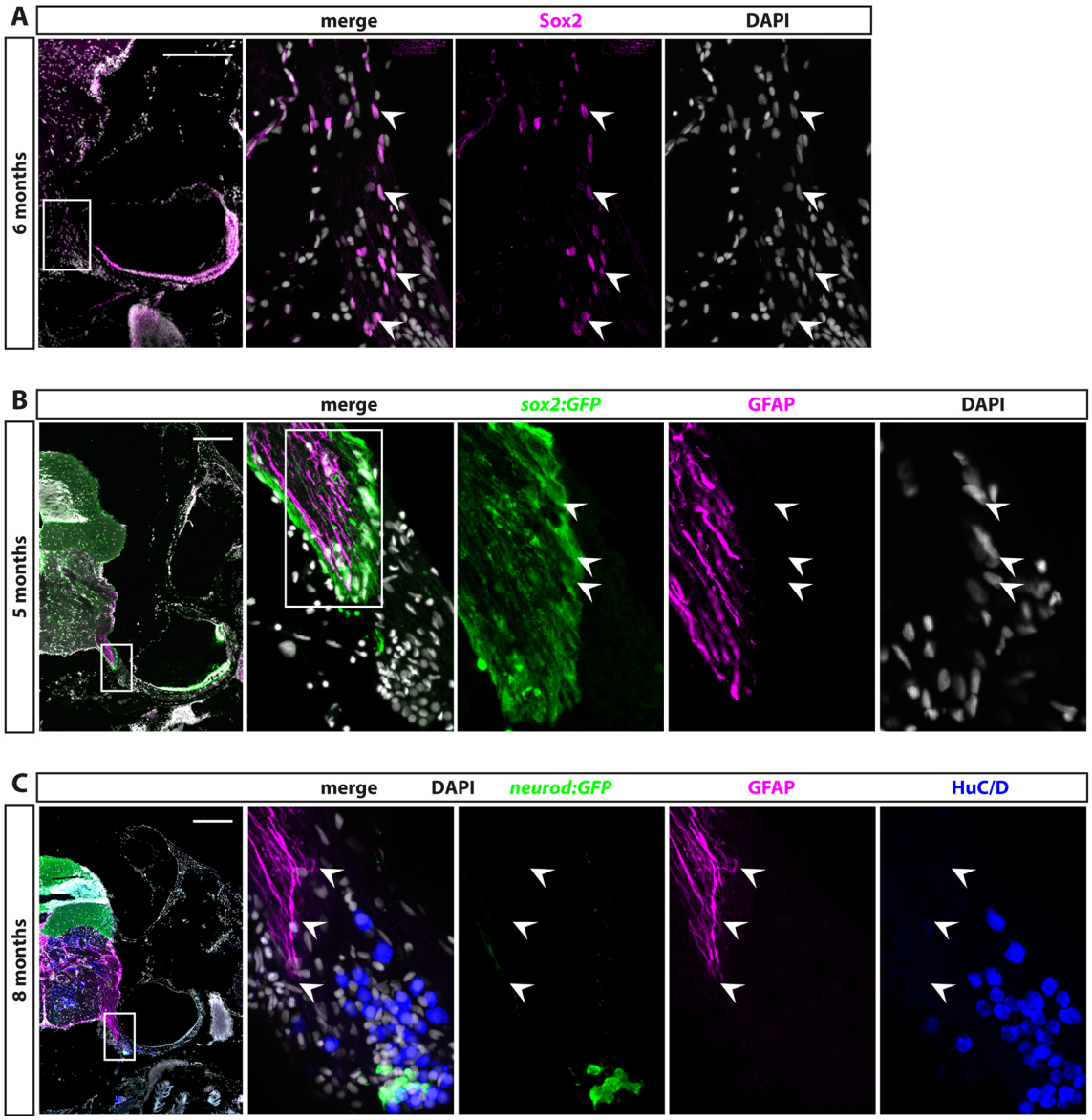

Fig. 8. Sox2-positive cells reside along the PCTZ outside the NeuroD/Nestin-positive progenitor pool in the SAG. (A) Antibody staining against Sox2 reveals that Sox2-positive cells (arrowheads) are present along a line in the medial portion of the adult SAG. (B) Co-staining for GFAP and *sox2*:GFP in the *sox2*:GFP reporter shows presence of *sox2*:GFP-positive cells (arrowheads) only a few microns lateral of the GFAP staining. (C) Co-staining for GFAP and *neurod*:GFP reveals presence of *neurod*:GFP-positive cells ∼50 µm away from the GFAP-positive zone (arrowheads). Panels on right show magnification of boxed areas in left panels. Scale bars: 200 µm. Cross-sections show dorsal to the top and lateral to the right.

neurons, and also the PCTZ (Fig. 9A). The PCTZ forms the boundary between the PNS and the CNS in the nerve roots of vertebrates and it is known that the CNS extension is exceptionally long in the mammalian cochlear nerve (Fraher and Delanty, 1987; Hu, 2013). In the zebrafish SAG, the PCTZ is characterized by a strong myelination pattern in the medial part (corresponding to the CNS) and a weaker myelination in the lateral part (corresponding to the PNS). In addition, the medial PCTZ is also marked by the presence of cells expressing glia markers such as GFAP, S100B and *her4.3*:GFP. Interestingly, the neural progenitor marker Sox2 is expressed in cells at the intersection from the medial to the lateral part of the PCTZ, making it a functional marker for this zone.

The phenomenon of programmed cell death leading to a loss of 20-80% of newly generated neurons is a physiological process during development and maturation of the vertebrate CNS and PNS (Oppenheim, 1991). Quantification of all HuC/D-positive neurons in the anterior SAG revealed that the overall number and the density of sensory neurons decreases as the SAG grows and increases in thickness (∼20% decrease on overall number of neurons from 2 to 8 months, Fig. 2). This suggests that a surplus of neurons are produced during juvenile stages that are either subsequently lost or gradually mature to innervate hair cells at later times.

Interestingly, our data show that neurogenesis still takes place at late juvenile and also even at adult stages independent of this surplus of sensory neurons. During mammalian inner ear development, NeuroD is required for neuronal differentiation and is expressed in a pool of transient-amplifying neuronal progenitor cells (Kim et al., 2001). At juvenile stages, the neurogenic niche is still highly active and Neurod/Nestin-positive cells proliferate and give rise to newborn neurons. Moreover, quantification after BrdU treatment shows that the percentage of BrdU/*neurod*:GFP-positive cells does not change significantly from a 7 day chase to later time points,

Development (2020) 147, dev176750. doi:10.1242/dev.176750

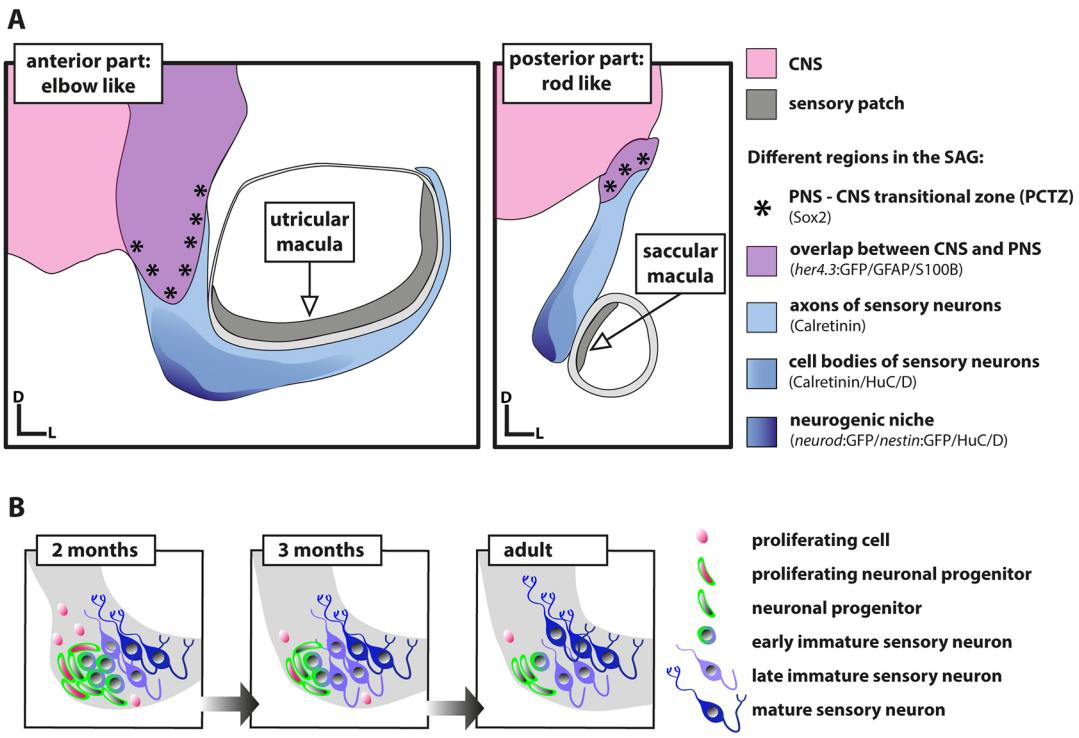

Fig. 9. Schematic of the adult zebrafish SAG and the course of neurogenesis from juvenile to adult stages. (A) The SAG connects the sensory patches of the inner ear to the CNS and can be morphologically divided into an anterior elbow-shaped part and a posterior rod-shaped part. The PCTZ is a strong landmark further dividing the SAG along the lateromedial axis into two parts: a lateral part corresponding to the PNS and characterized by weaker myelination and a lack of glia marker expression, and a medial part, corresponding to the CNS and characterized by a strong myelination pattern and expression of various glia markers. The anterior and the posterior part harbour a neurogenic niche at the ventromedial side consisting of Neurod/Nestin-double-positive cells. The cell bodies of the neurons are located around the neurogenic niche. In the anterior part of the SAG, neuronal cell bodies and the neurogenic niche are found between the lateral and the medial part, whereas in the posterior part of the SAG, both are located in the medial part. Neurons extend their axons in the medial part towards the CNS and their dendrites in the lateral part towards the sensory patches. D, dorsal; L, lateral. (B) Scheme depicting the potential development of the neurogenic niche from an active proliferating *neurod*:GFP-positive pool giving rise to new neurons in juvenile zebrafish to a more quiescent, non-proliferating *neurod*:GFP-positive pool with a very low neurogenesis rate in adult zebrafish.

indicating that some of the proliferating *neurod*:GFP-positive cells remain in the transient-amplifying progenitor pool and do not initiate differentiation within 28 days after proliferation. Whether these cells belong to a pool of progenitors with proliferative potential residing in the neurogenic niche or will eventually differentiate into new neurons at later time points is not yet clear.

In contrast, the Neurod/Nestin-positive progenitor pool is largely quiescent and does not proliferate at adulthood. Moreover, neurogenesis (*neurod*:GFP/HuC/D-positive cells) is reduced to extremely low levels. This indicates that neurogenesis from the *neurod*:GFP-positive progenitor pool in the adult SAG is independent of proliferation of these cells. This hypothesis is further supported by the fact that we do see a low neurogenesis rate at adult stages when using GFP persistence in the *neurod*:GFP line combined with an antibody staining against HuC/D as a short-term lineage tracing, but have almost no newborn neurons labelled after a 28 day-lasting trace of proliferating cells with the BrdU lineage tracing approach at adult stages. In this context, exhaustion of the Neurod/Nestin-positive progenitor pool would be anticipated over time, which is in contrast to our findings in aged fish that still display the *neurod*:GFP-positive cell pool. Consequently, a replenishing source can be postulated. Indeed, a small population of proliferating but otherwise marker-negative cells is present: this feeds into the *neurod*:GFP-positive progenitor pool and also gives rise to neurons at a low but steady-state level at the adult stage. Taken together, the Neurod/Nestin-positive cells represent a pool of neural progenitors capable of differentiating into new neurons in the juvenile as well as in the adult SAG. This is actively maintained throughout life by a proliferating but otherwise marker-negative stem cell population.

It is currently unclear whether neurogenesis occurs exclusively via the Neurod/Nestin-positive progenitor pool or whether alternative mechanisms such as proliferation followed by direct differentiation into mature neurons without expression of NeuroD or Nestin in an intermediate progenitor are also present. In the zebrafish telencephalon, some neuronal progenitors are GFAP/S100B/Her4.3-positive radial glia cells (Chapouton et al., 2011; Ganz et al., 2010). However, in the SAG we only find expression of these glia markers in the medial portion of the PCTZ, presumably in the CNS. Hence, we consider it very unlikely that glia cells serve as an alternative source of new sensory neurons in the SAG. Similarly, Sox2-positive cells in the SAG are also only located in the region close to the PCTZ, which is in contrast to neonatal mice, in which Sox2-expressing glia cells are distributed evenly within the spiral ganglion (Meas et al., 2018a). Interestingly, in cranial and dorsal root ganglia, a neural-crest-derived population called boundary cap cells is involved in CNS-PNS boundary formation and is transiently found at the peripheral nerve entry/exit points during development (Maro et al., 2004; Niederlander and Lumsden, 1996). It has been shown in various studies that boundary cap cells are capable of differentiating into glia cells and sensory neurons of the PNS and therefore serve as neural progenitor cells (Gresset et al., 2015; Maro

Development (2020) 147, dev176750. doi:10.1242/dev.176750

et al., 2004). However, whether Sox2-expressing cells found in the adult SAG are related to boundary cap cells found in the PCTZ of other vertebrates, and whether these Sox2-positive cells have the capacity to serve as neuronal progenitor cells for sensory neurons in the SAG remains elusive.

Our findings are in line with the production rate of hair cells reported for the inner ear of adult zebrafish and other teleost species. Studies on hair cell and ganglion cell generation in *Astronotus* have shown that the average ratio of hair cells to afferent ganglion cells increases from 30:1 in small/younger fish to 300:1 in larger/older fish (Popper and Hoxter, 1984). Quantification of saccular hair cells in zebrafish aged 2 to 20 months revealed an increase from 2800 hair cells in 6-month-old zebrafish to almost 3600 hair cells in 10-month-old zebrafish (Higgs et al., 2002). The addition of ∼800 hair cells within 4 months corresponds to a hair cell production rate in the magnitude of, on average, 6.5 hair cells per day within the whole saccule. As one sensory neuron innervates multiple hair cells, our experiments revealing a proliferation rate of less than one sensory neuron per day in the anterior part of the adult SAG fit perfectly well to the known literature.

In summary, the neurogenic niche of the zebrafish SAG switches from a high neurogenesis rate at juvenile stages to a low level production at adulthood. As the number of *neurod*:GFP cells remains constant throughout juvenile and adult stages, we hypothesize that the neurogenic niche is not depleted over time but maintained throughout life.

It will be interesting to investigate whether the neurogenic niche can adapt and increase its activity after loss of mature neurons due to injury. Regeneration of hair cells is known to occur in various vertebrate species, except mammals (reviewed by Rubel et al., 2013). In zebrafish, studies on hair cell regeneration, especially on hair cells in neuromasts of the lateral line, have been carried out confirming the regenerative capacity of hair cells after injury. This raises the question of whether neurons, which can undergo secondary degeneration after hair cell loss or be injured directly by various other factors such as noise, ototoxic drugs or infections, are also capable of regeneration? In various mammalian species, application of the neurotoxin ouabain, a potent inhibitor of the Na^+/K^+-ATPase pump, results in degeneration of auditory neurons with no visible sign of regeneration (Fu et al., 2012; Lang et al., 2011; Schmiedt et al., 2002). In contrast, the adult zebrafish CNS displays robust regeneration after brain injury (Kaslin et al., 2017; Kroehne et al., 2011). Regeneration requires the maintenance of the neurogenic niche into adulthood. In the zebrafish cerebellum, the stem cell niche arises during embryonic development from the rhombic lip and consists of two distinct populations with either radial glia or neuro-epithelial-like identity (Kaslin et al., 2009). However, only the neuro-epithelial-like stem cell pool persists throughout life whereas the radial glia stem cells are terminated during juvenile stages. Consequently, neuronal cell lineages of the epithelial-like stem cell pool are replaced but cell lineages of the cerebellar radial glia do not regenerate (Kaslin et al., 2017). Although it is not clear whether the findings from the CNS can be directly transferred to the PNS, we would expect that the neurogenic niche in the adult zebrafish SAG contributes to regeneration because the niche is not terminated but rather maintained at adulthood.

Independent of that, understanding neurogenesis in the adult zebrafish SAG during homeostasis and potentially regeneration will be of particular importance because it can provide significant insights into the cellular properties of the progenitors and help in the identification of mechanisms to rekindle regeneration in the mammalian inner ear. Currently, reprogramming of resident cells within the auditory system is considered a promising way to cure hearing loss (Meas et al., 2018b). To this aim, glia cells of the eighth cranial ganglion have been reprogrammed *in vitro* into neuron-like cells that display a transcriptome profile resembling that of endogenous inner ear neurons (Noda et al., 2018). Although the results indicate that reprogramming of glia represents a viable strategy, targeting progenitor-like cells to re-initiate proliferation and differentiation might provide a valid alternative. As we have shown, Nestin is expressed in the progenitor cells within the neurogenic niche that gives rise to new neurons in the juvenile SAG and that is in a quiescent state in the adult zebrafish SAG. More importantly, the analysis of *nestin*:GFP transgenic mice revealed a reduced but persisting expression of Nestin in cells of the eighth cranial ganglion, indicating the persistence of progenitor-like cells in the mammalian auditory system (Chow et al., 2016). In conclusion, we provide the first in-depth characterization of the neurogenic niche in the juvenile and adult zebrafish, which might help in the identification of mechanisms to rekindle neurogenesis in the mammalian inner ear.

MATERIALS AND METHODS

Ethical statement

All animal experiments were conducted according to the guidelines and under supervision of the Regierungspräsidium Dresden (permits: TVV 79/2016; TVV 21/2018; TVA 1/2017). All efforts were made to minimize animal suffering and the number of animals used.

Plasmid construction and germline transformation

To create the pTol *nestin*:mCherry-T2A-CreER^{T2} plasmid, the 3932-bp upstream promoter region of *nestin* (Lam et al., 2009) was PCR amplified flanked by *Apa*I and *Fse*I restriction sites that allowed substitution of the *hsp70l* promoter of the pTol *hsp70l*:mCherryT2ACreER^{T2} plasmid (Hans et al., 2011). For germline transformation, plasmid DNA and transposase mRNA were injected into fertilized eggs (F0), raised to adulthood and crossed to AB wild-type fish as previously described (Kawakami et al., 2004). To identify the *Tg(nestin:mCherry-T2A-CreER^{T2})* driver line, F1 embryos were examined under a fluorescent microscope and positive embryos were raised. Two independent F0 founder fish were tested for recombination by crossing to *Tg(EF1α:loxP-DsRed2-loxP EGFP)* and application of 4-hydroxy-tamoxifen (4-OHT; Hans et al., 2009), but recombination was elicited in one line only, which was subsequently established *Tg(nestin:mCherry-T2A-CreER^{T2})tud45*.

Zebrafish husbandry and lines

Zebrafish were kept and bred according to standard procedures (Brand et al., 2002; Westerfield, 2000). Our experiments were carried out using juvenile (2 and 3 months old) and adult (6 months and older) zebrafish from wild-type stocks with the AB genetic background and transgenic lines as follows: *TgBAC(neurod1:EGFP)nl1* (known as *neurod*:GFP; Obholzer et al., 2008), *Tg(pou4f3:GAP-GFP)^{s356}* (known as *pou4f3*:GFP; Xiao et al., 2005), *Tg(her4.3:GFP)y83* (known as *her4.3*:GFP; Yeo et al., 2007), *TgBAC(nes:EGFP)tud100* (known as *nestin*:GFP; Kaslin et al., 2009), *Tg(hsp70l:loxP-DsRed2-loxP-nlsEGFP)tud9* (known as *hsp70l*:loxP-DsRed2-loxP-nlsEGFP; Knopf et al., 2011), *Tg(nestin:mCherry-T2A-CreER^{T2})tud45* (known as *nestin*:mCherry-T2A-CreER^{T2}; Fig. S4) and *Tg(sox2:sox2-P2a-GFP)stl84* (known as *sox2*:GFP; Shin et al., 2014). Besides date of birth and genotype, sex and body length were also measured from the tip of the mouth to the base of the caudal fin for every fish. Age and body length were used as staging criteria: the body length of 2-month-old fish varied from 15.5 mm to 19 mm, the body length of 3-month-old fish varied from 20 mm to 27 mm, and the body length of adult fish (6 months and older) varied from 27 mm to 34 mm (for detailed information see Table S1).

Bromodeoxyuridine (BrdU) pulse chase experiment

To label cells in S-phase of the cell cycle, transgenic *neurod*:GFP zebrafish were immersed for 24 h in 5 mM BrdU (Sigma-Aldrich) solution (modified

Development (2020) 147, dev176750. doi:10.1242/dev.176750

after Grandel et al., 2006). Therefore, BrdU was dissolved in E3 medium and the pH was adjusted to pH 7.2-7.4 using freshly prepared HEPES buffer. Depending on age and size of the fish, up to five fish were kept under oxygen supply in beakers containing 500 ml of the 5 mM BrdU solution. After 24 h, fish were kept in the fish facility for 0, 7, 15 and 28 days in case of the juvenile (3 months old) zebrafish and for 0, 7, 14 and 29 days in case of the adult (8 months old) zebrafish before fish were sacrificed for analysis.

Long-term lineage tracing

To trace *nestin*-derived cells in the SAG, *nestin*:mCherry-T2A-CreER^{T2} was crossed to the Cre-dependent reporter line *hsp70l*:loxP-DsRed2-loxP-nlsEGFP (see Fig. S4). Subsequently, 4-OHT (Sigma-Aldrich, H7904) and heat-shock treatments during embryonic stages were performed as previously described (Hans et al., 2011; Hans et al., 2009). Briefly, recombination was achieved by immersing embryos from 8 to 24 h post fertilization (hpf) in 0.5 µM 4-OHT in E3 medium. At 24 hpf, embryos were heat shocked at 37°C for 0.5 h and GFP-positive embryos were raised. At 6 months, zebrafish were placed in a heat-shock tank and heat shocked four times for 1 h at 37°C at 6 h intervals at 27°C between the heat shocks. Afterwards, zebrafish were sacrificed to analyze *nestin*-derived cells.

H&E staining

Wild-type zebrafish were sacrificed and the skull plate was carefully removed with forceps to enable better fixation of the otic tissue underneath the brain. Samples were fixed overnight in 4% paraformaldehyde in 0.1 M phosphate buffer (PB) (pH 7.5) at 4°C and then incubated for 2 days in 0.5 M EDTA in 0.1 M PB (pH 7.5) at 4°C, refreshing the solution after the first day. Afterwards, samples were washed twice in PBS and prepared for paraffin embedding, which was carried out using a paraffin infiltration processor (STP 420, Zeiss) according to the following programme: ddH_2O: 1×1 min; 50% ethanol (EtOH) 1×5 min; 70% EtOH 1×10 min; 96% EtOH 1×25 min; 96% EtOH 2×20 min; 100% EtOH 2×20 min; xylene 2×20 min; paraffin 3×40 min at 60°C; paraffin 1×60 min at 60°C. After dehydration and paraffin infiltration, samples were embedded using an Embedding Center EG1160 (Leica) and cut into 10 µm thick sections using an Ultracut microtome (Microm, HM 340E). Subsequently, samples were counterstained using H&E (Sigma-Aldrich).

Tissue preparation for immunohistochemistry

Experimental animals were sacrificed and the skull plate was carefully removed with forceps to enable better fixation of the otic tissue underneath the brain. Samples were fixed overnight in 4% paraformaldehyde in 0.1 M PB (pH 7.5) at 4°C and then incubated overnight in 20% sucrose/20% EDTA in 0.1 M PB (pH 7.5) for decalcification and cryoprotection. Subsequently, samples were embedded in 7.5% gelatin/20% sucrose and stored at −80°C. Samples were cut into 12 µm thick transverse sections using a Microm HM 560 Cryostat and stored at −20°C.

Immunohistochemistry

For immunohistochemistry, sections were post-fixed for 20-30 min with 100% ice cold methanol at room temperature. Afterwards, sections were washed once with PBS and three times with PBS containing 0.3% Triton X-100 (PBST×0.3%) and were incubated at 4°C overnight with primary antibodies in PBST×0.3% (see Table S2). Next day, sections were washed three times with PBST×0.3% before incubation with Alexa 488-, 555- and 633-conjugated secondary antibodies (ThermoFisherScientific, see Table S2) in PBST×0.3% for 2 h at room temperature. Then, 4,6-diamidino-2-phenylindole (DAPI, 1 µg/ml, Invitrogen) was added to the secondary antibodies to counterstain nuclei. Sections were washed again three times with PBST×0.3% and once with PBS and were mounted in 70% glycerol/PBS.

Modifications for PCNA and HuC/D staining

For immunohistochemistry against PCNA and HuC/D, an antigen retrieval was performed before incubation with primary antibodies. Therefore, slides were incubated in 85-95°C preheated sodium citrate buffer (pH 6) (10 mM) for 15 min, followed by a 10 min cool down in the heated sodium citrate buffer at room temperature.

Modifications for Sox2 staining

For immunohistochemistry against Sox2, an antigen retrieval was performed before incubation with primary antibodies. Therefore, slides were incubated in 99°C preheated sodium citrate buffer (pH 6) (10 mM) for 10 min, followed by a 10 min cool down in the heated sodium citrate buffer at room temperature.

Modifications for BrdU staining

As samples were co-stained for *neurod*:GFP, BrdU and HuC/D, and BrdU and HuC/D both require different antigen retrieval, immunohistochemistry was performed sequentially. First, samples were stained for *neurod*:GFP and HuC/D as described above, without adding DAPI, while incubating with the secondary antibodies. Instead of mounting, samples were washed again with PBST×0.3% and afterwards slides were incubated for 13 min at 37°C in preheated 2 M HCl to retrieve the antigenicity of BrdU. Afterwards, slides were washed for 10 min in tetraborate buffer and then with PBST×0.3%. Slides were incubated with primary antibody against BrdU overnight at 4°C, washed with PBST×0.3%, incubated with all secondary antibodies plus DAPI for 2 h at room temperature, and then washed again and mounted as described above.

Image acquisition

Images were taken in the light microscopy facility of the Center for Molecular and Cellular Bioengineering (CMCB) technology platform with either a ZEISS Axio Imager upright microscope with Zeiss Plan-Apochromat 10×0.45, 20×0.8 and 40×0.95 korr objectives for magnification, or a Zeiss Axiovert 200 M inverted microscope with Zeiss Plan-Neofluar 10×0.30 and Zeiss Plan-Apochromat 20×0.8 or 40×0.95 korr objectives for magnification. An Axiocam MRm (1388×1040, 6.45×6.45 µm, b/w) or an Axiocam MRc (1388×1040 pixel, 6.45×6.45 µm, colour) was used for detection. Sequential image acquisition was used in samples co-stained with multiple fluorophores. For imaging, *z*-stacks were acquired to cover the full information in all three dimensions (typically 5-25 *z*-planes with an interval of 0.4-1.5 µm depending on the numerical aperture of the objective). Images were processed using ZEN blue 2012 and Fiji. Close-up images were generated from the original overview image. For overview images, a maximum projection was taken from several *z*-planes, whereas only 2-3 *z*-planes were used for the close-up images. Figures were assembled using Adobe Illustrator CS5.

Quantification and statistical analysis

Quantification of HuC/D-positive neurons in juvenile (2 month) and adult (8 month) zebrafish was carried out using the ZEISS Axio Imager upright microscope. Every HuC/D-positive cell in the entire anterior part of both SAGs, as well as every section containing HuC/D-positive cells, were counted on consecutive 12 µm thick sections, starting with the first section containing a HuC/D-positive cell and ending with the last section of the anterior part of the SAG (for detailed numbers, see Table S3). From these values, the overall number of HuC/D-positive neurons, the average number of HuC/D-positive neurons per section, the section with the highest number of HuC/D-positive neurons as well as the thickness of the anterior part of the SAG containing HuC/D-positive neurons were calculated. Values from the right and from the left SAG of one fish were averaged, resulting in one value per category and fish. In total, four fish were analyzed for both time points (n=4). For every other experiment, quantification was performed on acquired images comprising all *z*-planes using Fiji software. Therefore, one SAG per fish (either left or right side, depending on sample quality) was analyzed. To analyze the neurogenic niche, a square covering the neurogenic area and the surrounding cells was chosen as the region of interest (see overview images in Fig. 3A, Fig. 4B and Fig. 5B: size of square: 132 mm^2). For the proliferation analysis, cells were counted on 12 consecutive 12 µm thick sections (for detailed numbers, see Table S4). If a section was damaged, it was excluded from the analysis and less than twelve sections were taken into account. All values from one fish were averaged and the mean cell count/section was used for statistical analysis (in total: n=5 for the 2 month time point; n=3 for the 3 month time point; n=4 for the 8 month time point). For BrdU pulse chase experiments, cells were counted on either five or 12 consecutive 12 µm thick sections (if possible, see above). In the case of all BrdU-positive cells, the average cell numbers/

Development (2020) 147, dev176750. doi:10.1242/dev.176750

section for each fish, four fish per time point for the experiment with juvenile fish and four to five fish for the experiment with adult fish (time point: 0/7/14 days post treatment n=5; time point: 29 days post treatment n=4), was calculated and used for statistical analysis (for detailed numbers, see Tables S5 and S6). For all other analysis, the average cell number/section for each fish was taken to calculate either the percentage of the specific cell group of all BrdU-positive cells (on a total of twelve sections) or the percentage of the specific cell group of all cells within that group of cell type, e.g. *neurod*:GFP/BrdU-positive cells per *neurod*:GFP-positive cell or HuC/D/BrdU-positive cells per HuC/D-positive cell (on a total of five sections). The corresponding percentage values, one per fish and cell group, were used for further analysis. For the *nestin* lineage tracing experiment, the number of HuC/D-positive and HuC/D/GFP-double-positive cells (derived from recombined *nestin*:mCherry-T2A-CreER^{T2} cells) as well as the percentage of recombined HuC/D/GFP-double-positive cells from all HuC/D-positive cells was quantified in the whole SAG on 12 consecutive 12 µm thick sections from three fish (where possible, see above; for detailed numbers, see Table S7). For statistical analysis the GraphPad Prism software was used to determine P-values with a one-way ANOVA test with a Tukey's Multiple Comparison Test for post hoc analysis. Chosen significance levels are ***$P\leq0.001$, **$P\leq0.01$, *$P\leq0.05$; values above $P>0.05$ are not considered significant; data are presented as mean±s.e.m.

In situ hybridization

Probe synthesis and *in situ* hybridization was essentially carried out as previously described (Westerfield, 2000). The following cDNA probes were used to detect expression: *neurod* (Andermann et al., 2002), *gfp* (Hans and Campos-Ortega, 2002), *nestin* (Mahler and Driever, 2007), *mCherry* and *CreER^{T2}* (Hans et al., 2011).

SAG dissection

Before dissection, experimental animals were sacrificed and placed on their ventral side in a Petri dish on ice. Initially, the skull plate was carefully removed using forceps. After cutting through the brain between optic tectum and cerebellum with dissection scissors, the entire anterior part of the brain including olfactory bulb, telencephalon and optic tectum was carefully removed. The cerebellum was carefully pushed to the side to localize the anterior part of SAG laying underneath the lapillus (otolith of the utricular macula). Both SAGs were cut at a 50-60° angle from the frontal plane including the medial parts of the SAG entering the brain. Afterwards, the brain was cut posterior of the brain stem and the brain was completely removed, so that the posterior parts of the inner ear also came into sight. The anterior part of the SAG, attached to the utricular macula and semicircular canals, was collected using forceps to grab the otolith within the utricle and carefully lift out the utricular macula, parts of the adjacent semicircular canals and the anterior SAG. The lapillus was removed from the utricular macula either before or after taking out the anterior part of the inner ear. If possible, parts of the posterior SAG were also collected and otoliths were removed from the posterior part of the inner ear. All dissected tissue was placed into an Eppendorf tube and stored on ice. In total, tissue from either eight male or eight female adult *Tg(neurod:GFP)* fish were pooled, generating two samples (male and female) with the tissue from 16 SAGs each. The whole dissection procedure did not take longer than 1:15 h to minimize the degree of tissue degradation.

Cell dissociation

To dissociate the inner ear tissue including the SAG, the Neural Tissue Dissociation Kit (*P*) (Miltenyi Biotec) was used, with some modifications to the manufacturer's protocol. After a primary enzymatic dissociation step in preheated enzyme mix 1 for 15 min at 28°C, enzyme mix 2 was added to stop enzymatic dissociation. Subsequently, samples were further sheared mechanically by carefully pipetting samples up and down through fire-polished glass Pasteur pipettes (230 mm). Four different opening sizes were used, starting with the pipette with the widest opening, and additional incubation steps at 28°C were carried out between changing from a pipette with a wide opening to one with a smaller opening. The acquired cell suspension was filtered drop wise through a Hanks' Balanced Salt Solution (HBSS; without Ca^{2+} and Mg^{2+})-equilibrated 70 µm cell strainer, collected in HBSS and the cell strainer was washed once with 5 ml HBSS. After centrifugation of the cell suspension for 15 min at 300 ***g*** and 4°C, the supernatant was removed and cells were resuspended in ∼400 µl fresh HBSS and stored on ice.

Fluorescence-activated cell sorting (FACS) of cells derived from the SAG

Calcein Violet at a final concentration of 8 µM was added to the cell suspension before FACS to distinguish live from dead cells. FACS was performed with the help of the Flow Cytometry Core Facility of the CMCB technology platform using a BD FACSAria III system. A total of 250 single live *neurod*:GFP-positive cells and 300 single live wild-type cells were sorted into PCR tubes and kept on ice.

Analysis of gene expression in *neurod*:GFP-positive cells

To analyze gene expression of *neurod* and *nestin*, RNA isolation and cDNA synthesis including an RNA amplification step from sorted *neurod*:GFP-positive cells as well as a wild-type negative control was performed by the deep sequencing facility of the CMCB technology platform. Primers (see Table S8) were designed in a way that primers were either located in two neighbouring exons (*neurod*) or that one primer was exon-junction spanning (*nestin* forward primer) and the corresponding primer was located in the neighbouring exon (*nestin* reverse primer) to exclude amplification of amplicons derived from genomic DNA. PCR was performed with both samples (*neurod*:GFP-positive male, *neurod*:GFP-positive female) and a genomic DNA (gDNA) sample as a negative control. We used 40 PCR cycles (30 s/94°C denaturation, 30 s/59°C annealing, 30 s/72°C elongation) and the amplification products were separated on a 2% agarose gel.

Acknowledgements

We thank Drs U. Strähle and N. Ninov for sharing reagents and M. Fischer, J. Michling and D. Mögel for excellent zebrafish care. In addition, we thank Dr M. Brand and the members of his laboratory for continued support and discussions as well as helpful comments on the manuscript. This work was supported by the Light Microscopy Facility, a core facility of the CMCB at the Technische Universität Dresden.

Competing interests

The authors declare no competing or financial interests.

Author contributions

Conceptualization: S.S., S.H.; Formal analysis: S.S.; Investigation: S.S., N.A., O.B., J.C., V.K., J.K., S.H.; Resources: J.K., S.H.; Writing - original draft: S.S., S.H.; Writing - review & editing: S.S., N.A., O.B., V.K., J.K., S.H.; Supervision: S.H.; Funding acquisition: S.H.

Funding

Funding was provided by the Deutsche Forschungsgemeinschaft (HA 6362/1-1) and the Technische Universität Dresden.

Supplementary information

Supplementary information available online at
http://dev.biologists.org/lookup/doi/10.1242/dev.176750.supplemental

References

Andermann, P., Ungos, J. and Raible, D. W. (2002). Neurogenin1 defines zebrafish cranial sensory ganglia precursors. *Dev. Biol.* **251**, 45-58. doi:10.1006/dbio.2002.0820

Bang, P. I., Sewell, W. F. and Malicki, J. J. (2001). Morphology and cell type heterogeneities of the inner ear epithelia in adult and juvenile zebrafish (Danio rerio). *J. Comp. Neurol.* **438**, 173-190. doi:10.1002/cne.1308

Barald, K. F. and Kelley, M. W. (2004). From placode to polarization: new tunes in inner ear development. *Development* **131**, 4119-4130. doi:10.1242/dev.01339

Bermingham, N. A., Hassan, B. A., Price, S. D., Vollrath, M. A., Ben-Arie, N., Eatock, R. A., Bellen, H. J., Lysakowski, A. and Zoghbi, H. Y. (1999). Math1: an essential gene for the generation of inner ear hair cells. *Science* **284**, 1837-1841. doi:10.1126/science.284.5421.1837

Bever, M. M. and Fekete, D. M. (2002). Atlas of the developing inner ear in zebrafish. *Dev. Dyn.* **223**, 536-543. doi:10.1002/dvdy.10062

Bojrab, D., Zhang, B., Jiang, H., Zhang, L., Cohen, D. S., Luo, X. and Hu, Z. (2017). Expression of oligodendrocyte marker during peripheral-central

transitional zone formation of the postnatal mouse cochlear nerve. *Otolaryngol. Head Neck Surg.* **157**, 488-492. doi:10.1177/0194599817718806

Brand, M., Granato, M., Nüsslein-Volhard, C. (2002). Keeping and raising zebrafish. *In Zebrafish, A Practical Approach* (ed. C. Nüsslein-Volhard and R. Dahm), pp. 7-37. Oxford: Oxford University Press.

Chapouton, P., Webb, K. J., Stigloher, C., Alunni, A., Adolf, B., Hesl, B., Topp, S., Kremmer, E. and Bally-Cuif, L. (2011). Expression of Hairy/enhancer of split genes in neural progenitors and neurogenesis domains of the adult zebrafish brain. *J. Comp. Neurol.* **519**, 1748-1769. doi:10.1002/cne.22599

Chow, C. L., Trivedi, P., Pyle, M. P., Matulle, J. T., Fettiplace, R. and Gubbels, S. P. (2016). Evaluation of nestin expression in the developing and adult mouse inner ear. *Stem Cells Dev.* **25**, 1419-1432. doi:10.1089/scd.2016.0176

Corwin, J. and Cotanche, D. (1988). Regeneration of sensory hair cells after acoustic trauma. *Science* **240**, 1772-1774. doi:10.1126/science.3381100

Cowan, W., Fawcett, J., O'Leary, D. and Stanfield, B. (1984). Regressive events in neurogenesis. *Science* **225**, 1258-1265. doi:10.1126/science.6474175

Fraher, J. P. (1999). The transitional zone and CNS regeneration. *J. Anat.* **194**, 161-182. doi:10.1046/j.1469-7580.1999.19420161.x

Fraher, J. P. and Delanty, F. J. (1987). The development of the central-peripheral transitional zone of the rat cochlear nerve. A light microscopic study. *J. Anat.* **155**, 109-118.

Fritzsch, B. and Elliott, K. L. (2017). Gene, cell, and organ multiplication drives inner ear evolution. *Dev. Biol.* **431**, 3-15. doi:10.1016/j.ydbio.2017.08.034

Fu, Y., Ding, D., Jiang, H. and Salvi, R. (2012). Ouabain-induced cochlear degeneration in rat. *Neurotox. Res.* **22**, 158-169. doi:10.1007/s12640-012-9320-0

Furman, A. C., Kujawa, S. G. and Liberman, M. C. (2013). Noise-induced cochlear neuropathy is selective for fibers with low spontaneous rates. *J. Neurophysiol.* **110**, 577-586. doi:10.1152/jn.00164.2013

Ganz, J., Kaslin, J., Hochmann, S., Freudenreich, D. and Brand, M. (2010). Heterogeneity and Fgf dependence of adult neural progenitors in the zebrafish telencephalon. *Glia* **58**, 1345-1363. doi:10.1002/glia.21012

Grandel, H., Kaslin, J., Ganz, J., Wenzel, I. and Brand, M. (2006). Neural stem cells and neurogenesis in the adult zebrafish brain: origin, proliferation dynamics, migration and cell fate. *Dev. Biol.* **295**, 263-277. doi:10.1016/j.ydbio.2006.03.040

Gresset, A., Coulpier, F., Gerschenfeld, G., Jourdon, A., Matesic, G., Richard, L., Vallat, J.-M., Charnay, P. and Topilko, P. (2015). Boundary caps give rise to neurogenic stem cells and terminal glia in the skin. *Stem Cell Reports* **5**, 278-290. doi:10.1016/j.stemcr.2015.06.005

Haddon, C. and Lewis, J. (1996). Early ear development in the embryo of the Zebrafish, Danio rerio. *J. Comp. Neurol.* **365**, 113-128. doi:10.1002/(SICI)1096-9861(19960129)365:1<113::AID-CNE9>3.0.CO;2-6

Hagey, D. W., Klum, S., Kurtsdotter, I., Zaouter, C., Topcic, D., Andersson, O., Bergsland, M. and Muhr, J. (2018). SOX2 regulates common and specific stem cell features in the CNS and endoderm derived organs. *PLoS Genet.* **14**, e1007224. doi:10.1371/journal.pgen.1007224

Hans, S. and Campos-Ortega, J. A. (2002). On the organisation of the regulatory region of the zebrafish deltaD gene. *Development* **129**, 4773-4784.

Hans, S., Kaslin, J., Freudenreich, D. and Brand, M. (2009). Temporally-controlled site-specific recombination in Zebrafish. *PLoS ONE* **4**, e4640. doi:10.1371/journal.pone.0004640

Hans, S., Freudenreich, D., Geffarth, M., Kaslin, J., Machate, A. and Brand, M. (2011). Generation of a non-leaky heat shock–inducible Cre line for conditional Cre/lox strategies in zebrafish. *Dev. Dyn.* **240**, 108-115. doi:10.1002/dvdy.22497

Higgs, D. M., Souza, M. J., Wilkins, H. R., Presson, J. C. and Popper, A. N. (2002). Age- and size-related changes in the inner ear and hearing ability of the adult zebrafish (Danio rerio). *J. Assoc. Res. Otolaryngol.* **3**, 174-184. doi:10.1007/s101620020035

Hu, Z. (2013). Formation of the peripheral-central transitional zone in the postnatal mouse cochlear nerve. *Otolaryngol. Head Neck Surg.* **149**, 296-300. doi:10.1177/0194599813489663

Hu, Z., Zhang, B., Luo, X., Zhang, L., Wang, J., Bojrab, D. and Jiang, H. (2014). The astroglial reaction along the mouse cochlear nerve following inner ear damage. *Otolaryngol. Head Neck Surg.* **150**, 121-125. doi:10.1177/0194599813512097

Kaslin, J., Ganz, J., Geffarth, M., Grandel, H., Hans, S. and Brand, M. (2009). Stem cells in the adult zebrafish cerebellum: initiation and maintenance of a novel stem cell niche. *J. Neurosci.* **29**, 6142-6153. doi:10.1523/JNEUROSCI.0072-09.2009

Kaslin, J., Kroehne, V., Ganz, J., Hans, S. and Brand, M. (2017). Distinct roles of neuroepithelial-like and radial glia-like progenitor cells in cerebellar regeneration. *Development* **144**, 1462-1471. doi:10.1242/dev.144907

Kawakami, K., Takeda, H., Kawakami, N., Kobayashi, M., Matsuda, N. and Mishina, M. (2004). A transposon-mediated gene trap approach identifies developmentally regulated genes in Zebrafish. *Dev. Cell* **7**, 133-144. doi:10.1016/j.devcel.2004.06.005

Kiernan, A. E., Pelling, A. L., Leung, K. K. H., Tang, A. S. P., Bell, D. M., Tease, C., Lovell-Badge, R., Steel, K. P. and Cheah, K. S. E. (2005). Sox2 is required for sensory organ development in the mammalian inner ear. *Nature* **434**, 1031-1035. doi:10.1038/nature03487

Kim, W. Y., Fritzsch, B., Serls, A., Bakel, L. A., Huang, E. J., Reichardt, L. F., Barth, D. S. and Lee, J. E. (2001). NeuroD-null mice are deaf due to a severe loss of the inner ear sensory neurons during development. *Development* **128**, 417-426.

Knopf, F., Hammond, C., Chekuru, A., Kurth, T., Hans, S., Weber, C. W., Mahatma, G., Fisher, S., Brand, M., Schulte-Merker, S. et al. (2011). Bone regenerates via dedifferentiation of osteoblasts in the Zebrafish fin. *Dev. Cell* **20**, 713-724. doi:10.1016/j.devcel.2011.04.014

Kroehne, V., Freudenreich, D., Hans, S., Kaslin, J. and Brand, M. (2011). Regeneration of the adult zebrafish brain from neurogenic radial glia-type progenitors. *Development* **138**, 4831-4841. doi:10.1242/dev.072587

Ladher, R. K. (2017). Changing shape and shaping change: inducing the inner ear. *Semin. Cell Dev. Biol.* **65**, 39-46. doi:10.1016/j.semcdb.2016.10.006

Lam, C. S., März, M. and Strähle, U. (2009). gfap and nestin reporter lines reveal characteristics of neural progenitors in the adult zebrafish brain. *Dev. Dyn.* **238**, 475-486. doi:10.1002/dvdy.21853

Lang, H., Li, M., Kilpatrick, L. A., Zhu, J., Samuvel, D. J., Krug, E. L. and Goddard, J. C. (2011). Sox2 up-regulation and glial cell proliferation following degeneration of spiral ganglion neurons in the adult mouse inner ear. *J. Assoc. Res. Otolaryngol.* **12**, 151-171. doi:10.1007/s10162-010-0244-1

Li, H., Liu, H. and Heller, S. (2003). Pluripotent stem cells from the adult mouse inner ear. *Nat. Med.* **9**, 1293-1299. doi:10.1038/nm925

Liberman, M. (2017). Noise-induced and age-related hearing loss: new perspectives and potential therapies [version 1; referees: 4 approved]. *F1000Res.* **6**, 927. doi:10.12688/f1000research.11310.1

Lindsey, B. W., Hall, Z. J., Heuzé, A., Joly, J.-S., Tropepe, V. and Kaslin, J. (2018). The role of neuro-epithelial-like and radial-glial stem and progenitor cells in development, plasticity, and repair. *Prog. Neurobiol.* **170**, 99-114. doi:10.1016/j.pneurobio.2018.06.004

Ma, Q., Chen, Z., Barrantes, I. d. B., Luis de la Pompa, J. and Anderson, D. J. (1998). Neurogenin1 is essential for the determination of neuronal precursors for proximal cranial sensory ganglia. *Neuron* **20**, 469-482. doi:10.1016/S0896-6273(00)80988-5

Mahler, J. and Driever, W. (2007). Expression of the zebrafish intermediate neurofilament Nestin in the developing nervous system and in neural proliferation zones at postembryonic stages. *BMC Dev. Biol.* **7**, 89. doi:10.1186/1471-213X-7-89

Maro, G. S., Vermeren, M., Voiculescu, O., Melton, L., Cohen, J., Charnay, P. and Topilko, P. (2004). Neural crest boundary cap cells constitute a source of neuronal and glial cells of the PNS. *Nat. Neurosci.* **7**, 930-938. doi:10.1038/nn1299

Meas, S. J., Nishimura, K., Scheibinger, M. and Dabdoub, A. (2018a). In vitro methods to cultivate spiral ganglion cells, and purification of cellular subtypes for induced neuronal reprogramming. *Front. Neurosci.* **12**, 822-822. doi:10.3389/fnins.2018.00822

Meas, S. J., Zhang, C.-L. and Dabdoub, A. (2018b). Reprogramming glia into neurons in the peripheral auditory system as a solution for sensorineural hearing loss: lessons from the central nervous system. *Front. Mol. Neurosci.* **11**, 77. doi:10.3389/fnmol.2018.00077

Münzel, E. J., Schaefer, K., Obirei, B., Kremmer, E., Burton, E. A., Kuscha, V., Becker, C. G., Brüsamle, C., Williams, A. and Becker, T. (2012). Claudin k is specifically expressed in cells that form myelin during development of the nervous system and regeneration of the optic nerve in adult zebrafish. *Glia* **60**, 253-270. doi:10.1002/glia.21260

Niederlander, C. and Lumsden, A. (1996). Late emigrating neural crest cells migrate specifically to the exit points of cranial branchiomotor nerves. *Development* **122**, 2367-2374.

Noda, T., Meas, S. J., Nogami, J., Amemiya, Y., Uchi, R., Ohkawa, Y., Nishimura, K. and Dabdoub, A. (2018). Direct reprogramming of spiral ganglion non-neuronal cells into neurons: toward ameliorating sensorineural hearing loss by gene therapy. *Front. Cell Dev. Biol.* **6**, 16. doi:10.3389/fcell.2018.00016

Obholzer, N., Wolfson, S., Trapani, J. G., Mo, W., Nechiporuk, A., Busch-Nentwich, E., Seiler, C., Sidi, S., Söllner, C., Duncan, R. N. et al. (2008). Vesicular glutamate transporter 3 is required for synaptic transmission in zebrafish hair cells. *J. Neurosci.* **28**, 2110-2118. doi:10.1523/JNEUROSCI.5230-07.2008

Oppenheim, R. W. (1991). Cell death during development of the nervous system. *Annu. Rev.* **14**, 453-501. doi:10.1146/annurev.ne.14.030191.002321

Pinzon-Olejua, A., Welte, C., Chekuru, A., Bosak, V., Brand, M., Hans, s. and Stuerme, C. A. (2007). Cre-inducible site-specific recombination in zebrafish oligodendrocytes. *Dev. Dyn.* **246**, 41-49. doi:10.1002/dvdy.24458

Popper, A. N. and Hoxter, B. (1984). Growth of a fish ear: 1. Quantitative analysis of hair cell and ganglion cell proliferation. *Hear. Res.* **15**, 133-142. doi:10.1016/0378-5955(84)90044-3

Retzius, G. (1872). Anatomische Untersuchungen. Studien über den Bau des Gehörlabyrinthes. I. Das Gehörorgan der Knochenfische. Klemmings Antiquariat, Stockholm.

Rubel, E. W., Furrer, S. A. and Stone, J. S. (2013). A brief history of hair cell regeneration research and speculations on the future. *Hear. Res.* **297**, 42-51. doi:10.1016/j.heares.2012.12.014

Ryals, B. and Rubel, E. (1988). Hair cell regeneration after acoustic trauma in adult Coturnix quail. *Science* **240**, 1774-1776. doi:10.1126/science.3381101

Santi, P. A., Johnson, S. B., Hillenbrand, M., Grandpre, P. Z., Glass, T. J. and Leger, J. R. (2009). Thin-sheet laser imaging microscopy for optical sectioning of thick tissues. *BioTechniques* **46**, 287-294. doi:10.2144/000113087

Sapède, D. and Pujades, C. (2010). Hedgehog signaling governs the development of otic sensory epithelium and its associated innervation in zebrafish. *J. Neurosci.* **30**, 3612-3623. doi:10.1523/JNEUROSCI.5109-09.2010

Sapède, D., Dyballa, S. and Pujades, C. (2012). Cell lineage analysis reveals three different progenitor pools for neurosensory elements in the otic vesicle. *J. Neurosci.* **32**, 16424-16434. doi:10.1523/JNEUROSCI.3686-12.2012

Schmiedt, R. A., Okamura, H.-O., Lang, H. and Schulte, B. A. (2002). Ouabain application to the round window of the gerbil cochlea: a model of auditory neuropathy and apoptosis. *J. Assoc. Res. Otolaryngol.* **3**, 223-233. doi:10.1007/s1016200220017

Schuck, J. B. and Smith, M. E. (2009). Cell proliferation follows acoustically-induced hair cell bundle loss in the zebrafish saccule. *Hear. Res.* **253**, 67-76. doi:10.1016/j.heares.2009.03.008

Schwander, M., Kachar, B. and Müller, U. (2010). Review series: the cell biology of hearing. *J. Cell Biol.* **190**, 9-20. doi:10.1083/jcb.201001138

Seal, R. P., Akil, O., Yi, E., Weber, C. M., Grant, L., Yoo, J., Clause, A., Kandler, K., Noebels, J. L., Glowatzki, E. et al. (2008). Sensorineural deafness and seizures in mice lacking vesicular glutamate transporter 3. *Neuron* **57**, 263-275. doi:10.1016/j.neuron.2007.11.032

Shin, J., Chen, J. and Solnica-Krezel, L. (2014). Efficient homologous recombination-mediated genome engineering in zebrafish using TALE nucleases. *Development* **141**, 3807-3818. doi:10.1242/dev.108019

Stone, J. S. and Rubel, E. W. (2000). Temporal, spatial, and morphologic features of hair cell regeneration in the avian basilar papilla. *J. Comp. Neurol.* **417**, 1-16. doi:10.1002/(SICI)1096-9861(20000131)417:1<1::AID-CNE1>3.0.CO;2-E

Torper, O. and Götz, M. (2017). Chapter 3 - Brain repair from intrinsic cell sources: turning reactive glia into neurons. In *Progress in Brain Research* (ed. S. B. Dunnett and A. Björklund), pp. 69-97. Elsevier.

Trevarrow, B., Marks, D. L. and Kimmel, C. B. (1990). A Organization of hindbrain segments in the zebrafish embryo. *Neuron* **4**, 669-679. doi:10.1016/0896-6273(90)90194-k

Vemaraju, S., Kantarci, H., Padanad, M. S. and Riley, B. B. (2012). A spatial and temporal gradient of Fgf differentially regulates distinct stages of neural development in the zebrafish inner ear. *PLoS Genet.* **8**, e1003068. doi:10.1371/journal.pgen.1003068

Wang, J., Zhang, B., Jiang, H., Zhang, L., Liu, D., Xiao, X., Ma, H., Luo, X., Bojrab, D., II and Hu, Z. (2013). Myelination of the postnatal mouse cochlear nerve at the peripheral-central nervous system transitional zone. *Front. Pediatr.* **1**, 43-43. doi:10.3389/fped.2013.00043

Waterman, R. E. and Bell, D. H. (1984). Epithelial fusion during early semicircular canal formation in the embryonic zebrafish, Brachydanio rerio. *Anat. Rec.* **210**, 101-114. doi:10.1002/ar.1092100113

Westerfield, M. (2000). *The Zebrafish Book. A Guide for the Laboratory Use of Zebrafish (Danio rerio)*, 4th edn. Eugene: Univ. of Oregon Press.

Wiese, C., Rolletschek, A., Kania, G., Blyszczuk, P., Tarasov, K. V., Tarasova, Y., Wersto, R. P., Boheler, K. R. and Wobus, A. M. (2004). Nestin expression – a property of multi-lineage progenitor cells? *Cell. Mol. Life Sci. CMLS* **61**, 2510-2522. doi:10.1007/s00018-004-4144-6

Xiao, T., Roeser, T., Staub, W. and Baier, H. (2005). A GFP-based genetic screen reveals mutations that disrupt the architecture of the zebrafish retinotectal projection. *Development* **132**, 2955-2967. doi:10.1242/dev.01861

Yeo, S.-Y., Kim, M., Kim, H.-S., Huh, T.-L. and Chitnis, A. B. (2007). Fluorescent protein expression driven by her4 regulatory elements reveals the spatiotemporal pattern of Notch signaling in the nervous system of zebrafish embryos. *Dev. Biol.* **301**, 555-567. doi:10.1016/j.ydbio.2006.10.020

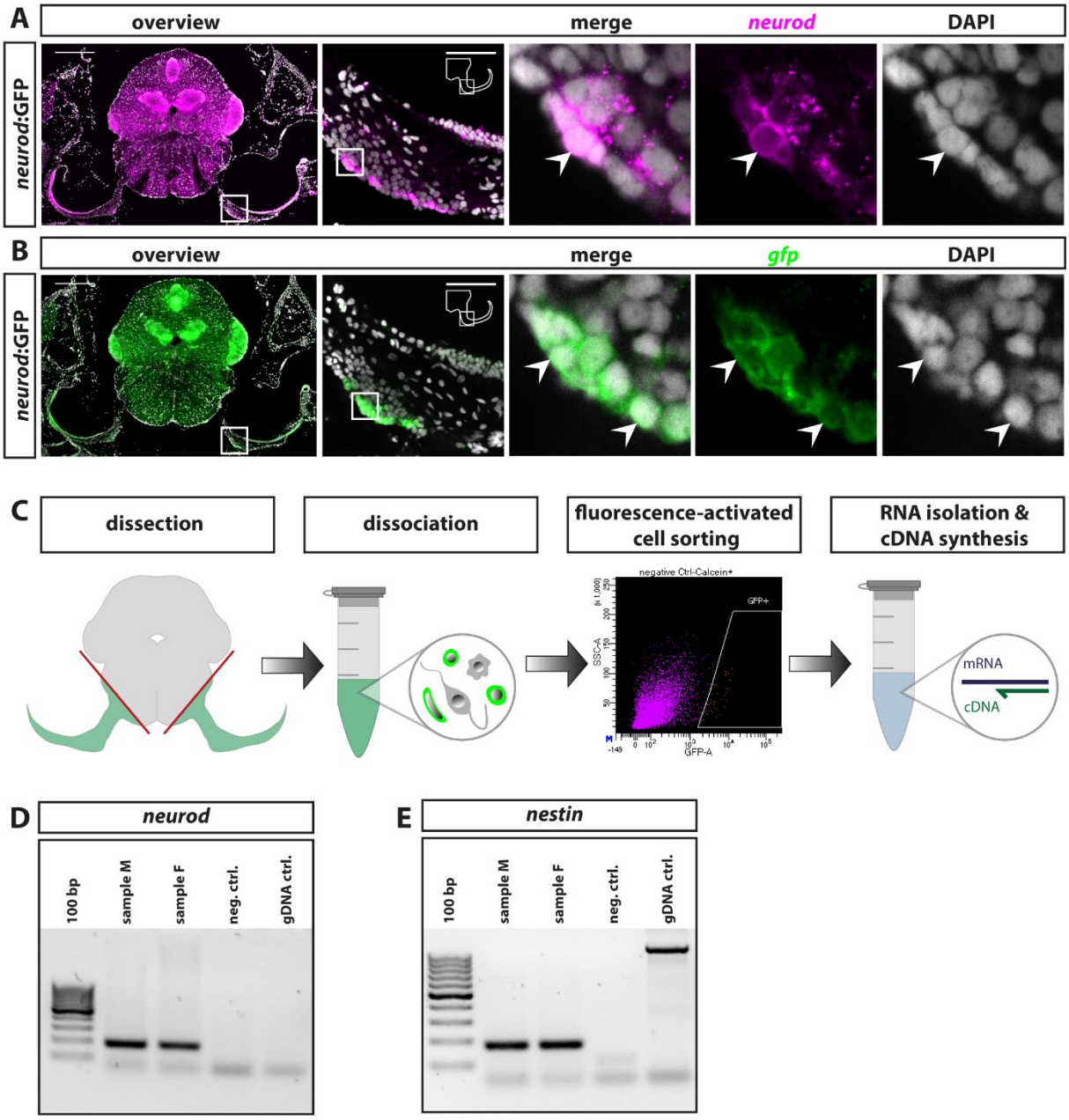

Fig. S1: *Tg(neurod:GFP)* faithfully recapitulates endogenous *neurod* expression in the zebrafish SAG. (**A,B**) *in situ* hybridization against *neurod* (**A**) and *gfp* (**B**) on a series of SAG sections from adult, transgenic *Tg(neurod:GFP)* fish shows expression of *neurod* and *gfp* in the same cell population. (**C**) Scheme depicting the workflow of SAG dissection, dissociation, fluorescence-activated cell sorting, RNA-isolation and cDNA synthesis to analyze the expression of *neurod* and *nestin* in the pool of *neurod*:GFP-positive progenitor cells. (**D,E**) PCR for *neurod* (**D**) and *nestin* (**E**) on cDNA obtain from *neurod*:GFP-positive cells isolated from the adult SAG of male (sample M) and female (sample F) *Tg(neurod:GFP)* transgenic fish further confirms expression of *neurod* and *nestin* in the adult zebrafish SAG; lanes from the left to the right: 100 base pair ladder; sample M; sample F; negative control w/o DNA; negative control with genomic DNA (gDNA). Scale bar overview: 300 µm, scale bar close-up: 50 µm; cross sections showing dorsal to the top and lateral to the right.

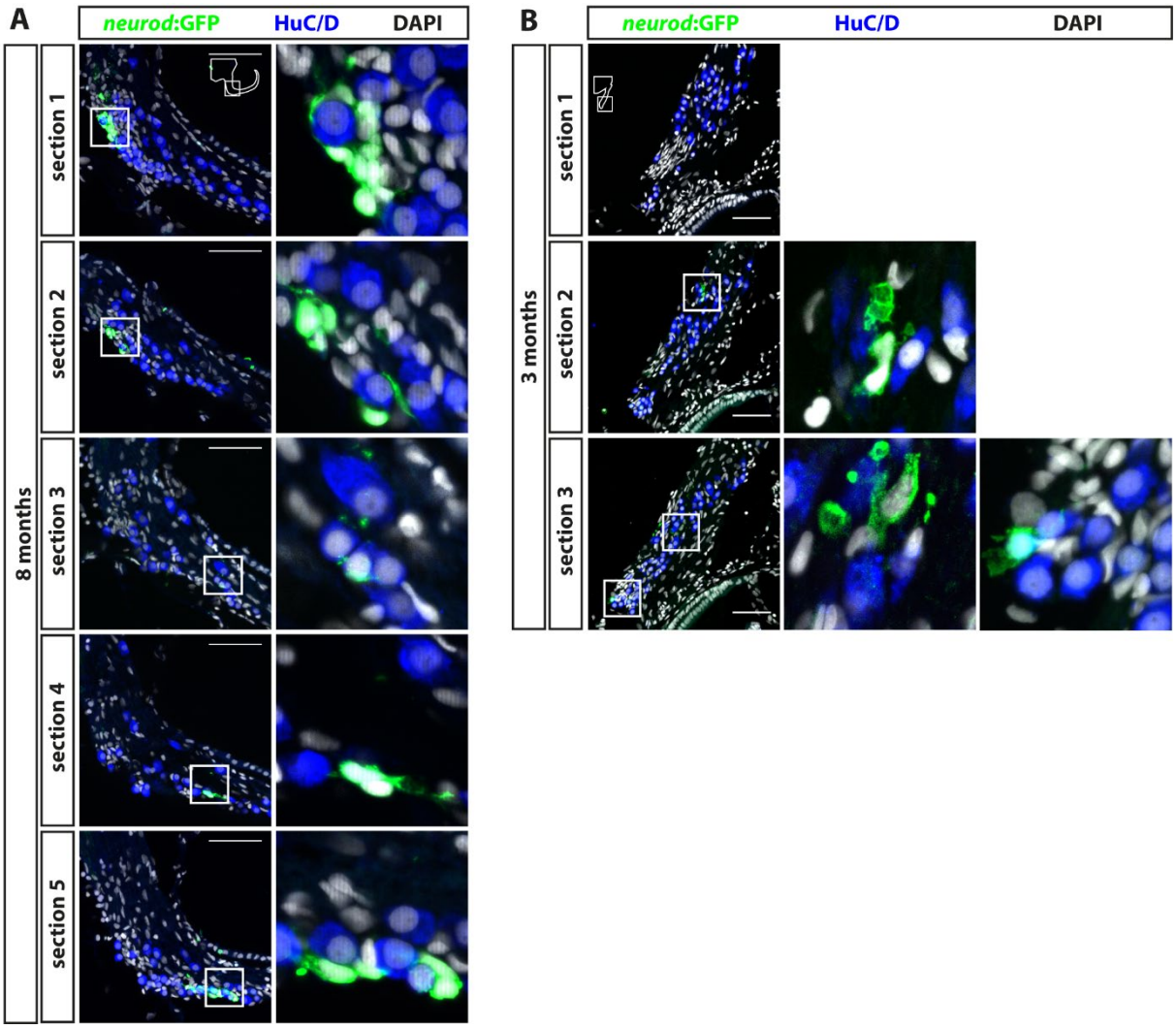

Fig. S2: Dispersed groups of *neurod*:GFP-positive cells reside at the ventromedial side in the posterior part of the zebrafish SAG. (**A,B**) Antibody staining against HuC/D and GFP in the *neurod*:GFP reporter with (**A**) five consecutive sections of the anterior part of the SAG from a 8 months old fish and (**B**) three consecutive sections of the posterior part of the SAG from 3 months old fish. Two groups of *neurod*:GFP-positive cells at different positions illustrate that the *neurod*:GFP-positive domain is not a continues band within the SAG but rather divided into several islets located within the SAG. The area in which the majority of *neurod*:GFP-positive cells (the neurogenic niche) reside in the adult SAG are depicted in Fig. 9. Scale bar: 50 µm; cross sections showing dorsal to the top and lateral to the right.

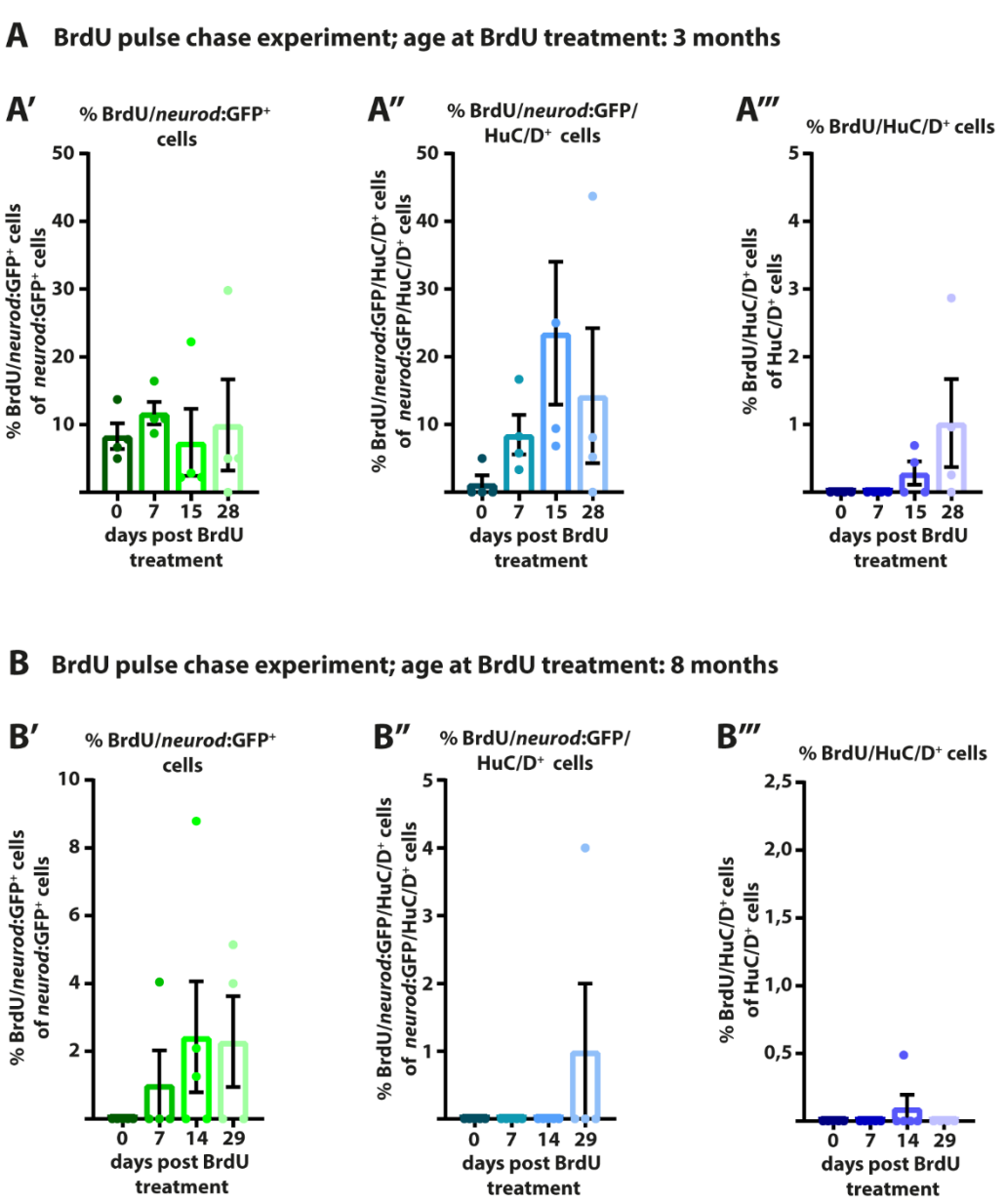

Fig. S3: Long term lineage tracing reveals proliferation of *neurod*:GFP-positive progenitor cells and neurogenesis in the juvenile SAG and the presence of proliferating stem/progenitor cells replenishing the pool of *neurod*:GFP-positive cells in the adult SAG. (**A**) Quantification of the percentage of BrdU/*neurod*:GFP-positive cells per *neurod*:GFP-positive progenitor cells (**A'**), BrdU/*neurod*:GFP/HuC/D-positive cells per *neurod*:GFP/HuC/D-positive immature neurons (**A''**) and BrdU/HuC/D-positive cells per HuC/D-positive neurons (**A'''**) after long term lineage tracing in the juvenile SAG shows proliferation of *neurod*:GFP-positive cells (**A'**, 0 dpt) which give rise to new BrdU/*neurod*:GFP/HuC/D and BrdU/HuC/D-positive neurons (**A''**, all time points; and **A'''**, 15 and 28 dpt) (see also Fig. 4). (**B**) Quantification of the percentage of BrdU/*neurod*:GFP-positive cells per *neurod*:GFP-positive progenitor cells (**B'**), BrdU/*neurod*:GFP/HuC/D-positive cells per *neurod*:GFP/HuC/D-positive immature neurons (**B''**) and BrdU/HuC/D-positive cells per HuC/D-positive neurons (**B'''**) after long term lineage tracing in the adult SAG reveals the presence of proliferating stem/progenitor cell which differentiate into BrdU/*neurod*:GFP-positive cells as early as 7 dpt (**B'**) and are able to further differentiate into neurons (presence of BrdU/*neurod*:GFP/HuC/D-positive cells at 29 dpt (**B''**) and BrdU/HuC/D-positive cells at 14 dpt, (**B'''**)) (see also Fig. 5).

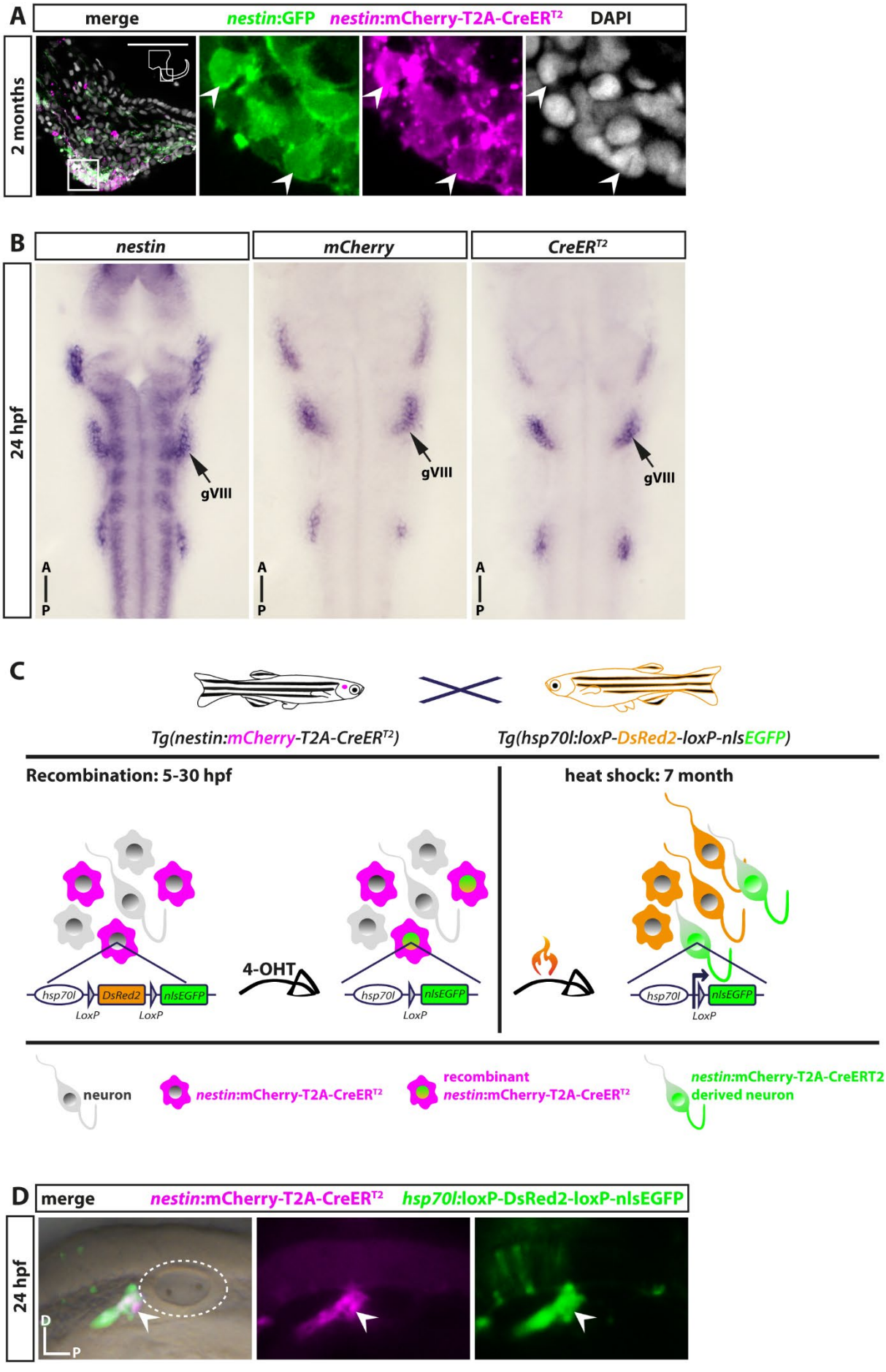

Fig. S4: Expression pattern of transgenic line *Tg(nestin:mCherry-T2A-CreER^{T2})* used for long term lineage tracing. (**A**) Antibody staining against *nestin*:GFP and *nestin:*mCherry-T2A-CreER^{T2} in 2 months old double transgenic fish shows that both transgenic lines label the same cell population in the SAG. (**B**) *in situ* hybridization against endogenous *nestin*, *mCherry* and *CreER^{T2}* in transgenic *Tg(nestin:mCherry-T2A-CreER^{T2})* embryos at 24 hours post fertilization (hpf). *nestin* is expressed widely throughout the developing central nervous system and in the developing cranial ganglia (compare Mahler and Driever, 2007). Expression of *mCherry* and *CreER^{T2}* is restricted to the developing statoacoustic ganglion (gVIII) and the neighboring ganglia. (**C**) Scheme depicting experimental set-up for long term lineage tracing experiment; *Tg (nestin*:mCherry-T2A-CreER^{T2}*)* was crossed to the Cre-dependent reporter line *Tg (hsp70l:loxP-DsRed2-loxP-nlsEGFP).* To induce recombination, embryos were immersed in 0.5 µM 4-hydroxy-tamoxifen (4-OHT) in E3 medium from 5 to 30 hpf. At 7 months, zebrafish were heat shocked to induce EGFP expression in successful recombined, *nestin*:mCherry-T2A-CreER^{T2}-derived cells. **(D)** Similar expression patterns of mCherry and EGFP after heat shock in double transgenic *Tg (nestin*:mCherry-T2A-CreER^{T2}*)*; *Tg (hsp70l:loxP-DsRed2-loxP-nlsEGFP)* embryos at 24 hpf reveals successful recombination in *nestin*:mCherry-T2A-CreER^{T2}-positive cells in the SAG and neighboring cranial ganglia. (**A**) Scale bar: 50 µm; cross sections showing dorsal to the top and lateral to the right. (**B**) dorsal views, anterior facing upwards. (**D**) lateral views with anterior to the left.

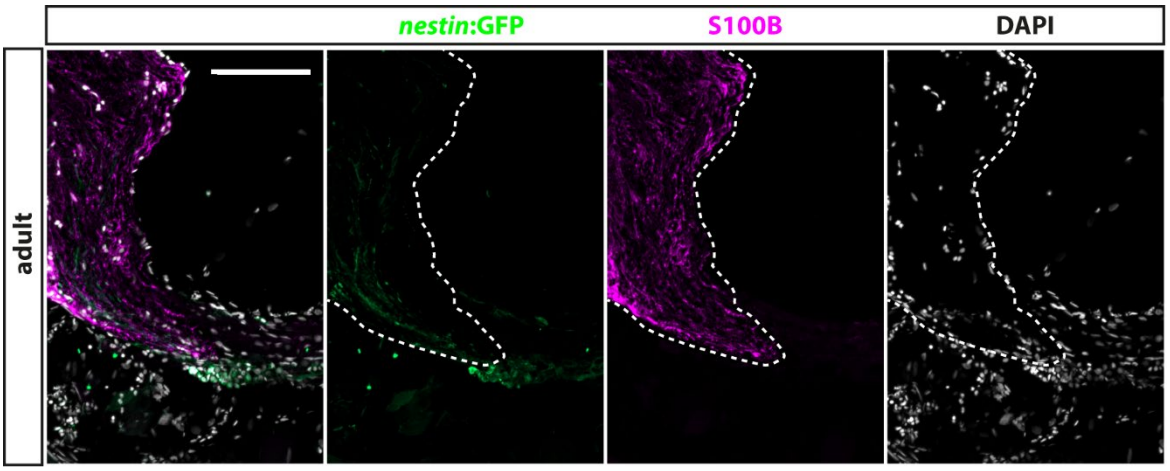

Fig. S5: Expression of glia marker GFAP marks the peripheral and central nervous system transitional zone (PCTZ) in the SAG. Antibody staining against S100B and *nestin*:GFP showing the PCTZ (dashed line) as a sharp boundary medial of *nestin*:GFP-positive cells in the SAG of adult zebrafish. Scale bar: 100 µm; cross sections showing dorsal to the top and lateral to the right.

Table S1: detailed staging criteria for animals used in this study.

No.	Genotype	age	sex	length	figure
60	WT gol stem cell	11,5 month	female	4 *	Fig.1
614	*Tg(pou4f3:GAP-GFP)^{s356}*	5,5 month	female	2,7	Fig.1
903	*TgBAC(neurod1:EGFP)nl1*	2 month	-	1,85	Fig.2
904	*TgBAC(neurod1:EGFP)nl1*	2 month	-	1,45	Fig.2
905	*TgBAC(neurod1:EGFP)nl1*	2 month	-	1,6	Fig.2
906	*TgBAC(neurod1:EGFP)nl1*	2 month	-	1,9	Fig.2
859	*TgBAC(neurod1:EGFP)nl1*	8,5 month	male	2,2	Fig.2
860	*TgBAC(neurod1:EGFP)nl1*	8,5 month	female	2,85	Fig.2
861	*TgBAC(neurod1:EGFP)nl1*	8,5 month	female	3	Fig.2
862	*TgBAC(neurod1:EGFP)nl1*	8,5 month	female	2,7	Fig.3/Fig. S2
368	*TgBAC(neurod1:EGFP)nl1*	2 month	-	1,7	Fig.3
359	*TgBAC(neurod1:EGFP)nl1*	3 month	female	2,7	Fig.3
860	*TgBAC(neurod1:EGFP)nl1*	8,5 month	female	2,85	Fig.3
676	*TgBAC(neurod1:EGFP)nl1*	19 month	female	3,35	Fig.3
367	*TgBAC(neurod1:EGFP)nl1*	2 month	-	1,5	Fig.3
369	*TgBAC(neurod1:EGFP)nl1*	2 month	-	1,85	Fig.3
904	*TgBAC(neurod1:EGFP)nl1*	2 month	-		Fig.3
906	*TgBAC(neurod1:EGFP)nl1*	2 month	-		Fig.3
360	*TgBAC(neurod1:EGFP)nl1*	3 month	female	2,5	Fig.3
362	*TgBAC(neurod1:EGFP)nl1*	3 month	female	2,7	Fig.3
410	*TgBAC(neurod1:EGFP)nl1*	8 month	male	3	Fig.3
411	*TgBAC(neurod1:EGFP)nl1*	8 month	male	2,8	Fig.3
413	*TgBAC(neurod1:EGFP)nl1*	8 month	male	2,8	Fig.3
a	*TgBAC(neurod1:EGFP)nl1*	3 month	male	2	Fig.4
b	*TgBAC(neurod1:EGFP)nl1*	3 month	male	2	Fig.4
c	*TgBAC(neurod1:EGFP)nl1*	3 month	male	2	Fig.4
d	*TgBAC(neurod1:EGFP)nl1*	3 month	male	2	Fig.4
k	*TgBAC(neurod1:EGFP)nl1*	3,25 month	female	2,2	Fig.4
j	*TgBAC(neurod1:EGFP)nl1*	3,25 month	male	2	Fig.4
h	*TgBAC(neurod1:EGFP)nl1*	3,25 month	female	-	Fig.4
l	*TgBAC(neurod1:EGFP)nl1*	3,25 month	male	2	Fig.4
m	*TgBAC(neurod1:EGFP)nl1*	3,5 month	female	2,2	Fig.4
p	*TgBAC(neurod1:EGFP)nl1*	3,5 month	female	2,5	Fig.4
q	*TgBAC(neurod1:EGFP)nl1*	3,5 month	female	2,5	Fig.4
n	*TgBAC(neurod1:EGFP)nl1*	3,5 month	female	2,5	Fig.4
4	*TgBAC(neurod1:EGFP)nl1*	4 month	male	2,2	Fig.4
5	*TgBAC(neurod1:EGFP)nl1*	4 month	female	2	Fig.4
6	*TgBAC(neurod1:EGFP)nl1*	4 month	male	2,1	Fig.4
1	*TgBAC(neurod1:EGFP)nl1*	4 month	male	2,1	Fig.4
419	*TgBAC(neurod1:EGFP)nl1*	7,75 month	m	2,8	Fig.5
420	*TgBAC(neurod1:EGFP)nl1*	7,75 month	m	2,8	Fig.5
421	*TgBAC(neurod1:EGFP)nl1*	7,75 month	m	2,8	Fig.5
422	*TgBAC(neurod1:EGFP)nl1*	7,75 month	f	2,8	Fig.5
423	*TgBAC(neurod1:EGFP)nl1*	7,75 month	f	2,8	Fig.5
424	*TgBAC(neurod1:EGFP)nl1*	8 month	-	-	Fig.5
425	*TgBAC(neurod1:EGFP)nl1*	8 month	-	-	Fig.5
426	*TgBAC(neurod1:EGFP)nl1*	8 month	-	-	Fig.5
427	*TgBAC(neurod1:EGFP)nl1*	8 month	-	-	Fig.5
428	*TgBAC(neurod1:EGFP)nl1*	8 month	-	-	Fig.5
434	*TgBAC(neurod1:EGFP)nl1*	8,25 month	f	2,8	Fig.5
435	*TgBAC(neurod1:EGFP)nl1*	8,25 month	f	2,7	Fig.5

436	*TgBAC(neurod1:EGFP)nl1*	8,25 month	m	2,85	Fig.5
437	*TgBAC(neurod1:EGFP)nl1*	8,25 month	m	2,85	Fig.5
438	*TgBAC(neurod1:EGFP)nl1*	8,25 month	f	2,65	Fig.5
439	*TgBAC(neurod1:EGFP)nl1*	8,75 month	f	2,7	Fig.5
440	*TgBAC(neurod1:EGFP)nl1*	8,75 month	f	2,95	Fig.5
441	*TgBAC(neurod1:EGFP)nl1*	8,75 month	f	2,8	Fig.5
443	*TgBAC(neurod1:EGFP)nl1*	8,75 month	m	2,9	Fig.5
571	*TgBAC(nes:EGFP)tud100*	2 month	-	1,55	Fig.6
877	*Tg(nestin*:mCherry-T2A-CreER^{T2}*)tud45 Tg(hsp70l:loxP-DsRed2-loxP-nlsEGFP)tud9*	12 month	female	2,7	Fig.6
878	*Tg(nestin*:mCherry-T2A-CreER^{T2}*)tud45 Tg(hsp70l:loxP-DsRed2-loxP-nlsEGFP)tud9*	12 month	female	2,8	Fig.6
879	*Tg(nestin*:mCherry-T2A-CreER^{T2}*)tud45 Tg(hsp70l:loxP-DsRed2-loxP-nlsEGFP)tud9*	12 month	female	2,8	Fig.6
622	*TgBAC(neurod1:EGFP)nl1 Tg(nestin*:mCherry-T2A-CreER^{T2}*)tud45*	2 month	-	1,9	Fig.6
690	*TgBAC(neurod1:EGFP)nl1 Tg(nestin*:mCherry-T2A-CreER^{T2}*)tud45*	4,75 month	male	3,2	Fig.6
134	*Tg(her4.3:GFP)y83*	11 month	female	4,1*	Fig.7
298	*Tg(her4.3:GFP)y83*	2,5 month	male	1,9	Fig.7
658	WT AB	2 month	-	1,85	Fig.7
859	*TgBAC(neurod1:EGFP)nl1*	8,5 month	male	2,2	Fig.8
952	*Tg(sox2:sox2-P2a-GFP)stl84*	4 month	male	3	Fig.8
161	WT AB	6 month	male	3,3*	Fig.8
852	*TgBAC(neurod1:EGFP)nl1*	13 month	male	2,8	Fig. S1
365	*TgBAC(neurod1:EGFP)nl1*	3 month	female	2,6	Fig. S2
624	*TgBAC(nes:EGFP)tud100 Tg(nestin*:mCherry-T2A-CreER^{T2}*)tud45*	2 month	-	1,9	Fig. S4
110	*TgBAC(nes:EGFP)tud100*	10 month	female	4*	Fig. S5

* length measured including caudal fin

Table S2: Primary and secondary antibodies used for immunohistochemistry on sections.

Antigen	Species	Isotype	Company	Catalogue Code	Dilution
BrdU	rat	polyclonal	Abcam	ab6326	1:500
Calretinin	rabbit	polyclonal	Swant Inc.	7699/4	1:2000
ClaudinK	rat	polyclonal	non-commercial (Münzel et al., 2012)		1:1000
GFP	chicken	polyclonal	Abcam	ab13970	1:2000
HuC/D	mouse	IgG2b, k	ThermoFisherScientific	A21271	1:500 - 1:300
Mbp	rabbit	polyclonal	non-commercial (Pinzon-Olejua et al., 2017)		1:100
mCherry	mouse	IgG1	Clontech	632543	1:500
PCNA	mouse	IgG2a, k	Dako	M0879	1:500
Sox2	rabbit	polyclonal	Millipore	AB5603	1:2000 - 1:1000
Zrf1/GFAP	mouse	IgG1	Zebrafish International Resource Center (Trevarrow et al., 1990)	CM-Zrf1-OG2B96	1:100

Secondary antibody	Fluorophore	Company	Catalogue Code	Dilution
Goat anti-Mouse IgG1	Alexa Fluor 488	ThermoFisherScientific	A21121	1:500
Goat anti-Mouse IgG1	Alexa Fluor 555	ThermoFisherScientific	A21127	1:500
Goat anti-Mouse IgG1	Alexa Fluor 633	ThermoFisherScientific	A21126	1:500
Goat anti-Mouse IgG (H+L)	Alexa Fluor 555	ThermoFisherScientific	A21424	1:500
Goat anti-Mouse IgG2a	Alexa Fluor 488	ThermoFisherScientific	A21131	1:500
Goat anti-Mouse IgG2a	Alexa Fluor 555	ThermoFisherScientific	A21137	1:500
Goat anti-Mouse IgG2a	Alexa Fluor 633	ThermoFisherScientific	A21136	1:500
Goat anti-Mouse IgG2b	Alexa Fluor 488	ThermoFisherScientific	A21141	1:500
Goat anti-Mouse IgG2b	Alexa Fluor 555	ThermoFisherScientific	A21147	1:500
Goat anti-Mouse IgG2b	Alexa Fluor 633	ThermoFisherScientific	A21146	1:500
Goat anti-Chicken IgY (H+L)	Alexa Fluor 488	ThermoFisherScientific	A11039	1:500
Goat anti-Rabbit IgG (H+L)	Alexa Fluor 488	ThermoFisherScientific	A11034	1:500
Goat anti-Rabbit IgG (H+L)	Alexa Fluor 555	ThermoFisherScientific	A21428	1:500
Goat anti-Rabbit IgG (H+L)	Alexa Fluor 633	ThermoFisherScientific	A31576	1:500
Goat anti-Rat IgG (H+L)	Alexa Fluor 555	ThermoFisherScientific	A21434	1:500

Table S3: Quantification of all neurons.

2 months

Slide	Row	Head	left HuC/D+	right HuC/D+
903.1	3	3		1
903.1	3	4		3
903.1	3	5		6
903.1	3	6		10
903.1	3	7		30
903.1	3	8		34,5
903.1	3	9		39
903.1	3	10		42
903.1	3	11		50
903.1	3	12		51
903.1	4	1		74
903.1	4	2		79
903.1	4	3		117
903.1	4	4		137
903.1	4	5		134
903.1	4	6		96
903.1	4	7		56
903.1	4	8		54
903.1	4	9		48
903.1	4	10		60
903.1	4	11		54
903.1	5	1		52
903.1	5	2	1	92
903.1	5	3	6	105
903.1	5	4	16	114
903.1	5	5	27	97
903.1	5	6	34	88
903.2	1	1	44	95
903.2	1	2	55	122
903.2	1	3	95	93
903.2	1	4	125	105
903.2	1	5	138	88
903.2	1	6	131	57
903.2	1	7	124	26
903.2	1	8	92	
903.2	1	9	85	
903.2	1	10	79	
903.2	2	1	42	
903.2	2	2	56	
903.2	2	3	70	
903.2	2	4	99	
903.2	2	5	139	
903.2	2	6	135	
903.2	2	7	131	
903.2	2	8	88	
903.2	3	1	71	
903.2	3	2	72	
903.2	3	3	86	
903.2	3	4	66	
903.2	3	5	32	
903.2	3	6	20	

Total	2159,00	2309,50
Average	74,45	67,93
Slides	29,00	34,00
Thickness in microns	348,00	408,00
Highest value	137,00	139,00

Slide	Row	Head	left HuC/D+	right HuC/D+
905.1	2	10	2	
905.1	3	1	5	
905.1	3	2	13	
905.1	3	3	18	
905.1	3	4	35	2
905.1	3	5	56	7
905.1	3	6	80	7
905.1	3	7	86	14
905.1	3	8	131	22
905.1	3	9	134	41
905.1	3	10	145	46
905.1	4	1	71	66
905.1	4	2	73	87
905.1	4	3	87	124
905.1	4	4	97	128
905.1	4	5	122	153
905.1	4	6	99	88
905.1	4	7	97	83
905.1	4	8	90	64
905.1	4	9	105	66
905.1	4	10	107	80
905.2	3	1	88	99
905.2	3	2	84	104
905.2	3	3	114	110
905.2	3	4	53	132
905.2	3	5	53	110
905.2	3	6	37	121
905.2	3	7	15	89
905.2	3	8		129
905.2	3	9		105
905.2	4	1		68
905.2	4	2		38
905.2	4	3		8

Total	2097,00	2191,00
Average	74,89	75,55
Slides	28,00	29,00
Thickness in microns	336,00	348,00
Highest value	145,00	153,00

Slide	Row	Head	left HuC/D+	right HuC/D+
904.1	4	5	1	
904.1	4	6	1	
904.1	4	7	5	
904.1	4	8	17	
904.1	4	9	27	
904.1	4	10	44	
904.1	4	11	61	
904.1	5	1	37	
904.1	5	2	99	
904.1	5	3	127	
904.1	5	4	167	
904.1	5	5	102	5
904.1	5	6	101	16
904.1	5	7	100	27
904.1	5	8	73	52
904.1	5	9	74	62
904.1	5	10	95	74
904.1	6	1	116	86
904.1	6	2	79	156
904.1	6	3	135	137
904.1	6	4	122	117
904.1	6	5	98	110
904.1	6	6	82	86
904.1	6	7	53	93
904.1	6	8	33	64
904.1	6	9	16,5	112
904.2	1	1		83
904.2	1	2		148
904.2	1	3		104
904.2	1	4		103
904.2	1	5		100
904.2	1	6		91
904.2	1	7		79
904.2	1	8		64
904.2	1	9		29
904.2	2	1		3

Total	1865,50	2001,00
Average	71,75	80,04
Slides	26,00	25,00
Thickness in microns	312,00	300,00
Highest value	167,00	156,00

Slide	Row	Head	left HuC/D+	right HuC/D+
906.1	4	3	1	
906.1	4	4	7	
906.1	4	5	8	
906.1	4	6	15	
906.1	4	7	23	
906.1	4	8	31	
906.1	4	9	51	
906.1	4	10	69	
906.2	1	1	75	
906.2	1	2	96	
906.2	1	3	128	
906.2	1	4	141	
906.2	1	5	150	
906.2	1	6	108	
906.2	1	7	81	
906.2	1	8	83	
906.2	1	9	75	
906.2	1	10	99	
906.2	2	1	107	11
906.2	2	2	105	22
906.2	2	3	117	49
906.2	2	4	89	107
906.2	2	5	84	128
906.2	2	6	80	162
906.2	2	7	95	135
906.2	2	8	104	117
906.2	3	1	82	122
906.2	3	2	32	104
906.2	3	3	5	73
906.2	3	4		121
906.2	3	5		109
906.2	3	6		129
906.2	3	7		124
906.2	3	8		102
906.2	3	9		121
906.2	3	10		124
906.2	4	1		96
906.2	4	2		101
906.2	4	3		73
906.2	4	4		37
906.2	4	5		5
906.2	4	6		2

Total	2141,00	2174,00
Average	73,83	90,58
Slides	29,00	24,00
Thickness in microns	348,00	288,00
Highest value	150,00	162,00

adult

Slide	Row	Head	left HuC/D+	right HuC/D+
859.1	3	7	1	
859.1	3	8	1	
859.1	3	9	5	
859.1	4	1	29	
859.1	4	2	31	
859.1	4	3	39	
859.1	4	4	46	
859.1	4	5	60	
859.1	4	6	70	
859.1	4	7	68	1
859.1	4	8	67	1
859.2	1	1	58	3
859.2	1	2	72	8
859.2	1	3	71	17
859.2	1	4	73	23
859.2	1	5	79	30
859.2	1	6	78	51
859.2	1	7	77	56
859.2	1	8	70	68
859.2	2	1	57	70
859.2	2	2	49	73
859.2	2	3	37	65
859.2	2	4	39	75
859.2	2	5	50	60
859.2	2	6	80	44
859.2	2	7	74	61
859.2	2	8	78	68
859.2	3	1	77	52
859.2	3	2	112	70
859.2	3	3	95	70
859.2	3	4	111	61
859.2	3	5	86	72
859.2	3	6	45	59
859.2	3	7	1	74
859.2	3	8		81
859.2	4	1		72
859.2	4	2		62
859.2	4	3		53
859.2	4	4		37
859.2	4	5		26
859.2	4	6		12

Total	1986,00	1575,00
Average	58,41	49,22
Slides	34,00	32,00
Thickness in microns	408,00	384,00
Highest value	112,00	81,00

Slide	Row	Head	left HuC/D+	right HuC/D+
860.1	3	1	4	
860.1	3	2	5	
860.1	3	3	7	1
860.1	3	4	11	0
860.1	3	5	13	0
860.1	3	6	25	1
860.1	3	7	37	13
860.1	4	1	37	20
860.1	4	2	51	26
860.1	4	3	49	24
860.1	4	4	52	43
860.1	4	5	40	28
860.1	4	6	60	33
860.1	4	7	53	48
860.1	4	8	63	64
860.2	1	1	37	55
860.2	1	2	55	74
860.2	1	3	32	60
860.2	1	4	38	53
860.2	1	5	24	49
860.2	1	6	36	41
860.2	1	7	31	35
860.2	2	1	29	37
860.2	2	2	24	45
860.2	2	3	39	37
860.2	2	4	39	31
860.2	2	5	22	31
860.2	2	6	40	42
860.2	2	7	35	38
860.2	2	8	38	40
860.2	3	1	40	39
860.2	3	2	48	45
860.2	3	3	44	26
860.2	3	4	46	49
860.2	3	5	65	48
860.2	3	6	60	45
860.2	3	7	86	49
860.2	3	8	102	67
860.2	4	1	83	44
860.2	4	2	56	55
860.2	4	3	28	58
860.2	4	4	2	75
860.2	4	5		62
860.2	4	6		46
860.2	4	7		27

Total	1686,00	1704,00
Average	40,14	39,63
Slides	42,00	43,00
Thickness in microns	504,00	516,00
Highest value	102,00	75,00

Slide	Row	Head	left HuC/D+	right HuC/D+
861.2	2	4		2
861.2	2	5		3
861.2	2	6		3
861.2	2	7		1
861.2	3	1		9
861.2	3	2		12
861.2	3	3		17
861.2	3	4		22
861.2	3	5		28
861.2	3	6	1	23
861.2	3	7	1	26
861.2	4	1	3	35
861.2	4	2	2	46
861.2	4	3	7	52
861.2	4	4	18	54
861.2	4	5	21	56
861.2	4	6	25	58
861.2	4	7	23	59
861.3	1	1	30	49
861.3	1	2	37	52
861.3	1	3	64	78
861.3	1	4	60	50
861.3	1	5	54	26
861.3	1	6	55	34
861.3	1	7	50	52
861.3	2	1	48	44
861.3	2	2	43	46
861.3	2	3	46	45
861.3	2	4	44	41
861.3	2	5	42	49
861.3	2	6	40	63
861.3	2	7	41	72
861.3	3	1	40	58
861.3	3	2	39	62
861.3	3	3	49	65
861.3	3	4	60	81
861.3	3	5	47	88
861.3	3	6	45	91
861.3	3	7	44	109
861.3	4	1	35	63
861.3	4	2	38	29
861.3	4	3	54	
861.3	4	4	67	
861.3	4	5	116	
861.3	4	6	130	
861.3	4	7	120	
861.4	1	1	81	
861.4	1	2	28	
861.4	1	3	2	

Total	1750,00	1853,00
Average	43,75	45,20
Slides	40,00	41,00
Thickness in microns	480,00	492,00
Highest value	130,00	109,00

Slide	Row	Head	left HuC/D+	right HuC/D+
862.1	4	3		2
862.1	4	4	2	3
862.1	4	5	1	12
862.1	4	6	5	12
862.1	4	7	6	17
862.1	4	8	11	26
862.1	4	9	7	21
862.2	1	1	7	26
862.2	1	2	7	53
862.2	1	3	11	58
862.2	1	4	10	53
862.2	1	5	24	43
862.2	1	6	27	46
862.2	1	7	45	34
862.2	1	8	68	39
862.2	2	1	72	50
862.2	2	2	81	48
862.2	2	3	51	55
862.2	2	4	36	47
862.2	2	5	39	42
862.2	2	6	33	48
862.2	2	7	35	43
862.2	2	8	36	30
862.2	3	1	26	36
862.2	3	2	25	33
862.2	3	3	51	36
862.2	3	4	65	36
862.2	3	5	39	42
862.2	3	6	42	46
862.2	3	7	45	65
862.2	3	8	50	47
862.2	4	1	53	49
862.2	4	2	51	54
862.2	4	3	52	63
862.2	4	4	58	90
862.2	4	5	62	69
862.2	4	6	64	49
862.2	4	7	80	10
862.3	1	1	44	5
862.3	1	2	18	
862.3	1	3	10	

Total	1449,00	1538,00
Average	36,23	39,44
Slides	40,00	39,00
Thickness in microns	480,00	468,00
Highest value	81,00	90,00

summary								
2 months								
Sample number	903		904		905		906	
Side	left	right	left	right	left	right	left	right
Total	2309,50	2159,00	2097,00	2191,00	1865,50	2001,00	2141,00	2174,00
Average	67,93	74,45	74,89	75,55	71,75	80,04	73,83	90,58
Slides	34,00	29,00	28,00	29,00	26,00	25,00	29,00	24,00
Thickness in microns	408,00	348,00	336,00	348,00	312,00	300,00	348,00	288,00
Highest value	137,00	139,00	145,00	153,00	167,00	156,00	150,00	162,00

Sample number	903	904	905	906	AVERAGE
Total	2234,25	2144,00	1933,25	2157,50	2117,25
Average	71,19	75,22	75,90	82,21	76,13
Slides	31,50	28,50	25,50	26,50	28,00
Thickness in microns	378,00	342,00	306,00	318,00	336,00
Highest value	138,00	149,00	161,50	156,00	151,13

adult								
Sample number	859		860		861		862	
Side	left	right	left	right	left	right	left	right
Total	1986,00	1575,00	1686,00	1704,00	1750,00	1853,00	1449,00	1538,00
Average	58,41	49,22	40,14	39,63	43,75	45,20	36,23	39,44
Slides	34,00	32,00	42,00	43,00	40,00	41,00	40,00	39,00
Thickness in microns	408,00	384,00	504,00	516,00	480,00	492,00	480,00	468,00
Highest value	112,00	81,00	102,00	75,00	130,00	109,00	81,00	90,00

Sample number	859	860	861	862	AVERAGE
Total	1780,50	1695,00	1801,50	1493,50	1692,63
Average	53,82	39,89	44,47	37,83	44,00
Slides	33,00	42,50	40,50	39,50	38,88
Thickness in microns	396,00	510,00	486,00	474,00	466,50
Highest value	96,50	88,50	119,50	85,50	97,50

Table S4: Quantification of proliferation and neurogenesis.

2 months							
Sample	Row.Head	all neurod	only neurod+	neurod/ HuC/D+	all PCNA+	only PCNA	neurod/ PCNA+
367.2	3.2	30	7	21	16	14	2
367.2	3.3	53	7	39	26	19	7
367.2	3.4	50	12	26	19	7	12
367.2	3.5	38	11	14	17	4	13
367.2	3.6	36	11	12	23	10	13
367.2	3.7	20	6	8	19	13	6
367.2	3.8	16	5	4	19	12	7
367.2	3.9	4	2	0	7	5	2
367.2	3.10	19	3	13	8	5	3
367.2	3.11	59	23	21	28	13	15
367.2	4.2	63	25	25	29	16	13
367.2	4.1	68	32	24	19	7	12
	Total	456	144	207	230	125	105
	Average	38	12	17,25	19,16666667	10,41666667	8,75
	SD	20,73205686	9,572688423	10,86382655	6,899714531	4,832810839	4,788717801
	Median	37	9	17,5	19	11	9,5

Sample	Row.Head	all neurod	only neurod+	neurod/ HuC/D+	all PCNA+	only PCNA	neurod/ PCNA+
368.1	1.1	39	1	18	45	25	20
368.1	1.2	56	0	33	50	27	23
368.1	1.3	71	7	24	64	24	40
368.1	1.4	73	11	20	63	21	42
368.1	1.5	34	2	5	53	26	27
368.1	1.6	29	3	12	26	12	14
368.1	1.7	65	18	27	41	21	20
368.1	1.8	41	2	11	46	18	28
368.1	1.9	24	5	10	29	20	9
368.1	1.10	75	14	38	40	17	23
368.1	2.1	76	33	10	51	18	33
368.1	2.2	41	8	6	41	14	27
	Total	624	104	214	549	243	306
	Average	52	8,666666667	17,83333333	45,75	20,25	25,5
	SD	19,40009372	9,461244713	10,75202588	11,59251326	4,712169931	9,662486034
	Median	48,5	6	15	45,5	20,5	25

Sample	Row.Head	all neurod	only neurod+	neurod/ HuC/D+	all PCNA+	only PCNA	neurod/ PCNA+
369.2	1.2	33	8	14	17	6	11
369.2	1.3	39	13	16	17	7	10
369.2	1.4	16	9	4	22	19	3
369.2	1.5	80	30	25	44	19	25
369.2	1.6	51	19	26	23	17	6
369.2	1.7	37	19	6	33	21	12
369.2	1.8	41	23	10	28	20	8
369.2	1.9	85	22	32	48	17	31
369.2	1.10	47	19	12	45	29	16
369.2	2.1	42	19	14	36	27	9
369.2	2.2	64	23	18	56	33	23
369.2	2.3	36	8	12	25	9	16
	Total	571	212	189	394	224	170
	Average	47,58333333	17,66666667	15,75	32,83333333	18,66666667	14,16666667
	SD	19,85611119	6,866696087	8,313461154	12,9673249	8,445906306	8,386497084
	Median	41,5	19	14	30,5	19	11,5

Sample	Row.Head	all neurod	only neurod+	neurod/ HuC/D+	all PCNA+	only PCNA	neurod/ PCNA+
904.1	5.5	67	9	49	24	15	9
904.1	5.6	55	3	43	35	26	9
904.1	5.7	94	41	28	46	21	25
904.1	5.8	56	13	30	38	25	13
904.1	5.9	27	6	18	25	22	3
904.1	5.10-lost		0			0	
904.1	6.1	76	18	51	31	24	7
904.1	6.2	56	17	29	33	23	10
904.1	6.3	99	20	56	46	23	23
904.1	6.4	56	22	29	14	9	5
904.1	6.5	37	6	22	37	28	9
904.1	6.6	35	4	29	12	10	2
	Total	658	159	384	341	226	115
	Average	59,81818182	13,25	34,90909091	31	18,83333333	10,45454545
	SD	23,0165948	11,35481476	12,63688684	11,35781669	8,494204798	7,421100139
	Median	56	11	29	33	22,5	9

Sample	Row.Head	all neurod	only neurod+	neurod/ HuC/D+	all PCNA+	only PCNA	neurod/ PCNA+
906.2	1.6	63	33	16	21	7	14
906.2	1.7	47	20	15	22	10	12
906.2	1.8	43	19	15	25	16	9
906.2	1.9	39	10	18	20	9	11
906.2	1.10	37	15	20	15	13	2
906.2	2.1	32	13	13	11	5	6
906.2	2.2	67	22	33	32	20	12
906.2	2.3	60	21	30	24	15	9
906.2	2.4	68	23	33	26	14	12
906.2	2.5	66	15	46	17	12	5
906.2	2.6	57	8	42	23	16	7
906.2	2.7	66	15	44	21	14	7
	Total	645	214	325	257	151	106
	Average	53,75	17,83333333	27,08333333	21,41666667	12,58333333	8,833333333
	SD	13,30157202	6,712719722	12,39837477	5,451577475	4,231018217	3,537676005
	Median	58,5	17	25	21,5	13,5	9

3 months							
Sample	Row.Head	all neurod	only neurod+	neurod/ HuC/D+	all PCNA+	only PCNA	neurod/ PCNA+
359.2	2.4	21	0	21	6	6	0
359.2	2.5	38	23	13	8	6	2
359.2	3.1	16	13	1	5	3	2
359.2	3.2	1	0	1	9	9	0
359.3	1.1	0	0	0	5	5	0
359.4	1.2	1	1	0	11	11	0
359.5	1.4	7	5	2	2	2	0
359.6	1.5	25	17	4	12	8	4
359.7	1.6	23	14	7	5	3	2
359.8	1.7	26	23	3	2	2	0
359.9	2.1	10	4	6	0	0	0
359.10	2.2	10	9	0	13	12	1
	Total	178	109	58	78	67	11
	Average	14,83333333	9,083333333	4,833333333	6,5	5,583333333	0,916666667
	SD	11,99115836	8,764166022	6,365151335	4,166969686	3,800916955	1,311372171
	Median	13	7	2,5	5,5	5,5	0

Sample	Row.Head	all neurod	only neurod+	neurod/ HuC/D+	all PCNA+	only PCNA	neurod/ PCNA+
360.1	1.3	19	17	1	6	5	1
360.1	1.4	23	19	2	5	3	2
360.1	1.5	38	31	7	14	14	0
360.1	1.6	39	34	4	1	0	1
360.1	1.7	12	12	0	2	2	0
360.1	1.8	9	9	0	2	2	0
360.1	2.1	5	5	0	1	1	0
360.1	2.2	11	11	0	1	1	0
360.1	2.3	41	35	6	0	0	0
360.1	2.4	22	19	1	6	4	2
360.1	2.5	33	28	3	6	4	2
360.1	2.6	18	15	2	5	4	1
	Total	270	235	26	49	40	9
	Average	22,5	19,58333333	2,166666667	4,083333333	3,333333333	0,75
	SD	12,53721732	10,1395565	2,40580107	3,872005197	3,749747466	0,866025404
	Median	20,5	18	1,5	3,5	2,5	0,5

Sample	Row.Head	all neurod	only neurod+	neurod/ HuC/D+	all PCNA+	only PCNA	neurod/ PCNA+
362.2	2.2	33	19	14	5	5	0
362.2	2.3	37	31	4	8	6	2
362.2	2.4	18	13	3	10	8	2
362.2	2.5	21	13	7	2	1	1
362.2	2.6	36	29	6	2	1	1
362.2	2.7	15	14	0	3	2	1
362.2	2.8	23	19	4	3	3	0
362.2	3.1	2	1	1	0	0	0
362.2	3.2	33	20	10	6	3	3
362.2	3.3	9	7	2	1	1	0
362.2	3.4	34	30	4	1	1	0
362.2	3.5	17	11	6	1	1	0
	Total	278	207	61	42	32	10
	Average	23,16666667	17,25	5,083333333	3,5	2,666666667	0,833333333
	SD	11,48780645	9,333468614	3,918680978	3,1188576	2,46182982	1,029857301
	Median	22	16,5	4	2,5	1,5	0,5

adult							
Sample	Row.Head	all neurod	only neurod+	neurod/ HuC/D+	all PCNA+	only PCNA	neurod/ PCNA+
410.2	2.4	15	15	0	2	2	0
410.2	2.5	19	19	0	1	1	0
410.2	2.6	20	20	0	3	3	0
410.2	2.7	29	28	0	3	2	1
410.2	3.1	8	8	0	0	0	0
410.2	3.2	4	4	0	0	0	0
410.2	3.3	13	11	2	0	0	0
410.2	3.4	11	11	0	0	0	0
410.2	3.5	15	13	2	2	2	0
410.2	3.6	32	31	1	3	3	0
410.3	1.1	8	7	1	3	3	0
410.3	1.3	2	2	0	0	0	0
	Total	176	169	6	17	16	1
	Average	14,66666667	14,08333333	0,5	1,416666667	1,333333333	0,083333333
	SD	9,208033383	9,019759454	0,797724035	1,378954369	1,302677895	0,288675135
	Median	14	12	0	1,5	1,5	0

Sample	Row.Head	all neurod	only neurod+	neurod/ HuC/D+	all PCNA+	only PCNA	neurod/ PCNA+
413.2	2.7	7	7	0	0	0	0
413.2	2.8	18	18	0	1	1	0
413.2	2.9	31	31	0	0	0	0
413.2	3.1	15	15	0	2	2	0
413.2	3.2	18	18	0	0	0	0
413.2	3.3	13	13	0	3	3	0
413.2	3.4	2	2	0	0	0	0
413.2	3.5	2	2	0	2	2	0
413.2	3.6	6	5	1	2	2	0
413.2	3.7	11	11	0	0	0	0
413.2	4.1	17	17	0	2	2	0
413.2	4.2	13	13	0	1	1	0
	Total	153	152	1	13	13	0
	Average	12,75	12,66666667	0,083333333	1,083333333	1,083333333	0
	SD	8,114241128	8,194602806	0,288675135	1,083624669	1,083624669	0
	Median	13	13	0	1	1	0

Sample	Row.Head	all neurod	only neurod+	neurod/ HuC/D+	all PCNA+	only PCNA	neurod/ PCNA+
411.4	2.2	7	7	0	2	2	0
411.4	2.3	1	1	0	0	0	0
411.4	2.4	4	4	0	0	0	0
411.4	2.5	40	40	0	2	2	0
411.4	2.6	32	32	0	3	3	0
411.4	2.7	29	29	0	2	2	0
411.4	2.8	25	25	0	3	3	0
411.4	2.9	8	8	0	1	1	0
411.4	3.6	14	14	0	3	3	0
411.4	3.7	16	15	1	1	1	0
411.4	3.8	9	9	0	0	0	0
411.4	3.9	13	13	0	1	1	0
	Total	198	197	1	18	18	0
	Average	16,5	16,41666667	0,083333333	1,5	1,5	0
	SD	12,26599142	12,27309203	0,288675135	1,167748416	1,167748416	0
	Median	13,5	13,5	0	1,5	1,5	0

Sample	Row.Head	all neurod	only neurod+	neurod/ HuC/D+	all PCNA+	only PCNA	neurod/ PCNA+
860.2	1.4	21	11	10	0	0	0
860.2	1.5	25	18	7	0	0	0
860.2	1.6	20	18	2	0	0	0
860.2	1.7	5	5	0	1	1	0
860.2	2.1	1	1	0	2	2	0
860.2	2.2	3	3	0	0	0	0
860.2	2.3	2	2	0	0	0	0
860.2	2.4	2	2	0	0	0	0
860.2	2.5	5	5	0	2	2	0
860.2	2.6	4	4	0	0	0	0
860.2	2.7	23	23	0	0	0	0
860.2	2.8	22	22	0	0	0	0
	Total	133	114	19	5	5	0
	Average	11,08333333	9,5	1,583333333	0,416666667	0,416666667	0
	SD	9,949493668	8,436931799	3,342789617	0,792961461	0,792961461	0
	Median	5	5	0	0	0	0

Table S5: Quantification of BrdU-positive cells in juveniles.

0dpt

Slide	Row	Head	BrdU+	only BrdU	% only per all BrdU	neurod/ BrdU+	% neurod/ BrdU per all BrdU	BrdU/ HuC/D+	% HuC/D/ BrdU per all BrdU	triple+	% triple+ per all BrdU	only neurod+	only neurod+ and neurod/ BrdU+	% neurod/ BrdU+ per specific cell type	only neuroD/ HuC/D+	neurod/ HuC/D+ and triple+	% triple+ per specific cell type	only HuC/D+	HuC/D+ and HuC/D/ BrdU+	% HuC/D/ BrdU+ per specific cell type
a-1	2	1	2	2	100	0	0	0	0	0	0									
a-1	2	2	9	5	55,55555556	4	44,44444444	0	0	0	0									
a-1	2	3	14	6	42,85714286	8	57,14285714	0	0	0	0									
a-1	2	4	10	9	90	1	10	0	0	0	0									
a-1	2	5	8	8	100	0	0	0	0	0	0									
a-1	3	11	3	3	100	0	0	0	0	0	0									
a-1	3	10	2	2	100	0	0	0	0	0	0									
a-1	3	9	15	6	40	9	60	0	0	0	0	32	41	21,95121951	5	5	0	42	42	0
a-1	3	8	10	6	60	4	40	0	0	0	0	29	33	12,12121212	8	8	0	57	57	0
a-1	3	7	8	6	75	2	25	0	0	0	0	40	42	4,761904762	8	8	0	56	56	0
a-1	3	6	9	5	55,55555556	4	44,44444444	0	0	0	0	44	48	8,333333333	6	6	0	53	53	0
a-1	3	5	9	6	66,66666667	3	33,33333333	0	0	0	0	11	14	21,42857143	9	9	0	66	66	0
	Sum		99	64	885,6349206	35	314,3650794	0	0	0	0	156	178	68,59624116	36	36	0	274	274	0
	Average		8,25	5,333333333	73,80291005	2,916666667	26,19708995	0	0	0	0	31,2	35,6	13,71924823	7,2	7,2	0	54,8	54,8	0
	SD		4,180582821	2,14617348	23,38722312	3,088345639	23,38722312	0	0	0	0	12,79453008	13,20227253	7,729728586	1,643167673	1,643167673	0	8,642916175	8,642916175	0

Slide	Row	Head	BrdU+	only BrdU	% only per all BrdU	neurod/ BrdU+	% neurod/ BrdU per all BrdU	BrdU/ HuC/D+	% HuC/D/ BrdU per all BrdU	triple+	% triple+ per all BrdU	only neurod+	only neurod+ and neurod/ BrdU+	% neurod/ BrdU+ per specific cell type	only neuroD/ HuC/D+	neurod/ HuC/D+ and triple+	% triple+ per specific cell type	only HuC/D+	HuC/D+ and HuC/D/ BrdU+	% HuC/D/ BrdU+ per specific cell type
b-2	1	1	4	2	50	2	50	0	0	0	0									
b-2	1	2	2	2	100	0	0	0	0	0	0									
b-2	1	3	2	2	100	0	0	0	0	0	0									
b-2	1	4	0	0		0		0		0										
b-2	2	4	7	2	28,57142857	5	71,42857143	0	0	0	0	28	33	15,15151515	10	10	0	52	52	0
b-2	2	5	7	3	42,85714286	4	57,14285714	0	0	0	0	31	35	11,42857143	17	17	0	53	53	0
b-2	2	6	5	5	100	0	0	0	0	0	0	44	44	0	7	7	0	44	44	0
b-2	2	8	5	3	60	2	40	0	0	0	0	14	16	12,5	6	6	0	63	63	0
b-2	2	9	3	3	100	0	0	0	0	0	0	31	31	0	12	12	0	76	76	0
b-2	2	10	3	3	100	0	0	0	0	0	0									
b-2	2	11	6	4	66,66666667	2	33,33333333	0	0	0	0									
b-2	2	12	9	3	33,33333333	6	66,66666667	0	0	0	0									
	Sum		53	32	781,4285714	21	318,5714286	0	0	0	0	148	159	39,08008658	52	52	0	288	288	0
	Average		4,416666667	2,666666667	71,03896104	1,75	28,96103896	0	0	0	0	29,6	31,8	7,816017316	10,4	10,4	0	57,6	57,6	0
	SD		2,574643253	1,23091491	29,65930367	2,179449472	29,65930367	0	0	0	0	10,69111781	10,13410085	7,262575694	4,393176527	4,393176527	0	12,3004065	12,3004065	

Slide	Row	Head	BrdU+	only BrdU	% only per all BrdU	neurod/ BrdU+	% neurod/ BrdU per all BrdU	BrdU/ HuC/D+	% HuC/D/ BrdU per all BrdU	triple+	% triple+ per all BrdU	only neurod+	only neurod+ and neurod/ BrdU+	% neurod/ BrdU+ per specific cell type	only neuroD/ HuC/D+	neurod/ HuC/D+ and triple+	% triple+ per specific cell type	only HuC/D+	HuC/D+ and HuC/D/ BrdU+	% HuC/D/ BrdU+ per specific cell type
c-2	3	1	0	0	0	1	100	0	0	0	0									
c-2	3	2	0	0		0		0		0										
c-2	3	3	1	1	100	0	0	0	0	0	0									
c-2	3	4	3	3	100	0	0	0	0	0	0									
c-2	3	5	4	4	100	0	0	0	0	0	0									
c-2	3	6	3	3	100	0	0	0	0	0	0									
c-2	3	7	2	2	100	0	0	0	0	0	0									
c-2	4	7	6	6	100	0	0	0	0	0	0	2	2	0	0	0		55	55	0
c-2	4	8	4	4	100	0	0	0	0	0	0	30	30	0	29	29	0	84	84	0
c-2	4	9	3	3	100	0	0	0	0	0	0	30	30	0	4	4	0	57	57	0
c-2	4	10	3	3	100	0	0	0	0	0	0	17	17	0	6	6	0	45	45	0
c-2	4	11	1	0	0	1	100	0	0	0	0	2	3	33,33333333	0	0		23	23	0
	Sum		31	29	900	2	200	0	0	0	0	81	82	33,33333333	39	39	0	264	264	0
	Average		2,583333333	2,416666667	81,81818182	0,166666667	18,18181818	0	0	0	0	16,2	16,4	6,666666667	7,8	7,8	0	52,8	52,8	0
	SD		1,676486224	1,880924982	40,45199175	0,389249472	40,45199175	0	0	0	0	14,00714104	13,75863365	14,90711985	12,13260071	12,13260071	0	22,04994331	22,04994331	0

Slide	Row	Head	BrdU+	only BrdU	% only per all BrdU	neurod/ BrdU+	% neurod/ BrdU per all BrdU	BrdU/ HuC/D+	% HuC/D/ BrdU per all BrdU	triple+	% triple+ per all BrdU	only neurod+	only neurod+ and neurod/ BrdU+	% neurod/ BrdU+ per specific cell type	only neuroD/ HuC/D+	neurod/ HuC/D+ and triple+	% triple+ per specific cell type	only HuC/D+	HuC/D+ and HuC/D/ BrdU+	% HuC/D/ BrdU+ per specific cell type
d-3	1	1	4	3	75	1	25	0	0	0	0									
d-3	1	2	4	1	25	2	50	0	0	1	25	27	29	6,896551724	0	1	100	38	38	0
d-3	1	3	2	2	100	0	0	0	0	0	0	15	15	0	3	3	0	22	22	0
d-3	1	4	6	6	100	0	0	0	0	0	0	21	21	0	9	9	0	52	52	0
d-3	1	5	3	3	100	0	0	0	0	0	0	17	17	0	6	6	0	47	47	0
d-3	1	6	5	2	40	3	60	0	0	0	0	10	13	23,07692308	2	2	0	30	30	0
d-3	1	7	0	0		0		0		0										
d-3	1	8	0	0		0		0		0										
d-3	1	9	0	0		0		0		0										
lost																				
lost																				
lost																				
	Sum		24	17	440	6	135	0	0	1	25	90	95	29,9734748	20	21	100	189	189	0
	Average		2,666666667	1,888888889	73,33333333	0,666666667	22,5	0	0	0,111111111	4,166666667	18	19	5,99469496	4	4,2	20	37,8	37,8	0
	SD		2,291287847	1,96497102	33,41656276	1,118033989	27,15695123	0	0	0,333333333	10,20620726	6,403124237	6,32455532	10,00531067	3,535533906	3,271085447	44,72135955	12,21474519	12,21474519	0

Summary
0dpt

Sample	BrdU+	only BrdU	% only per all BrdU	neurod/ BrdU+	% neurod/ BrdU per all BrdU	BrdU/ HuC/D+	% HuC/D/ BrdU per all BrdU	triple+	% triple+ per all BrdU	only neurod+	only neurod+ and neurod/ BrdU+	% neurod/ BrdU+ per specific cell type	only neuroD/ HuC/D+	neurod/ HuC/D+ and triple+	% triple+ per specific cell type	only HuC/D+	HuC/D+ and HuC/D/ BrdU+	% HuC/D/ BrdU+ per specific cell type
B-a	8,25	5,333333333	73,80291005	2,916666667	26,19708995	0	0	0	0	31,2	35,6	13,71924823	7,2	7,2	0	54,8	54,8	0
B-b	4,416666667	2,666666667	71,03896104	1,75	28,96103896	0	0	0	0	29,6	31,8	7,816017316	10,4	10,4	0	57,6	57,6	0
B-c	2,583333333	2,416666667	81,81818182	0,166666667	18,18181818	0	0	0	0	16,2	16,4	6,666666667	7,8	7,8	0	52,8	52,8	0
B-d	2,666666667	1,888888889	73,33333333	0,666666667	22,5	0	0	0,111111111	4,166666667	18	19	5,99469496	4	4,2	20	37,8	37,8	0
Sum	17,91666667	12,30555556	299,9933862	5,5	95,83994709	0	0	0,111111111	4,166666667	95	102,8	34,19662717	29,4	29,6	20	203	203	0
Average	4,479166667	3,076388889	74,99834656	1,375	23,95998677	0	0	0,027777778	1,041666667	23,75	25,7	8,549156794	7,35	7,4	5	50,75	50,75	0
SD	2,65219598	1,53916213	4,704190477	1,221906525	4,673825958	0	0	0,055555556	2,083333333	7,741446893	9,426911831	3,527812509	2,62995564	2,545584412	10	8,854942123	8,854942123	0

7dpt

Slide	Row	Head	BrdU+	only BrdU	% only per all BrdU	neurod/ BrdU+	% neurod/ BrdU per all BrdU	BrdU/ HuC/D+	% HuC/D/ BrdU per all BrdU	triple+	% triple+ per all BrdU	only neurod+	only neurod+ and neurod/ BrdU+	% neurod/ BrdU+ per specific cell type	only neuroD/ HuC/D+	neurod/ HuC/D+ and triple+	% triple+ per specific cell type	only HuC/D+	HuC/D+ and HuC/D/ BrdU+	% HuC/D/ BrdU+ per specific cell type
k.2	3	2	9	7	77,77777778	2	22,22222222	0	0	0	0	12	14	14,28571429	2	2	0	42	42	0
k.2	3	3	12	12	100	0	0	0	0	0	0	24	24	0	12	12	0	19	19	0
k.2	3	4	14	13	92,85714286	1	7,142857143	0	0	0	0	11	12	8,333333333	2	2	0	34	34	0
k.2	3	5	25	23	92	2	8	0	0	0	0									
k.2	3	6	21	19	90,47619048	2	9,523809524	0	0	0	0									
k.2	3	7	21	20	95,23809524	1	4,761904762	0	0	0	0									
k.2	3	8	29	28	96,55172414	1	3,448275862	0	0	0	0									
k.2	3	9	26	25	96,15384615	1	3,846153846	0	0	0	0									
k.2	3	10	21	20	95,23809524	1	4,761904762	0	0	0	0									
k.2	4	9	21	17	80,95238095	2	9,523809524	1	4,761904762	1	4,761904762									
k.2	4	10	16	16	100	0	0	0	0	0	0	6	6	0	0	0	0	32	32	0
k.2	4	11	33	30	90,90909091	3	9,090909091	0	0	0	0	7	10	30	4	4	0	37	37	0
		Sum	248	230	1108,154344	16	82,32184674	1	4,761904762	1	4,761904762	60	66	52,61904762	20	20	0	164	164	0
		Average	20,66666667	19,16666667	92,34619531	1,333333333	6,860153895	0,083333333	0,396825397	0,083333333	0,396825397	12	13,2	10,52380952	4	4	0	32,8	32,8	0
		SD	7,049607769	6,726248898	6,836221719	0,887625365	5,879026935	0,288675135	1,374643498	0,288675135	1,374643498	7,176350047	6,723094526	12,44762269	4,69041576	4,69041576	0	8,584870413	8,584870413	0

Slide	Row	Head	BrdU+	only BrdU	% only per all BrdU	neurod/ BrdU+	% neurod/ BrdU per all BrdU	BrdU/ HuC/D+	% HuC/D/ BrdU per all BrdU	triple+	% triple+ per all BrdU	only neurod+	only neurod+ and neurod/ BrdU+	% neurod/ BrdU+ per specific cell type	only neuroD/ HuC/D+	neurod/ HuC/D+ and triple+	% triple+ per specific cell type	only HuC/D+	HuC/D+ and HuC/D/ BrdU+	% HuC/D/ BrdU+ per specific cell type
j.2	5	1	9	9	100	0	0	0	0	0	0									
j.2	5	2	15	15	100	0	0	0	0	0	0	21	21	0	0	0		53	53	0
j.2	5	3	30	25	83,33333333	2	6,666666667	0	0	3	10	44	46	4,347826087	16	19	15,78947368	52	52	0
j.2	5	4	28	21	75	5	17,85714286	0	0	2	7,142857143	32	37	13,51351351	13	15	13,33333333	91	91	0
j.2	5	5	21	16	76,19047619	4	19,04761905	0	0	1	4,761904762	7	11	36,36363636	25	26	3,846153846	85	85	0
j.2	5	6	24	24	100	0	0	0	0	0	0	0	0	0	43	43	0	81	81	0
j.2	5	7	28	28	100	0	0	0	0	0	0									
j.2	5	8	20	19	95	0	0	0	0	1	5									
j.2	6	4	32	30	93,75	2	6,25	0	0	0	0									
j.2	6	5	27	24	88,88888889	2	7,407407407	0	0	1	3,703703704									
j.2	6	6	30	30	100	0	0	0	0	0	0									
j.2	6	7	27	22	81,48148148	2	7,407407407	0	0	3	11,11111111									
		Sum	291	263	1093,64418	17	64,63624339	0	0	11	41,71957672	104	115	54,22497596	97	103	32,96896086	362	362	0
		Average	24,25	21,91666667	91,13701499	1,416666667	5,386353616	0	0	0,916666667	3,476631393	20,8	23	10,84499519	19,4	20,6	8,242240216	72,4	72,4	0
		SD	6,850680125	6,359793212	9,804896647	1,729862492	6,920207515	0	0	1,164500153	4,165079572	17,93599732	18,72164523	15,29512247	15,94678651	15,72577502	7,530826898	18,5148589	18,5148589	0

Slide	Row	Head	BrdU+	only BrdU	% only per all BrdU	neurod/ BrdU+	% neurod/ BrdU per all BrdU	BrdU/ HuC/D+	% HuC/D/ BrdU per all BrdU	triple+	% triple+ per all BrdU	only neurod+	only neurod+ and neurod/ BrdU+	% neurod/ BrdU+ per specific cell type	only neuroD/ HuC/D+	neurod/ HuC/D+ and triple+	% triple+ per specific cell type	only HuC/D+	HuC/D+ and HuC/D/ BrdU+	% HuC/D/ BrdU+ per specific cell type
h.2	5	5	16	16	100	0	0	0	0	0	0									
h.2	5	6	16	16	100	0	0	0	0	0	0									
h.2	5	7	18	16	88,88888889	2	11,11111111	0	0	0	0									
h.2	5	8	21	21	100	0	0	0	0	0	0									
h.2	5	9	21	20	95,23809524	0	0	1	4,761904762	0	0									
h.2	5	10	18	17	94,44444444	1	5,555555556	0	0	0	0									
h.3	1	lost																		
h.3	1	lost																		
h.3	1	3	8	4	50	4	50	0	0	0	0	14	18	22,22222222	0	0		27	27	0
h.3	1	4	19	18	94,73684211	0	0	1	5,263157895	0	0	23	23	0	3	3	0	68	69	1,449275362
h.3	1	5	19	17	89,47368421	2	10,52631579	0	0	0	0	14	16	12,5	1	1	0	50	50	0
h.3	1	6	10	9	90	0	0	0	0	1	10	10	10	0	1	2	50	49	49	0
		Sum	166	154	902,7819549	9	77,19298246	2	10,02506266	1	10	61	67	34,72222222	5	6	50	194	195	1,449275362
		Average	16,6	15,4	90,27819549	0,9	7,719298246	0,2	1,002506266	0,1	1	15,25	16,75	8,680555556	1,25	1,5	16,66666667	48,5	48,75	0,362318841
		SD	4,376706017	5,125101625	14,79626849	1,370320319	15,52506453	0,421637021	2,116768498	0,316227766	3,16227766	5,5	5,377421935	10,78067687	1,258305739	1,290994449	28,86751346	16,78292783	17,17313794	0,724637681

Slide	Row	Head	BrdU+	only BrdU	% only per all BrdU	neurod/ BrdU+	% neurod/ BrdU per all BrdU	BrdU/ HuC/D+	% HuC/D/ BrdU per all BrdU	triple+	% triple+ per all BrdU	only neurod+	only neurod+ and neurod/ BrdU+	% neurod/ BrdU+ per specific cell type	only neuroD/ HuC/D+	neurod/ HuC/D+ and triple+	% triple+ per specific cell type	only HuC/D+	HuC/D+ and HuC/D/ BrdU+	% HuC/D/ BrdU+ per specific cell type
l.2	2	2	11	5	45,45454545	3	27,27272727	0	0	3	27,27272727									
l.2	2	1	18	10	55,55555556	7	38,88888889	1	5,555555556	0	0	39	46	15,2173913	35	35	0	62	63	1,587301587
l.2	3	11	43	30	69,76744186	12	27,90697674	0	0	1	2,325581395	42	54	22,22222222	38	39	2,564102564	70	70	0
l.2	3	10	40	31	77,5	8	20	0	0	1	2,5	31	39	20,51282051	15	16	6,25	78	78	0
l.2	3	9	32	27	84,375	5	15,625	0	0	0	0	46	51	9,803921569	12	12	0	59	59	0
l.2	3	8	35	27	77,14285714	6	17,14285714	0	0	2	5,714285714	36	42	14,28571429	8	10	20	49	49	0
l.2	3	7	19	17	89,47368421	2	10,52631579	0	0	0	0									
l.2	3	6	28	28	100	0	0	0	0	0	0									
l.2	3	5	32	32	100	0	0	0	0	0	0									
l.2	3	4	18	17	94,44444444	0	0	0	0	1	5,555555556									
l.2	3	3	21	21	100	0	0	0	0	0	0									
l.2	3	2	10	10	100	0	0	0	0	0	0									
		Sum	307	255	993,7135287	43	157,3627658	1	5,555555556	8	43,36814994	194	232	82,04206989	108	112	28,81410256	318	319	1,587301587
		Average	25,58333333	21,25	82,80946072	3,583333333	13,11356382	0,083333333	0,462962963	0,666666667	3,614012495	38,8	46,4	16,40841398	21,6	22,4	5,762820513	63,6	63,8	0,317460317
		SD	10,96654693	9,304202374	18,4214654	4,010403139	13,55185834	0,288675135	1,603750748	0,984731928	7,759124861	5,718391382	6,188699379	5,004753448	13,86722755	13,57571361	8,360421949	11,01362792	10,98635517	0,70986285

Summary
7dpt

Sample	BrdU+	only BrdU	% only per all BrdU	neurod/ BrdU+	% neurod/ BrdU per all BrdU	BrdU/ HuC/D+	% HuC/D/ BrdU per all BrdU	triple+	% triple+ per all BrdU	only neurod+	only neurod+ and neurod/ BrdU+	% neurod/ BrdU+ per specific cell type	only neuroD/ HuC/D+	neurod/ HuC/D+ and triple+	% triple+ per specific cell type	only HuC/D+	HuC/D+ and HuC/D/ BrdU+	% HuC/D/ BrdU+ per specific cell type
B-k	20,66666667	19,16666667	92,34619531	1,333333333	6,860153895	0,083333333	0,396825397	0,083333333	0,396825397	12	13,2	10,52380952	4	4	0	32,8	32,8	0
B-j	24,25	21,91666667	91,13701499	1,416666667	5,386353616	0	0	0,916666667	3,476631393	20,8	23	10,84499519	19,4	20,6	8,242240216	72,4	72,4	0
B-h	16,6	15,4	90,27819549	0,9	7,719298246	0,2	1,002506266	0,1	1	15,25	16,75	8,680555556	1,25	1,5	16,66666667	48,5	48,75	0,362318841
B-i	25,58333333	21,25	82,80946072	3,583333333	13,11356382	0,083333333	0,462962963	0,666666667	3,614012495	38,8	46,4	16,40841398	21,6	22,4	5,762820513	63,6	63,8	0,317460317
Sum	87,1	77,73333333	356,5708665	7,233333333	33,07936958	0,366666667	1,862294625	1,766666667	8,487469285	86,85	99,35	46,45777425	46,25	48,5	30,6717274	217,3	217,75	0,679779158
Average	21,775	19,43333333	89,14271663	1,808333333	8,269842394	0,091666667	0,465573656	0,441666667	2,121867321	21,7125	24,8375	11,61444356	11,5625	12,125	7,667931849	54,325	54,4375	0,16994479
SD	4,026497881	2,932922951	4,306543248	1,204812879	3,369790563	0,082214714	0,412225098	0,41688883	1,66295308	11,95703245	14,93493527	3,335235353	10,41980286	10,89812675	6,921793757	17,41634768	17,42447393	0,197088026

15dpt

Slide	Row	Head	BrdU+	only BrdU	% only per all BrdU	neurod/ BrdU+	% neurod/ BrdU per all BrdU	BrdU/ HuC/D+	% HuC/D/ BrdU per all BrdU	triple+	% triple+ per all BrdU	only neurod+	only neurod+ and neurod/ BrdU+	% neurod/ BrdU+ per specific cell type	only neuroD/ HuC/D+	neurod/ HuC/D+ and triple+	% triple+ per specific cell type	only HuC/D+	HuC/D+ and HuC/D/ BrdU+	% HuC/D/ BrdU+ per specific cell type
m.2	2	7	51	41	80,39215686	5	9,803921569	0	0	11	21,56862745									
m.2	2	6	71	65	91,54929577	3	4,225352113	0	0	5	7,042253521									
m.2	2	5	45	37	82,22222222	4	8,888888889	0	0	5	11,11111111									
m.2	2	4	26	18	69,23076923	4	15,38461538	0	0	5	19,23076923									
m.2	2	3	20	14	70	3	15	0	0	0	0									
m.2	2	2	19	15	78,94736842	2	10,52631579	0	0	0	0									
m.2	2	1	4	4	100	0	0	0	0	0	0									
m.2	3	lost																		
m.2	3	11	64	55	85,9375	4	6,25	1	1,5625	7	10,9375	46	50	8	17	24	29,16666667	56	57	1,754385965
m.2	3	10	59	43	72,88135593	8	13,55932203	0	0	5	8,474576271	14	22	36,36363636	14	19	26,31578947	65	65	0
m.2	3	9	72	58	80,55555556	7	9,722222222	0	0	5	6,944444444	14	21	33,33333333	4	9	55,55555556	55	55	0
m.2	3	8	54	50	92,59259259	2	3,703703704	0	0	4	7,407407407	16	18	11,11111111	0	4	100	42	42	0
	Sum		485	400	904,3088166	42	97,06434417	1	1,5625	47	92,71668944	90	111	88,80808081	35	56	211,0380117	218	219	1,754385965
	Average		44,09090909	36,36363636	82,20989242	3,818181818	8,824031064	0,090909091	0,142045455	4,272727273	8,428789949	22,5	27,75	22,2020202	8,75	14	52,75950292	54,5	54,75	0,438596491
	SD		23,26565944	20,56342738	9,729613643	2,272363607	4,900311343	0,301511345	0,471111476	3,319364671	7,218941352	15,69500982	14,93039406	14,71012289	8,057087977	9,128709292	34,13392437	9,469248474	9,53502316	0,877192982

Slide	Row	Head	BrdU+	only BrdU	% only per all BrdU	neurod/ BrdU+	% neurod/ BrdU per all BrdU	BrdU/ HuC/D+	% HuC/D/ BrdU per all BrdU	triple+	% triple+ per all BrdU	only neurod+	only neurod+ and neurod/ BrdU+	% neurod/ BrdU+ per specific cell type	only neuroD/ HuC/D+	neurod/ HuC/D+ and triple+	% triple+ per specific cell type	only HuC/D+	HuC/D+ and HuC/D/ BrdU+	% HuC/D/ BrdU+ per specific cell type
p.3	1	1	4	4	100	0	0	0	0	0	0									
p.3	1	2	10	10	100	0	0	0	0	0	0									
p.3	1	3	18	16	88,88888889	2	11,11111111	0	0	0	0	8	10	20	1	1	0	36	36	0
p.3	1	4	26	26	100	0	0	0	0	0	0	12	12	0	1	1	0	27	27	0
p.3	1	5	22	22	100	0	0	0	0	0	0	14	14	0	5	5	0	41	41	0
p.3	1	6	34	31	91,17647059	0	0	0	0	3	8,823529412	14	14	0	8	11	27,27272727	35	35	0
p.3	1	7	24	24	100	0	0	0	0	0	0	17	17	0	2	2	0	35	35	0
p.3	1	8	38	36	94,73684211	2	5,263157895	0	0	0	0									
p.3	1	9	24	23	95,83333333	0	0	1	4,166666667	0	0									
p.3	1	10	24	22	91,66666667	0	0	0	0	2	8,333333333									
p.3	2	9	33	33	100	0	0	0	0	0	0									
p.3	2	10	32	29	90,625	3	9,375	0	0	0	0									
	Sum		289	276	1152,927202	7	25,74926901	1	4,166666667	5	17,15686275	65	67	20	17	20	27,27272727	174	174	0
	Average		24,08333333	23	96,0772668	0,583333333	2,145772417	0,083333333	0,347222222	0,416666667	1,429738562	13	13,4	4	3,4	4	5,454545455	34,8	34,8	0
	SD		9,912878064	9,34198733	4,462515024	1,083624669	4,087632955	0,288675135	1,202813061	0,99620492	3,340784985	31,31662479	2,607680962	8,94427191	3,049590136	4,242640687	12,19673442	5,019960159	5,019960159	0

Slide	Row	Head	BrdU+	only BrdU	% only per all BrdU	neurod/ BrdU+	% neurod/ BrdU per all BrdU	BrdU/ HuC/D+	% HuC/D/ BrdU per all BrdU	triple+	% triple+ per all BrdU	only neurod+	only neurod+ and neurod/ BrdU+	% neurod/ BrdU+ per specific cell type	only neuroD/ HuC/D+	neurod/ HuC/D+ and triple+	% triple+ per specific cell type	only HuC/D+	HuC/D+ and HuC/D/ BrdU+	% HuC/D/ BrdU+ per specific cell type
q.3	1	1	6	6	100	0	0	0	0	0	0									
q.3	1	2	15	12	80	3	20	0	0	0	0									
q.3	1	3	11	10	90,90909091	1	9,090909091	0	0	0	0									
q.3	1	4	7	7	100	0	0	0	0	0	0									
q.3	1	5	14	14	100	0	0	0	0	0	0	19	19	0	1	1	0	48	48	0
q.3	1	6	21	20	95,23809524	0	0	0	0	1	4,761904762	47	47	0	8	9	11,11111111	67	67	0
q.3	1	7	19	15	78,94736842	3	15,78947368	0	0	1	5,263157895	45	48	6,25	6	7	14,28571429	74	74	0
q.3	1	8	10	8	80	0	0	0	0	2	20	33	33	0	13	15	13,33333333	81	81	0
q.3	1	9	14	12	85,71428571	1	7,142857143	0	0	1	7,142857143	19	20	5	11	12	8,333333333	58	58	0
q.3	2	8	15	15	100	0	0	0	0	0	0									
q.3	2	9	5	4	80	0	0	0	0	1	20									
q.3	2	10	5	5	100	0	0	0	0	0	0									
	Sum		142	128	1090,80884	8	52,02323992	0	0	6	57,1679198	163	167	11,25	39	44	47,06349206	328	328	0
	Average		11,83333333	10,66666667	90,90073669	0,666666667	4,335269993	0	0	0,5	4,763993317	32,6	33,4	2,25	7,8	8,8	9,412698413	65,6	65,6	0
	SD		5,390789002	4,849242365	9,337393936	1,154700538	7,118718759	0	0	0,674199862	7,56216292	13,52035502	14,01071019	3,112474899	4,65832588	5,310367219	5,73947271	13,01153335	13,01153335	0

Slide	Row	Head	BrdU+	only BrdU	% only per all BrdU	neurod/ BrdU+	% neurod/ BrdU per all BrdU	BrdU/ HuC/D+	% HuC/D/ BrdU per all BrdU	triple+	% triple+ per all BrdU	only neurod+	only neurod+ and neurod/ BrdU+	% neurod/ BrdU+ per specific cell type	only neuroD/ HuC/D+	neurod/ HuC/D+ and triple+	% triple+ per specific cell type	only HuC/D+	HuC/D+ and HuC/D/ BrdU+	% HuC/D/ BrdU+ per specific cell type
n.2	5	1	5	5	100	0	0	0	0	0	0									
n.2	5	2	11	11	100	0	0	0	0	0	0									
n.2	5	3	10	9	90	1	10	0	0	0	0									
n.2	5	4	17	17	100	0	0	0	0	0	0									
n.2	5	5	20	20	100	0	0	0	0	0	0									
n.2	6	1	12	11	91,66666667	0	0	0	0	1	8,333333333	28	28	0	3	4	25	51	51	0
n.2	6	2	6	6	100	0	0	0	0	0	0	31	31	0	6	6	0	63	63	0
n.2	6	3	18	18	100	0	0	0	0	0	0	32	32	0	1	1	0	56	56	0
n.2	6	4	12	11	91,66666667	1	8,333333333	0	0	0	0	8	9	11,11111111	1	1	0	37	37	0
n.2	6	5	24	22	91,66666667	0	0	0	0	2	8,333333333	19	19	0	0	2	100	50	50	0
n.2	6	6	8	8	100	0	0	0	0	0	0									
n.2	6	lost																		
	Sum		143	138	1065	2	18,33333333	0	0	3	16,66666667	118	119	11,11111111	11	14	125	257	257	0
	Average		13	12,54545455	96,81818182	0,181818182	1,666666667	0	0	0,272727273	1,515151515	23,6	23,8	2,222222222	2,2	2,8	25	51,4	51,4	0
	SD		6,033241252	5,785561967	4,438126823	0,404519917	3,726779962	0	0	0,646669791	3,370999312	10,11434625	9,731392501	4,96903995	2,387467277	2,167948339	43,30127019	9,555103348	9,555103348	0

Summary 15dpt

Sample	BrdU+	only BrdU	% only per all BrdU	neurod/ BrdU+	% neurod/ BrdU per all BrdU	BrdU/ HuC/D+	% HuC/D/ BrdU per all BrdU	triple+	% triple+ per all BrdU	only neurod+	only neurod+ and neurod/ BrdU+	% neurod/ BrdU+ per specific cell type	only neuroD/ HuC/D+	neurod/ HuC/D+ and triple+	% triple+ per specific cell type	only HuC/D+	HuC/D+ and HuC/D/ BrdU+	% HuC/D/ BrdU+ per specific cell type
B-m	44,09090909	36,36363636	82,20989242	3,818181818	8,824031064	0,090909091	0,142045455	4,272727273	8,428789949	22,5	27,75	22,2020202	8,75	14	52,75950292	54,5	54,75	0,438596491
B-p	24,08333333	23	96,0772668	0,583333333	2,145772417	0,083333333	0,347222222	0,416666667	1,429738562	13	13,4	4	3,4	4	5,454545455	34,8	34,8	0
B-q	11,83333333	10,66666667	90,90073669	0,666666667	4,335269993	0	0	0,5	4,763993317	32,6	33,4	2,25	7,8	8,8	9,412698413	65,6	65,6	0
B-n	13	12,54545455	96,81818182	0,181818182	1,666666667	0	0	0,272727273	1,515151515	23,6	23,8	2,222222222	2,2	2,8	25	51,4	51,4	0
Sum	93,00757576	82,57575758	366,0060777	5,25	16,97174014	0,174242424	0,489267677	5,462121212	16,13767334	91,7	98,35	30,67424242	22,15	29,6	92,62674679	206,3	206,55	0,438596491
Average	23,25189394	20,64393939	91,50151943	1,3125	4,242935035	0,043560606	0,122316919	1,365530303	4,034418336	22,925	24,5875	7,668560606	5,5375	7,4	23,1566867	51,575	51,6375	0,109649123
SD	14,94925527	11,80100733	6,730518439	1,683811893	3,26752793	0,05039445	0,164209691	1,940403531	3,315310119	8,015557789	8,434885397	9,724594003	3,222156369	5,106858134	21,46305004	12,7369214	12,75665676	0,219298246

28dpt

Slide	Row	Head	BrdU+	only BrdU	% only per all BrdU	neurod/ BrdU+	% neurod/ BrdU per all BrdU	BrdU/ HuC/D+	% HuC/D/ BrdU per all BrdU	triple+	% triple+ per all BrdU	only neurod+	only neurod+ and neurod/ BrdU+	% neurod/ BrdU+ per specific cell type	only neuroD/ HuC/D+	neurod/ HuC/D+ and triple+	% triple+ per specific cell type	only HuC/D+	HuC/D+ and HuC/D/ BrdU+	% HuC/D/ BrdU+ per specific cell type
4.3		4 3	2	2	100	0	0	0	0	0	0									
4.3		4 4	15	15	100	0	0	0	0	0	0									
4.3		4 5	3	3	100	0	0	0	0	0	0									
4.3		4 6	21	18	85,71428571	3	14,28571429	0	0	0	0									
4.3		4 7	24	18	75	5	20,83333333	0	0	1	4,166666667									
4.3		4 8	17	16	94,11764706	0	0	0	0	1	5,882352941									
4.3		4 9	27	22	81,48148148	2	7,407407407	0	0	3	11,11111111									
4.3		4 10	19	13	68,42105263	3	15,78947368	0	0	3	15,78947368	53	56	5,357142857	17	20	15	72	72	0
4.3		3 1	3	2	66,66666667	1	33,33333333	0	0	0	0	19	20	5	13	13	0	58	58	0
4.3		3 2	3	3	100	0	0	0	0	0	0	12	12	0	12	12	0	84	84	0
4.3		3 3	13	12	92,30769231	1	7,692307692	0	0	0	0	37	38	2,631578947	16	16	0	91	91	0
4.3		3 4	21	16	76,19047619	3	14,28571429	1	4,761904762	1	4,761904762	22	25	12	8	9	11,11111111	77	78	1,282051282
		Sum	168	140	1039,899302	18	113,627284	1	4,761904762	9	41,71150917	143	151	24,9887218	66	70	26,11111111	382	383	1,282051282
		Average	14	11,66666667	86,65827517	1,5	9,468940335	0,083333333	0,396825397	0,75	3,475959097	28,6	30,2	4,997744361	13,2	14	5,222222222	76,4	76,6	0,256410256
		SD	9,09545341	7,227892102	12,80981807	1,678744119	10,62039608	0,288675135	1,374643498	1,138180366	5,243313437	16,41036258	17,23948955	4,464777258	3,563705936	4,183300133	7,281805501	12,54192968	12,561847	0,573350763

Slide	Row	Head	BrdU+	only BrdU	% only per all BrdU	neurod/ BrdU+	% neurod/ BrdU per all BrdU	BrdU/ HuC/D+	% HuC/D/ BrdU per all BrdU	triple+	% triple+ per all BrdU	only neurod+	only neurod+ and neurod/ BrdU+	% neurod/ BrdU+ per specific cell type	only neuroD/ HuC/D+	neurod/ HuC/D+ and triple+	% triple+ per specific cell type	only HuC/D+	HuC/D+ and HuC/D/ BrdU+	% HuC/D/ BrdU+ per specific cell type
5.3		3 2	12	12	100	0	0	0	0	0	0									
5.3		3 3	23	22	95,65217391	1	4,347826087	0	0	0	0									
5.3		3 4	37	34	91,89189189	2	5,405405405	0	0	1	2,702702703									
5.3		3 5	34	24	70,58823529	8	23,52941176	1	2,941176471	1	2,941176471	32	40	20	6	7	14,28571429	50	51	1,960784314
5.3		3 6	56	50	89,28571429	5	8,928571429	0	0	1	1,785714286	25	30	16,66666667	7	8	12,5	53	53	0
5.3		3 7	52	29	55,76923077	18	34,61538462	4	7,692307692	1	1,923076923	20	38	47,36842105	2	3	33,33333333	48	52	7,692307692
5.3		3 8	52	38	73,07692308	11	21,15384615	0	0	3	5,769230769	11	22	50	1	4	75	43	43	0
5.3		3 9	56	42	75	6	10,71428571	3	5,357142857	5	8,928571429	34	40	15	1	6	83,33333333	61	64	4,6875
5.3		3 10	44	35	79,54545455	6	13,63636364	1	2,272727273	2	4,545454545									
5.3		2 1	3	3	100	0	0	0	0	0	0									
5.3		2 2	5	4	80	1	20	0	0	0	0									
5.3		2 3	11	10	90,90909091	1	9,090909091	0	0	0	0									
		Sum	385	303	1001,718715	59	151,4220039	9	18,26335429	14	28,59592713	122	170	149,0350877	17	28	218,452381	255	263	14,34059201
		Average	32,08333333	25,25	83,47655956	4,916666667	12,61850032	0,75	1,521946191	1,166666667	2,382993927	24,4	34	29,80701754	3,4	5,6	43,69047619	51	52,6	2,868118401
		SD	20,4870617	15,39849461	13,46865012	5,418123347	10,44403709	1,356801051	2,591779715	1,527525232	2,834251048	9,343446901	7,874007874	17,35117875	2,880972058	2,073644135	33,52834114	6,670832032	7,503332593	3,311284237

Slide	Row	Head	BrdU+	only BrdU	% only per all BrdU	neurod/ BrdU+	% neurod/ BrdU per all BrdU	BrdU/ HuC/D+	% HuC/D/ BrdU per all BrdU	triple+	% triple+ per all BrdU	only neurod+	only neurod+ and neurod/ BrdU+	% neurod/ BrdU+ per specific cell type	only neuroD/ HuC/D+	neurod/ HuC/D+ and triple+	% triple+ per specific cell type	only HuC/D+	HuC/D+ and HuC/D/ BrdU+	% HuC/D/ BrdU+ per specific cell type
6.2		5 4	18	17	94,44444444	0	0	0	0	1	5,555555556	33	33	0	6	7	14,28571429	60	60	0
6.2		5 5	12	7	58,33333333	5	41,66666667	0	0	0	0	27	32	15,625	3	3	0	32	32	0
6.2		5 6	23	20	86,95652174	1	4,347826087	0	0	2	8,695652174	21	22	4,545454545	18	20	10	66	66	0
6.2		5 7	19	25	131,5789474	0	0	0	0	0	0	9	9	0	0	0		67	67	0
6.2		5 lost																		
6.2		5 lost																		
6.3		1 1	2	2	100	0	0	0	0	0	0									
6.3		1 2	7	6	85,71428571	0	0	0	0	1	14,28571429									
6.3		1 3	8	8	100	0	0	0	0	0	0									
6.3		1 4	12	11	91,66666667	1	8,333333333	0	0	0	0									
6.3		1 5	13	12	92,30769231	1	7,692307692	0	0	0	0									
6.3		1 6	23	23	100	0	0	0	0	0	0									
		Sum	137	131	941,0018916	8	62,04013378	0	0	4	28,53692202	90	96	20,17045455	27	30	24,28571429	225	225	0
		Average	13,7	13,1	94,10018916	0,8	6,204013378	0	0	0,4	2,853692202	22,5	24	5,042613636	6,75	7,5	8,095238095	56,25	56,25	0
		SD	6,992853495	7,781031066	18,00912591	1,549193338	12,90449071	0	0	0,699205899	5,04562082	10,24695077	11,16542282	7,373148872	7,889866919	8,812869378	7,330859199	16,45954637	16,45954637	0

Slide	Row	Head	BrdU+	only BrdU	% only per all BrdU	neurod/ BrdU+	% neurod/ BrdU per all BrdU	BrdU/ HuC/D+	% HuC/D/ BrdU per all BrdU	triple+	% triple+ per all BrdU	only neurod+	only neurod+ and neurod/ BrdU+	% neurod/ BrdU+ per specific cell type	only neuroD/ HuC/D+	neurod/ HuC/D+ and triple+	% triple+ per specific cell type	only HuC/D+	HuC/D+ and HuC/D/ BrdU+	% HuC/D/ BrdU+ per specific cell type
1.3		3 5	23	22	95,65217391	0	0	1	4,347826087	0	0	13	13	0	1	1	0	37	38	2,631578947
1.3		3 6	28	28	100	0	0	0	0	0	0	14	14	0	3	3	0	45	45	0
1.3		3 7	33	33	100	0	0	0	0	0	0	15	15	0	3	3	0	37	37	0
1.3		3 8	25	24	96	0	0	1	4	0	0	13	13	0	1	1	0	45	46	2,173913043
1.3		3 9	20	20	100	0	0	0	0	0	0	7	7	0	0	0		39	39	0
1.3		2 lost																		
1.3		2 2	8	8	100	0	0	0	0	0	0									
1.3		2 3	17	16	94,11764706	1	5,882352941	0	0	0	0									
1.3		2 4	19	19	100	0	0	0	0	0	0									
1.3		2 5	26	24	92,30769231	2	7,692307692	0	0	0	0									
1.3		2 6	29	22	75,86206897	2	6,896551724	0	0	5	17,24137931									
1.3		2 7	41	39	95,12195122	0	0	0	0	2	4,87804878									
		Sum	269	255	1049,061533	5	20,47121236	2	8,347826087	7	22,11942809	62	62	0	8	8	0	203	205	4,805491991
		Average	24,45454545	23,18181818	95,36923031	0,454545455	1,861019305	0,181818182	0,758893281	0,636363636	2,010857099	12,4	12,4	0	1,6	1,6	0	40,6	41	0,961098398
		SD	8,721968085	8,268230546	7,065607075	0,820199532	3,213079178	0,404519917	1,690221363	1,566698904	5,259101743	3,130495168	3,130495168	0	1,341640786	1,341640786	0	4,098780306	4,183300133	1,325948248

Summary
28dpt

Sample	BrdU+	only BrdU	% only per all BrdU	neurod/ BrdU+	% neurod/ BrdU per all BrdU	BrdU/ HuC/D+	% HuC/D/ BrdU per all BrdU	triple+	% triple+ per all BrdU	only neurod+	only neurod+ and neurod/ BrdU+	% neurod/ BrdU+ per specific cell type	only neuroD/ HuC/D+	neurod/ HuC/D+ and triple+	% triple+ per specific cell type	only HuC/D+	HuC/D+ and HuC/D/ BrdU+	% HuC/D/ BrdU+ per specific cell type
B-4	14	11,66666667	86,65827517	1,5	9,468940335	0,083333333	0,396825397	0,75	3,475959097	28,6	30,2	4,997744361	13,2	14	5,222222222	76,4	76,6	0,256410256
B-5	32,08333333	25,25	83,47655956	4,916666667	12,61850032	0,75	1,521946191	1,166666667	2,382993927	24,4	34	29,80701754	3,4	5,6	43,69047619	51	52,6	2,868118401
B-6	13,7	13,1	94,10018916	0,8	6,204013378	0	0	0,4	2,853692202	22,5	24	5,042613636	6,75	7,5	8,095238095	56,25	56,25	0
B-1	24,45454545	23,18181818	95,36923031	0,454545455	1,861019305	0,181818182	0,758893281	0,636363636	2,010857099	12,4	12,4	0	1,6	1,6	0	40,6	41	0,961098398
Sum	84,23787879	73,19848485	359,6042542	7,671212121	30,15247334	1,015151515	2,677664869	2,953030303	10,72350232	87,9	100,6	39,84737554	24,95	28,7	57,00793651	224,25	226,45	4,085627056
Average	21,0594697	18,29962121	89,90106355	1,91780303	7,538118336	0,253787879	0,669416217	0,738257576	2,680875581	21,975	25,15	9,961843885	6,2375	7,175	14,25198413	56,0625	56,6125	1,021406764
SD	8,889132232	6,908346626	5,753938699	2,046000068	4,602450224	0,339052182	0,647363197	0,320662229	0,632371628	6,873317976	9,446516113	13,44011857	5,108713961	5,171959654	19,90967929	15,03736319	14,82657383	1,296466018

Summary:

0dpt																		
Sample	BrdU+	only BrdU	% only per all BrdU	neurod/ BrdU+	% neurod/ BrdU per all BrdU	BrdU/ HuC/D+	% HuC/D/ BrdU per all BrdU	triple+	% triple+ per all BrdU	only neurod+	only neurod+ and neurod/ BrdU+	% neurod/ BrdU+ per specific cell type	only neuroD/ HuC/D+	neurod/ HuC/D+ and triple+	% triple+ per specific cell type	only HuC/D+	HuC/D+ and HuC/D/ BrdU+	% HuC/D/ BrdU+ per specific cell type
B-a	8,25	5,333333333	73,80291005	2,916666667	26,19708995	0	0	0	0	31,2	35,6	13,71924823	7,2	7,2	0	54,8	54,8	0
B-b	4,416666667	2,666666667	71,03896104	1,75	28,96103896	0	0	0	0	29,6	31,8	7,816017316	10,4	10,4	0	57,6	57,6	0
B-c	2,583333333	2,416666667	81,81818182	0,166666667	18,18181818	0	0	0	0	16,2	16,4	6,666666667	7,8	7,8	0	52,8	52,8	0
B-d	2,666666667	1,888888889	73,33333333	0,666666667	22,5	0	0	0,111111111	4,166666667	18	19	5,99469496	4	4,2	20	37,8	37,8	0
Sum	17,91666667	12,30555556	299,9933862	5,5	95,83994709	0	0	0,111111111	4,166666667	95	102,8	34,19662717	29,4	29,6	20	203	203	0
Average	4,479166667	3,076388889	74,99834656	1,375	23,95998677	0	0	0,027777778	1,041666667	23,75	25,7	8,549156794	7,35	7,4	5	50,75	50,75	0
SD	2,65219598	1,53916213	4,704190477	1,221906525	4,673825958	0	0	0,055555556	2,083333333	7,741446893	9,426911831	3,527812509	2,62995564	2,545584412	10	8,854942123	8,854942123	0

7dpt																		
Sample	BrdU+	only BrdU	% only per all BrdU	neurod/ BrdU+	% neurod/ BrdU per all BrdU	BrdU/ HuC/D+	% HuC/D/ BrdU per all BrdU	triple+	% triple+ per all BrdU	only neurod+	only neurod+ and neurod/ BrdU+	% neurod/ BrdU+ per specific cell type	only neuroD/ HuC/D+	neurod/ HuC/D+ and triple+	% triple+ per specific cell type	only HuC/D+	HuC/D+ and HuC/D/ BrdU+	% HuC/D/ BrdU+ per specific cell type
B-k	20,66666667	19,16666667	92,34619531	1,333333333	6,860153895	0,083333333	0,396825397	0,083333333	0,396825397	12	13,2	10,52380952	4	4	0	32,8	32,8	0
B-j	24,25	21,91666667	91,13701499	1,416666667	5,386353616	0	0	0,916666667	3,476631393	20,8	23	10,84499519	19,4	20,6	8,242240216	72,4	72,4	0
B-h	16,6	15,4	90,27819549	0,9	7,719298246	0,2	1,002506266	0,1	1	15,25	16,75	8,680555556	1,25	1,5	16,66666667	48,5	48,75	0,362318841
B-l	25,58333333	21,25	82,80946072	3,583333333	13,11356382	0,083333333	0,462962963	0,666666667	3,614012495	38,8	46,4	16,40841398	21,6	22,4	5,762820513	63,6	63,8	0,317460317
Sum	87,1	77,73333333	356,5708665	7,233333333	33,07936958	0,366666667	1,862294625	1,766666667	8,487469285	86,85	99,35	46,45777425	46,25	48,5	30,6717274	217,3	217,75	0,679779158
Average	21,775	19,43333333	89,14271663	1,808333333	8,269842394	0,091666667	0,465573656	0,441666667	2,121867321	21,7125	24,8375	11,61444356	11,5625	12,125	7,667931849	54,325	54,4375	0,16994479
SD	4,026497881	2,932922951	4,306543248	1,204812879	3,369790563	0,082214714	0,412225098	0,41688883	1,66295308	11,95703245	14,93493527	3,335235353	10,41980286	10,89812675	6,921793757	17,41634768	17,42447393	0,197088026

15dpt																		
Sample	BrdU+	only BrdU	% only per all BrdU	neurod/ BrdU+	% neurod/ BrdU per all BrdU	BrdU/ HuC/D+	% HuC/D/ BrdU per all BrdU	triple+	% triple+ per all BrdU	only neurod+	only neurod+ and neurod/ BrdU+	% neurod/ BrdU+ per specific cell type	only neuroD/ HuC/D+	neurod/ HuC/D+ and triple+	% triple+ per specific cell type	only HuC/D+	HuC/D+ and HuC/D/ BrdU+	% HuC/D/ BrdU+ per specific cell type
B-m	44,09090909	36,36363636	82,20989242	3,818181818	8,824031064	0,090909091	0,142045455	4,272727273	8,428789949	22,5	27,75	22,2020202	8,75	14	52,75950292	54,5	54,75	0,438596491
B-p	24,08333333	23	96,0772668	0,583333333	2,145772417	0,083333333	0,347222222	0,416666667	1,429738562	13	13,4	4	3,4	4	5,454545455	34,8	34,8	0
B-q	11,83333333	10,66666667	90,90073669	0,666666667	4,335269993	0	0	0,5	4,763993317	32,6	33,4	2,25	7,8	8,8	9,412698413	65,6	65,6	0
B-n	13	12,54545455	96,81818182	0,181818182	1,666666667	0	0	0,272727273	1,515151515	23,6	23,8	2,222222222	2,2	2,8	25	51,4	51,4	0
Sum	93,00757576	82,57575758	366,0060777	5,25	16,97174014	0,174242424	0,489267677	5,462121212	16,13767334	91,7	98,35	30,67424242	22,15	29,6	92,62674679	206,3	206,55	0,438596491
Average	23,25189394	20,64393939	91,50151943	1,3125	4,242935035	0,043560606	0,122316919	1,365530303	4,034418336	22,925	24,5875	7,668560606	5,5375	7,4	23,1566867	51,575	51,6375	0,109649123
SD	14,94925527	11,80100733	6,730518439	1,683811893	3,26752793	0,05039445	0,164209691	1,940403531	3,315310119	8,015557789	8,434885397	9,724594003	3,222156369	5,106858134	21,46305004	12,7369214	12,75665676	0,219298246

28dpt																		
Sample	BrdU+	only BrdU	% only per all BrdU	neurod/ BrdU+	% neurod/ BrdU per all BrdU	BrdU/ HuC/D+	% HuC/D/ BrdU per all BrdU	triple+	% triple+ per all BrdU	only neurod+	only neurod+ and neurod/ BrdU+	% neurod/ BrdU+ per specific cell type	only neuroD/ HuC/D+	neurod/ HuC/D+ and triple+	% triple+ per specific cell type	only HuC/D+	HuC/D+ and HuC/D/ BrdU+	% HuC/D/ BrdU+ per specific cell type
B-4	14	11,66666667	86,65827517	1,5	9,468940335	0,083333333	0,396825397	0,75	3,475959097	28,6	30,2	4,997744361	13,2	14	5,222222222	76,4	76,6	0,256410256
B-5	32,08333333	25,25	83,47655956	4,916666667	12,61850032	0,75	1,521946191	1,166666667	2,382993927	24,4	34	29,80701754	3,4	5,6	43,69047619	51	52,6	2,868118401
B-6	13,7	13,1	94,10018916	0,8	6,204013378	0	0	0,4	2,853692202	22,5	24	5,042613636	6,75	7,5	8,095238095	56,25	56,25	0
B-1	24,45454545	23,18181818	95,36923031	0,454545455	1,861019305	0,181818182	0,758893281	0,636363636	2,010857099	12,4	12,4	0	1,6	1,6	0	40,6	41	0,961098398
Sum	84,23787879	73,19848485	359,6042542	7,671212121	30,15247334	1,015151515	2,677664869	2,953030303	10,72350232	87,9	100,6	39,84737554	24,95	28,7	57,00793651	224,25	226,45	4,085627056
Average	21,0594697	18,29962121	89,90106355	1,91780303	7,538118336	0,253787879	0,669416217	0,738257576	2,680875581	21,975	25,15	9,961843885	6,2375	7,175	14,25198413	56,0625	56,6125	1,021406764
SD	8,889132232	6,908346626	5,753938699	2,046000068	4,602450224	0,339052182	0,647363197	0,320662229	0,632371628	6,873317976	9,446516113	13,44011857	5,108713961	5,171959654	19,90967929	15,03736319	14,82657383	1,296466018

Table S6: Quantification of BrdU-positive cells in adults.

0dpt

Slide	Row	Head	BrdU+	only BrdU	% only per all BrdU	neurod/ BrdU+	% neurod/ BrdU per all BrdU	BrdU/ HuC/D+	% HuC/D/ BrdU per all BrdU	triple+	% triple+ per all BrdU	only neurod+	only neurod+ and neurod/ BrdU+	% neurod/ BrdU+ per specific cell type	only neuroD/ HuC/D+	neurod/ HuC/D+ and triple+	% triple+ per specific cell type	only HuC/D+	HuC/D+ and HuC/D/ BrdU+	% HuC/D/ BrdU+ per specific cell type
419.4	1	3	0	0		0		0		0										
419.4	1	4	0	0		0		0		0		18	18	0	1	1	0	46	46	0
419.4	1	5	1	1	100	0	0	0	0	0	0	10	10	0	1	1	0	56	56	0
419.4	1	6	5	5	100	0	0	0	0	0	0	5	5	0	1	1	0	52	52	0
419.4	1	7	3	3	100	0	0	0	0	0	0	5	5	0	1	1	0	47	47	0
419.4	1	8	2	2	100	0	0	0	0	0	0	6	6	0	0	0		43	43	0
419.4	2	1	0	0		0		0		0										
419.4	2	2	0	0		0		0		0										
419.4	2	3	1	1	100	0	0	0	0	0	0									
419.4	2	4	1	1	100	0	0	0	0	0	0									
419.4	2	5	2	2	100	0	0	0	0	0	0									
419.4	2	6	0	0		0		0		0										
		Sum	15	15	700	0	0	0	0	0	0	44	44	0	4	4	0	244	244	0
		Average	1,25	1,25	100	0	0	0	0	0	0	8,8	8,8	0	0,8	0,8	0	48,8	48,8	0
		SD	1,544785952	1,544785952	0	0	0	0	0	0	0	5,540758071	5,540758071	0	0,447213595	0,447213595	0	5,167204273	5,167204273	0

Slide	Row	Head	BrdU+	only BrdU	% only per all BrdU	neurod/ BrdU+	% neurod/ BrdU per all BrdU	BrdU/ HuC/D+	% HuC/D/ BrdU per all BrdU	triple+	% triple+ per all BrdU	only neurod+	only neurod+ and neurod/ BrdU+	% neurod/ BrdU+ per specific cell type	only neuroD/ HuC/D+	neurod/ HuC/D+ and triple+	% triple+ per specific cell type	only HuC/D+	HuC/D+ and HuC/D/ BrdU+	% HuC/D/ BrdU+ per specific cell type
420.5	1	6	0	0		0		0		0										
420.5	1	7	1	1	100	0	0	0	0	0	0									
420.5	2	7	2	2	100	0	0	0	0	0	0	3	3	0	0	0		45	45	0
420.5	2	6	0	0		0		0		0		7	7	0	0	0		37	37	0
420.5	2	5	2	2	100	0	0	0	0	0	0	2	2	0	0	0		29	29	0
420.5	2	4	0	0		0		0		0		11	11	0	0	0		25	25	0
420.5	2	3	0	0		0		0		0		5	5	0	0	0		36	36	0
420.5	2	2	0	0		0		0		0										
420.5	2	1	0	0		0		0		0										
420.5	3	1	0	0		0		0		0										
420.5	3	2	0	0		0		0		0										
420.5	3	3	1	1	100	0	0	0	0	0	0									
		Sum	6	6	400	0	0	0	0	0	0	28	28	0	0	0	0	172	172	0
		Average	0,5	0,5	100	0	0	0	0	0	0	5,6	5,6	0	0	0	0	34,4	34,4	0
		SD	0,797724035	0,797724035	0	0	0	0	0	0	0	3,577708764	3,577708764	0	0	0	0	7,733045972	7,733045972	0

Slide	Row	Head	BrdU+	only BrdU	% only per all BrdU	neurod/ BrdU+	% neurod/ BrdU per all BrdU	BrdU/ HuC/D+	% HuC/D/ BrdU per all BrdU	triple+	% triple+ per all BrdU	only neurod+	only neurod+ and neurod/ BrdU+	% neurod/ BrdU+ per specific cell type	only neuroD/ HuC/D+	neurod/ HuC/D+ and triple+	% triple+ per specific cell type	only HuC/D+	HuC/D+ and HuC/D/ BrdU+	% HuC/D/ BrdU+ per specific cell type
422.3	2	3	0	0		0		0		0										
422.3	2	4																		
422.3	2	5	2	2	100	0	0	0	0	0	0	12	12	0	2	2	0	45	45	0
422.3	2	6	0	0		0		0		0		8	8	0	1	1	0	50	50	0
422.3	2	7	1	1	100	0	0	0	0	0	0	0	0		0	0		49	49	0
422.3	2	8	0	0		0		0		0		0	0		0	0		45	45	0
422.3	3	1	1	1	100	0	0	0	0	0	0									
422.3	3	2	0	0		0		0		0										
422.3	3	3	0	0		0		0		0										
422.3	3	4	1	1	100	0	0	0	0	0	0									
422.3	3	5	1	1	100	0	0	0	0	0	0									
422.3	3	6	0	0		0		0		0										
		Sum	6	6	500	0	0	0	0	0	0	20	20	0	3	3	0	189	189	0
		Average	0,545454545	0,545454545	100	0	0	0	0	0	0	5	5	0	0,75	0,75	0	47,25	47,25	0
		SD	0,687551651	0,687551651	0	0	0	0	0	0	0	6	6	0	0,957427108	0,957427108	0	2,62995564	2,62995564	0

Slide	Row	Head	BrdU+	only BrdU	% only per all BrdU	neurod/ BrdU+	% neurod/ BrdU per all BrdU	BrdU/ HuC/D+	% HuC/D/ BrdU per all BrdU	triple+	% triple+ per all BrdU	only neurod+	only neurod+ and neurod/ BrdU+	% neurod/ BrdU+ per specific cell type	only neuroD/ HuC/D+	neurod/ HuC/D+ and triple+	% triple+ per specific cell type	only HuC/D+	HuC/D+ and HuC/D/ BrdU+	% HuC/D/ BrdU+ per specific cell type
423.4	1	5	1	1	100	0	0	0	0	0	0	12	12	0	0	0		33	33	0
423.4	1	6	2	2	100	0	0	0	0	0	0	14	14	0	0	0		30	30	0
423.4	1	7	1	1	100	0	0	0	0	0	0	22	22	0	0	0		57	57	0
423.4	1	8	3	3	100	0	0	0	0	0	0	21	21	0	1	1	0	37	37	0
423.4	2	1	1	1	100	0	0	0	0	0	0	11	11	0	2	2	0	32	32	0
423.4	2	2	0	0		0		0		0										
423.4	2	3	0	0		0		0		0										
423.4	2	4	2	2	100	0	0	0	0	0	0									
423.4	2	5	0	0		0		0		0										
423.4	2	6	1	1	100	0	0	0	0	0	0									
423.4	2	7	0	0		0		0		0										
423.4	2	8	0	0		0		0		0										
		Sum	11	11	700	0	0	0	0	0	0	80	80	0	3	3	0	189	189	0
		Average	0,916666667	0,916666667	100	0	0	0	0	0	0	16	16	0	0,6	0,6	0	37,8	37,8	0
		SD	0,99620492	0,99620492	0	0	0	0	0	0	0	5,14781507	5,14781507	0	0,894427191	0,894427191	0	11,0317723	11,0317723	0

Slide	Row	Head	BrdU+	only BrdU	% only per all BrdU	neurod/ BrdU+	% neurod/ BrdU per all BrdU	BrdU/ HuC/D+	% HuC/D/ BrdU per all BrdU	triple+	% triple+ per all BrdU	only neurod+	only neurod+ and neurod/ BrdU+	% neurod/ BrdU+ per specific cell type	only neuroD/ HuC/D+	neurod/ HuC/D+ and triple+	% triple+ per specific cell type	only HuC/D+	HuC/D+ and HuC/D/ BrdU+	% HuC/D/ BrdU+ per specific cell type
421.3	3	1	1	1	100	0	0	0	0	0	0									
421.3	3	2	2	2	100	0	0	0	0	0	0									
421.3	3	3	1	1	100	0	0	0	0	0	0	7	7	0	0	0		62	62	0
421.3	3	4	0	0		0		0		0		7	7	0	1	1	0	58	58	0
421.3	3	5	1	1	100	0	0	0	0	0	0	2	2	0	2	2	0	33	33	0
421.3	3	6	0	0		0		0		0		8	8	0	0	0		47	47	0
421.3	3	7	0	0		0		0		0		4	4	0	0	0		35	35	0
421.3	4	1	1	1	100	0	0	0	0	0	0									
421.3	4	2	1	1	100	0	0	0	0	0	0									
421.3	4	3	0	0		0		0		0										
421.3	4	4	1	1	100	0	0	0	0	0	0									
421.3	4	5	0	0		0		0		0										
		Sum	8	8	700	0	0	0	0	0	0	28	28	0	3	3	0	235	235	0
		Average	0,666666667	0,666666667	100	0	0	0	0	0	0	5,6	5,6	0	0,6	0,6	0	47	47	0
		SD	0,651338947	0,651338947	0	0	0	0	0	0	0	2,50998008	2,50998008	0	0,894427191	0,894427191	0	13,09580085	13,09580085	0

Summary

0dpt

Sample	BrdU+	only BrdU	% only per all BrdU	neurod/ BrdU+	% neurod/ BrdU per all BrdU	BrdU/ HuC/D+	% HuC/D/ BrdU per all BrdU	triple+	% triple+ per all BrdU	only neurod+	only neurod+ and neurod/ BrdU+	% neurod/ BrdU+ per specific cell type	only neuroD/ HuC/D+	neurod/ HuC/D+ and triple+	% triple+ per specific cell type	only HuC/D+	HuC/D+ and HuC/D/ BrdU+	% HuC/D/ BrdU+ per specific cell type
419	1,25	1,25	100	0	0	0	0	0	0	8,8	8,8	0	0,8	0,8	0	48,8	48,8	0
420	0,5	0,5	100	0	0	0	0	0	0	5,6	5,6	0	0	0	0	34,4	34,4	0
422	0,545454545	0,545454545	100	0	0	0	0	0	0	5	5	0	0,75	0,75	0	47,25	47,25	0
423	0,916666667	0,916666667	100	0	0	0	0	0	0	16	16	0	0,6	0,6	0	37,8	37,8	0
421	0,666666667	0,666666667	100	0	0	0	0	0	0	5,6	5,6	0	0,6	0,6	0	47	47	0
Sum	3,878787879	3,878787879	500	0	0	0	0	0	0	41	41	0	2,75	2,75	0	215,25	215,25	0
Average	0,803030303	0,803030303	100	0	0	0	0	0	0	8,85	8,85	0	0,5375	0,5375	0	42,0625	42,0625	0
SD	0,351600042	0,351600042	0	0	0	0	0	0	0	5,050082508	5,050082508	0	0,368272997	0,368272997	0	7,051876228	7,051876228	0

7dpt

Slide	Row	Head	BrdU+	only BrdU	% only per all BrdU	neurod/ BrdU+	% neurod/ BrdU per all BrdU	BrdU/ HuC/D+	% HuC/D/ BrdU per all BrdU	triple+	% triple+ per all BrdU	only neurod+	only neurod+ and neurod/ BrdU+	% neurod/ BrdU+ per specific cell type	only neuroD/ HuC/D+	neurod/ HuC/D+ and triple+	% triple+ per specific cell type	only HuC/D+	HuC/D+ and HuC/D/ BrdU+	% HuC/D/ BrdU+ per specific cell type
424.5		1 2	0	0		0		0		0										
424.5		1 3	5	5	100	0	0	0	0	0	0									
424.5		1 4	5	5	100	0	0	0	0	0	0									
424.5	lost	5																		
424.5		1 6	0	0																
424.5	lost	7																		
424.5		1 8	4	4	100	0	0	0	0	0	0	10	10	0	1	1	0	49	49	0
424.5	lost	1																		
424.5		2 2	2	2	100	0	0	0	0	0	0	10	10	0	0	0		44	44	0
424.5		2 3	2	2	100	0	0	0	0	0	0	11	11	0	2	2	0	46	46	0
424.5		2 4	3	3	100	0	0	0	0	0	0	7	7	0	2	2	0	26	26	0
424.5		2 5	5	5	100	0	0	0	0	0	0	2	2	0	0	0		62	62	0
		Sum	26	26	700	0	0	0	0	0	0	30	30	0	4	4	0	178	178	0
		Average	2,888888889	2,888888889	100	0	0	0	0	0	0	7,5	7,5	0	1	1	0	44,5	44,5	0
		SD	2,02758751	2,02758751	0	0	0	0	0	0	0	4,041451884	4,041451884	0	1,154700538	1,154700538	0	14,73091986	14,73091986	0

Slide	Row	Head	BrdU+	only BrdU	% only per all BrdU	neurod/ BrdU+	% neurod/ BrdU per all BrdU	BrdU/ HuC/D+	% HuC/D/ BrdU per all BrdU	triple+	% triple+ per all BrdU	only neurod+	only neurod+ and neurod/ BrdU+	% neurod/ BrdU+ per specific cell type	only neuroD/ HuC/D+	neurod/ HuC/D+ and triple+	% triple+ per specific cell type	only HuC/D+	HuC/D+ and HuC/D/ BrdU+	% HuC/D/ BrdU+ per specific cell type
425.3		2 5	2	2	100	0	0	0	0	0	0									
425.3		2 6	0	0		0		0		0										
425.3		2 7	1	1	100	0	0	0	0	0	0									
425.3		3 1	0	0		0		0		0										
425.3		3 2	1	1	100	0	0	0	0	0	0									
425.3		3 3	0	0		0		0		0		0	0	x	x		x	x		
425.3		3 4	0	0		0		0		0		4	4	0	x	x	0	x	x	0
425.3		3 5	3	3	100	0	0	0	0	0	0	22	22	0	x	x	0	x	x	0
425.3		3 6	1	1	100	0	0	0	0	0	0	10	10	0	x	x	0	x	x	0
425.3		3 7	1	1	100	0	0	0	0	0	0	17	17	0	x	x	0	x	x	0
425.4		1 1	0	0		0		0		0										
425.4		1 2	1	1	100	0	0	0	0	0	0									
		Sum	10	10	700	0	0	0	0	0	0	53	53	0	x	x	0	x	x	0
		Average	0,833333333	0,833333333	100	0	0	0	0	0	0	10,6	10,6	0	x	x	0	x	x	0
		SD	0,937436867	0,937436867	0	0	0	0	0	0	0	9,044335244	9,044335244	0	x	x	0	x	x	0

Slide	Row	Head	BrdU+	only BrdU	% only per all BrdU	neurod/ BrdU+	% neurod/ BrdU per all BrdU	BrdU/ HuC/D+	% HuC/D/ BrdU per all BrdU	triple+	% triple+ per all BrdU	only neurod+	only neurod+ and neurod/ BrdU+	% neurod/ BrdU+ per specific cell type	only neuroD/ HuC/D+	neurod/ HuC/D+ and triple+	% triple+ per specific cell type	only HuC/D+	HuC/D+ and HuC/D/ BrdU+	% HuC/D/ BrdU+ per specific cell type
426.3		4 4	8	8	100	0	0	0	0	0	0									
426.3		4 5	5	5	100	0	0	0	0	0	0									
426.3		4 6	4	4	100	0	0	0	0	0	0									
426.3		4 7	4	4	100	0	0	0	0	0	0									
426.3		4 8	3	3	100	0	0	0	0	0	0									
426.4		1 1	0	0		0		0		0	#DIV/0!									
426.4		1 2									#DIV/0!									
426.4		1 3	3	3	100	0	0	0	0	0	0	lost			lost			lost		
426.4		1 4	4	4	100	0	0	0	0	0	0	lost			lost			lost		
426.4		1 5	4	4	100	0	0	0	0	0	0	lost			lost			lost		
426.4		1 6	5	5	100	0	0	0	0	0	0	lost			lost			lost		
426.4		1 7	4	3	75	1	25	0	0	0	0	lost			lost			lost		
		Sum	44	43	975	1	25	0	0	0	#DIV/0!	0	0	0	0	0	0	0	0	0
		Average	4	3,909090909	97,5	0,090909091	2,5	0	0	0	#DIV/0!									
		SD	1,897366596	1,921173884	7,90569415	0,301511345	7,90569415	0	0	0	#DIV/0!									

Slide	Row	Head	BrdU+	only BrdU	% only per all BrdU	neurod/ BrdU+	% neurod/ BrdU per all BrdU	BrdU/ HuC/D+	% HuC/D/ BrdU per all BrdU	triple+	% triple+ per all BrdU	only neurod+	only neurod+ and neurod/ BrdU+	% neurod/ BrdU+ per specific cell type	only neuroD/ HuC/D+	neurod/ HuC/D+ and triple+	% triple+ per specific cell type	only HuC/D+	HuC/D+ and HuC/D/ BrdU+	% HuC/D/ BrdU+ per specific cell type
427.4		1 2	2	2	100	0	0	0	0	0	0	18	0		1	0		36	0	
427.4		1 3	8	8	100	2	25	0	0	0	0	20	22	9,090909091	2	2	0	52	52	0
427.4		1 4	5	5	100	0	0	0	0	0	0	10	10	0	1	1	0	40	40	0
427.4		1 5	9	9	100	0	0	0	0	0	0	3	3	0	0	0		34	34	0
427.4		1 6	8	7	87,5	1	12,5	0	0	0	0	8	9	11,11111111	0	0		41	41	0
427.4		1 7	5	5	100	0	0	0	0	0	0	8	8	0	0	0		34	34	0
427.4		2 1	1	1	100	0	0	0	0	0	0									
427.4		2 2	4	3	75	1	25	0	0	0	0									
427.4		2 3	5	3	60	2	40	0	0	0	0									
427.4		2 4	3	3	100	0	0	0	0	0	0									
427.4		2 5	2	2	100	0	0	0	0	0	0									
427.4		2 6	3	3	100	0	0	0	0	0	0									
		Sum	55	51	1122,5	6	102,5	0	0	0	0	49	52	20,2020202	3	3	0	201	201	0
		Average	4,583333333	4,25	93,54166667	0,5	8,541666667	0	0	0	0	9,8	10,4	4,04040404	0,6	0,6	0	40,2	40,2	0
		SD	2,609713789	2,562846429	13,07575538	0,797724035	13,91771	0	0	0	0	6,260990337	7,021395873	5,57846516	0,894427191	0,894427191	0	7,362064928	7,362064928	0

Slide	Row	Head	BrdU+	only BrdU	% only per all BrdU	neurod/ BrdU+	% neurod/ BrdU per all BrdU	BrdU/ HuC/D+	% HuC/D/ BrdU per all BrdU	triple+	% triple+ per all BrdU	only neurod+	only neurod+ and neurod/ BrdU+	% neurod/ BrdU+ per specific cell type	only neuroD/ HuC/D+	neurod/ HuC/D+ and triple+	% triple+ per specific cell type	only HuC/D+	HuC/D+ and HuC/D/ BrdU+	% HuC/D/ BrdU+ per specific cell type
428.4		1 4	2	2	100	0	0	0	0	0	0	x	x		0	x	x	0	x	x	0
428.4		1 5	0	0		0		0		0	x	x		0	x	x	0	x	x	0
428.4		1 6	2	2	100	0	0	0	0	0	0	x	x		0	x	x	0	x	x	0
428.4		1 7	0	0		0		0		0	x	x		0	x	x	0	x	x	0
428.4		1 8	1	1	100	0	0	0	0	0	0	x	x		0	x	x	0	x	x	0
428.4		2 1	0	0		0		0		0										
428.4		2 2																		
428.4		2 3	0	0		0		0		0										
428.4		2 4	0	0		0		0		0										
428.4		2 5	0	0		0		0		0										
428.4		2 6	0	0		0		0		0										
428.4		2 7	1	1	100	0	0	0	0	0	0									
		Sum	6	6	400	0	0	0	0	0	0	x	x	0	x	x	0	x	x	0
		Average	0,545454545	0,545454545	100	0	0	0	0	0	0	x	x	0	x	x	0	x	x	0
		SD	0,820199532	0,820199532	0	0	0	0	0	0	0	x	x	0	x	x	0	x	x	0

Summary 7dpt

Sample	BrdU+	only BrdU	% only per all BrdU	neurod/ BrdU+	% neurod/ BrdU per all BrdU	BrdU/ HuC/D+	% HuC/D/ BrdU per all BrdU	triple+	% triple+ per all BrdU	only neurod+	only neurod+ and neurod/ BrdU+	% neurod/ BrdU+ per specific cell type	only neuroD/ HuC/D+	neurod/ HuC/D+ and triple+	% triple+ per specific cell type	only HuC/D+	HuC/D+ and HuC/D/ BrdU+	% HuC/D/ BrdU+ per specific cell type
424	2,888888889	2,888888889	100	0	0	0	0	0	0	7,5	7,5	0	1	1	0	44,5	44,5	0
425	0,833333333	0,833333333	100	0	0	0	0	0	0	10,6	10,6	0	x	x	0	x	x	0
426	4	3,909090909	97,5	0,090909091	2,5	0	0	0	0	lost	lost	lost	lost	lost	lost	lost	lost	lost
427	4,583333333	4,25	93,54166667	0,5	8,541666667	0	0	0	0	9,8	10,4	4,04040404	0,6	0,6	0	40,2	40,2	0
428	0,545454545	0,545454545	100	0	0	0	0	0	0	x	x	0	x	x	0	x	x	0
Sum	12,8510101	12,42676768	491,0416667	0,590909091	11,04166667	0	0	0	0	27,9	28,5	4,04040404	1,6	1,6	0	84,7	84,7	0
Average	2,57020202	2,485353535	98,20833333	0,118181818	2,208333333	0	0	0	0	9,3	9,5	1,01010101	0,8	0,8	0	42,35	42,35	0
SD	1,824479134	1,717281636	2,824434555	0,21704248	3,702242188	0	0	0	0	1,609347694	1,734935157	2,02020202	0,282842712	0,282842712	0	3,040559159	3,040559159	0

14dpt

Slide	Row	Head	BrdU+	only BrdU	% only per all BrdU	neurod/ BrdU+	% neurod/ BrdU per all BrdU	BrdU/ HuC/D+	% HuC/D/ BrdU per all BrdU	triple+	% triple+ per all BrdU	only neurod+	only neurod+ and neurod/ BrdU+	% neurod/ BrdU+ per specific cell type	only neuroD/ HuC/D+	neurod/ HuC/D+ and triple+	% triple+ per specific cell type	only HuC/D+	HuC/D+ and HuC/D/ BrdU+	% HuC/D/ BrdU+ per specific cell type
434.3	2	4	1	1	100	0	0	0	0	0	0									
434.3	2	5	4	4	100	0	0	0	0	0	0	8	8	0	3	3	0	54	54	0
434.3	2	6	2	2	100	0	0	0	0	0	0	13	13	0	0	0		40	40	0
434.3	2	7	1	0	0	1	100	0	0	0	0	11	12	8,333333333	0	0		47	47	0
434.3	2	8	1	1	100	0	0	0	0	0	0	5	5	0	0	0		63	63	0
434.3	3	lost																		
434.3	3	2	0	0		0		0		0										
434.3	3	3	0	0		0		0		0										
434.3	3	4	0	0		0		0		0										
434.3	3	5	0	0		0		0		0										
434.3	3	6	0	0		0		0		0										
434.3	3	7	2	2	100	0	0	0	0	0	0									
	Sum		11	10	500	1	100	0	0	0	0	37	38	8,333333333	3	3	0	204	204	0
	Average		1	0,909090909	83,33333333	0,090909091	16,66666667	0	0	0	0	9,25	9,5	2,083333333	0,75	0,75	0	51	51	0
	SD		1,264911064	1,300349603	40,82482905	0,301511345	40,82482905	0	0	0	0	3,5	3,696845502	4,166666667	1,5	1,5		9,831920803	9,831920803	0

Slide	Row	Head	BrdU+	only BrdU	% only per all BrdU	neurod/ BrdU+	% neurod/ BrdU per all BrdU	BrdU/ HuC/D+	% HuC/D/ BrdU per all BrdU	triple+	% triple+ per all BrdU	only neurod+	only neurod+ and neurod/ BrdU+	% neurod/ BrdU+ per specific cell type	only neuroD/ HuC/D+	neurod/ HuC/D+ and triple+	% triple+ per specific cell type	only HuC/D+	HuC/D+ and HuC/D/ BrdU+	% HuC/D/ BrdU+ per specific cell type
435.2	2	1	0	0		0		0		0		1	1	0	7	7	0	45	45	0
435.2	2	2	1	1	100	0	0	0	0	0	0	3	3	0	8	8	0	52	52	0
435.2	2	3	0	0		0		0		0		19	19	0	2	2	0	54	54	0
435.2	2	4	7	6	85,71428571	1	14,28571429	0	0	0	0	15	16	6,25	0	0		43	43	0
435.2	2	5	4	4	100	0	0	0	0	0	0	6	6	0	1	1	0	43	43	0
435.2	2	6	0	0		0		0		0										
435.2	2	7	1	1	100	0	0	0	0	0	0									
435.2	2	8	1	1	100	0	0	0	0	0	0									
435.2	3	1	1	1	100	0	0	0	0	0	0									
435.2	3	lost																		
435.2	3	3	1	1	100	0	0	0	0	0	0									
435.2	3	4	1	1	100	0	0	0	0	0	0									
	Sum		17	16	785,7142857	1	14,28571429	0	0	0	0	44	45	6,25	18	18	0	237	237	0
	Average		1,545454545	1,454545455	98,21428571	0,090909091	1,785714286	0	0	0	0	8,8	9	1,25	3,6	3,6	0	47,4	47,4	0
	SD		2,114882331	1,863525496	5,050762723	0,301511345	5,050762723	0	0	0	0	7,823042886	8,031189202	2,795084972	3,646916506	3,646916506	0	5,224940191	5,224940191	0

Slide	Row	Head	BrdU+	only BrdU	% only per all BrdU	neurod/ BrdU+	% neurod/ BrdU per all BrdU	BrdU/ HuC/D+	% HuC/D/ BrdU per all BrdU	triple+	% triple+ per all BrdU	only neurod+	only neurod+ and neurod/ BrdU+	% neurod/ BrdU+ per specific cell type	only neuroD/ HuC/D+	neurod/ HuC/D+ and triple+	% triple+ per specific cell type	only HuC/D+	HuC/D+ and HuC/D/ BrdU+	% HuC/D/ BrdU+ per specific cell type
437.3	1	1	1	1	100	0	0	0	0	0	0									
437.3	1	lost																		
437.3	1	3	5	5	100	0	0	0	0	0	0									
437.3	1	4	8	8	100	0	0	0	0	0	0									
437.3	1	lost																		
437.3	1	6	5	5	100	0	0	0	0	0	0	2	2	0	0	0		39	39	0
437.3	1	7	8	7	87,5	0	0	1	12,5	0	0	0	0		0	0		40	41	2,43902439
437.3	1	8	10	10	100	0	0	0	0	0	0	0	0		2	2	0	27	27	0
437.3	2	1	0	0		0		0		0		0	0		0	0		17	17	0
437.3	2	2	1	1	100	0	0	0	0	0	0	0	0		0	0		45	45	0
437.3	2	lost																		
437.3	2	lost																		
	Sum		38	37	687,5	0	0	1	12,5	0	0	2	2	0	2	2	0	168	169	2,43902439
	Average		4,75	4,625	98,21428571	0	0	0,125	1,785714286	0	0	0,4	0,4	0	0,4	0,4	0	33,6	33,8	0,487804878
	SD		3,770183777	3,662064211	4,724555913	0	0	0,353553391	4,724555913	0	0	0,894427191	0,894427191		0,894427191	0,894427191	#DIV/0!	11,39298029	11,54123044	1,090764867

Slide	Row	Head	BrdU+	only BrdU	% only per all BrdU	neurod/ BrdU+	% neurod/ BrdU per all BrdU	BrdU/ HuC/D+	% HuC/D/ BrdU per all BrdU	triple+	% triple+ per all BrdU	only neurod+	only neurod+ and neurod/ BrdU+	% neurod/ BrdU+ per specific cell type	only neuroD/ HuC/D+	neurod/ HuC/D+ and triple+	% triple+ per specific cell type	only HuC/D+	HuC/D+ and HuC/D/ BrdU+	% HuC/D/ BrdU+ per specific cell type
438.2	4	4	6	5	83,33333333	1	16,66666667	0	0	0	0	5	6	16,66666667	7	7	0	30	30	0
438.2		5	8	5	62,5	3	37,5	0	0	0	0	8	11	27,27272727	13	13	0	50	50	0
438.2		6	9	9	100	0	0	0	0	0	0	14	14	0	11	11	0	38	38	0
438.3	1	1	0	0		0		0		0		47	47	0	1	1	0	47	47	0
438.3		2	0	0		0		0		0		11	11	0	0	0		46	46	0
438.3		3	1	1	100	0	0	0	0	0	0									
438.3		4	0	0		0		0		0										
438.3		5	0	0		0		0		0										
438.3		lost		0																
438.3		7	4	1	25	3	75	0	0	0	0									
438.3	2	lost		0																
438.3		2	0	0		0		0		0										
	Sum		28	21	370,8333333	7	129,1666667	0	0	0	0	85	89	43,93939394	32	32	0	211	211	0
	Average		2,8	1,75	74,16666667	0,7	25,83333333	0	0	0	0	17	17,8	8,787878788	6,4	6,4	0	42,2	42,2	0
	SD		3,645392831	2,958039892	31,512784	1,251665557	31,512784	0	0	0	0	17,10263138	16,57407614	12,60402081	5,813776741	5,813776741	0	8,136338243	8,136338243	0

Slide	Row	Head	BrdU+	only BrdU	% only per all BrdU	neurod/ BrdU+	% neurod/ BrdU per all BrdU	BrdU/ HuC/D+	% HuC/D/ BrdU per all BrdU	triple+	% triple+ per all BrdU	only neurod+	only neurod+ and neurod/ BrdU+	% neurod/ BrdU+ per specific cell type	only neuroD/ HuC/D+	neurod/ HuC/D+ and triple+	% triple+ per specific cell type	only HuC/D+	HuC/D+ and HuC/D/ BrdU+	% HuC/D/ BrdU+ per specific cell type
436.2	3	1	0	0		0		0		0	x	x		0	x	x		0	x	x		0
436.2	3	2	0	0		0		0		0										
436.2	3	3	0	0		0		0		0										
436.2	3	4	1	1	100	0	0	0	0	0	0									
436.2	3	5	0	0		0		0		0										
436.2	3	6	3	3	100	0	0	0	0	0	0									
436.2	3	7	1	1	100	0	0	0	0	0	0									
436.2	3	8	0	0		0		0		0										
436.2	2	6	0	0		0		0		0	x	x		0	x	x		0	x	x		0
436.2	2	7	1	1	100	0	0	0	0	0	0	x	x	0	x	x		0	x	x		0
436.2	2	8	3	3	100	0	0	0	0	0	0	x	x	0	x	x		0	x	x		0
436.2	2	9	2	2	100	0	0	0	0	0	0	x	x	0	x	x		0	x	x		0
	Sum		11	11	600	0	0	0	0	0	0	0	0	0	0	0	0	0	0	0
	Average		0,916666667	0,916666667	100	0	0	0	0	0	0			0			0			0
	SD		1,164500153	1,164500153	0	0	0	0	0	0	0			0			0			0

Summary
14dpt

Sample	BrdU+	only BrdU	% only per all BrdU	neurod/ BrdU+	% neurod/ BrdU per all BrdU	BrdU/ HuC/D+	% HuC/D/ BrdU per all BrdU	triple+	% triple+ per all BrdU	only neurod+	only neurod+ and neurod/ BrdU+	% neurod/ BrdU+ per specific cell type	only neuroD/ HuC/D+	neurod/ HuC/D+ and triple+	% triple+ per specific cell type	only HuC/D+	HuC/D+ and HuC/D/ BrdU+	% HuC/D/ BrdU+ per specific cell type
434	1	0,909090909	83,33333333	0,090909091	16,66666667	0	0	0	0	9,25	9,5	2,083333333	0,75	0,75	0	51	51	0
435	1,545454545	1,454545455	98,21428571	0,090909091	1,785714286	0	0	0	0	8,8	9	1,25	3,6	3,6	0	47,4	47,4	0
437	4,75	4,625	98,21428571	0	0	0,125	1,785714286	0	0	0,4	0,4	0	0,4	0,4	0	33,6	33,8	0,487804878
438	2,8	1,75	74,16666667	0,7	25,83333333	0	0	0	0	17	17,8	8,787878788	6,4	6,4	0	42,2	42,2	0
436	0,916666667	0,916666667	100	0	0	0	0	0	0	x	x	0	x	x	0	x	x	0
Sum	11,01212121	9,65530303	453,9285714	0,881818182	44,28571429	0,125	1,785714286	0	0	35,45	36,7	12,12121212	11,15	11,15	0	174,2	174,4	0,487804878
Average	2,202424242	1,931060606	90,78571429	0,176363636	8,857142857	0,025	0,357142857	0	0	8,8625	9,175	2,424242424	2,7875	2,7875	0	43,55	43,6	0,097560976
SD	1,610733126	1,548432774	11,47825263	0,296229752	11,79070361	0,055901699	0,798595706	0	0	6,782007446	7,106980137	3,665543436	2,802491451	2,802491451	0	7,55314504	7,465476096	0,218152973

29dpt

Slide	Row	Head	BrdU+	only BrdU	% only per all BrdU	neurod/ BrdU+	% neurod/ BrdU per all BrdU	BrdU/ HuC/D+	% HuC/D/ BrdU per all BrdU	triple+	% triple+ per all BrdU	only neurod+	only neurod+ and neurod/ BrdU+	% neurod/ BrdU+ per specific cell type	only neuroD/ HuC/D+	neurod/ HuC/D+ and triple+	% triple+ per specific cell type	only HuC/D+	HuC/D+ and HuC/D/ BrdU+	% HuC/D/ BrdU+ per specific cell type
439.3		1	1	0	0		0		0		0									
439.3		1	2	0	0		0		0		0									
439.3		1	3	2	2	100	0	0	0	0	0	0								
439.3		1	4	0	0		0		0		0									
439.3		1	5	1	1	100	0	0	0	0	0	0								
439.3		1	6	2	2	100	0	0	0	0	0	0								
439.3		1	7	2	2	100	0	0	0	0	0	0	x	x		0	x	x	0	x	x	0
439.3		2	1	0	0		0		0		0	x	x	x		0	x	x	0	x	x	0
439.3		2	2	2	2	100	0	0	0	0	0	0	x	x		0	x	x	0	x	x	0
439.3		2	3	4	4	100	0	0	0	0	0	0	x	x		0	x	x	0	x	x	0
439.3		2	4	0	0		0		0		0	x	x	x		0	x	x	0	x	x	0
439.3		2	lost																			
		Sum	13	13	600	0	0	0	0	0	0	0	0	0	0	0	0	0	0	0	0	0
		Average	1,181818182	1,181818182	100	0	0	0	0	0	0	#DIV/0!	#DIV/0!	0	#DIV/0!	#DIV/0!	0	#DIV/0!	#DIV/0!	0
		SD	1,328019715	1,328019715	0	0	0	0	0	0	0	#DIV/0!	#DIV/0!	0	#DIV/0!	#DIV/0!	0	#DIV/0!	#DIV/0!	0

Slide	Row	Head	BrdU+	only BrdU	% only per all BrdU	neurod/ BrdU+	% neurod/ BrdU per all BrdU	BrdU/ HuC/D+	% HuC/D/ BrdU per all BrdU	triple+	% triple+ per all BrdU	only neurod+	only neurod+ and neurod/ BrdU+	% neurod/ BrdU+ per specific cell type	only neuroD/ HuC/D+	neurod/ HuC/D+ and triple+	% triple+ per specific cell type	only HuC/D+	HuC/D+ and HuC/D/ BrdU+	% HuC/D/ BrdU+ per specific cell type
440.3		1	1	0	0		0		0		0	38	38	0	10	10	0	60	60	0
440.3		1	2	0	0		0		0		0	37	37	0	4	4	0	64	64	0
440.3		1	3	8	2	25	5	62,5	0	0	1	12,5	30	35	14,28571429	4	5	20	39	39	0
440.3		1	4	6	2	33,33333333	4	66,66666667	0	0	0	0	31	35	11,42857143	3	3	0	56	56	0
440.3		1	5	1	1	100	0	0	0	0	0	0	19	19	0	1	1	0	48	48	0
440.2		3	3	0	0		0		0		0									
440.2		3	4	0	0		0		0		0									
440.2		3	5	2	2	100	0	0	0	0	0	0								
440.2		3	6	0	0		0		0		0									
440.2		3	7	0	0		0		0		0									
440.2		3	8	3	2	66,66666667	1	33,33333333	0	0	0	0								
440.2		3	9	1	1	100	0	0	0	0	0	0								
		Sum	21	10	425	10	162,5	0	0	1	12,5	155	164	25,71428571	22	23	20	267	267	0
		Average	1,75	0,833333333	70,83333333	0,833333333	27,08333333	0	0	0,083333333	2,083333333	31	32,8	5,142857143	4,4	4,6	4	53,4	53,4	0
		SD	2,667140109	0,937436867	34,86083444	1,749458791	31,81434861	0	0	0,288675135	5,103103631	7,582875444	7,823042886	7,114228342	3,361547263	3,361547263	8,94427191	9,989994995	9,989994995	0

Slide	Row	Head	BrdU+	only BrdU	% only per all BrdU	neurod/ BrdU+	% neurod/ BrdU per all BrdU	BrdU/ HuC/D+	% HuC/D/ BrdU per all BrdU	triple+	% triple+ per all BrdU	only neurod+	only neurod+ and neurod/ BrdU+	% neurod/ BrdU+ per specific cell type	only neuroD/ HuC/D+	neurod/ HuC/D+ and triple+	% triple+ per specific cell type	only HuC/D+	HuC/D+ and HuC/D/ BrdU+	% HuC/D/ BrdU+ per specific cell type
441.2		3	5	0	0		0		0		0									
441.2		3	6	2	2	100	0	0	0	0	0									
441.2		3	7	5	5	100	0	0	0	0	0									
441.2		3	8	3	3	100	0	0	0	0	0									
441.2		4	lost																	
441.2		4	2	0	0		0		0		0									
441.2		4	lost																	
441.2		4	4	1	1	100	0	0	0	0	0	6	6	0	0	0		45	45	0
441.2		4	5	0	0		0		0		0	8	8	0	0	0		49	49	0
441.2		4	6	0	0		0		0		0	21	21	0	0	0		37	37	0
441.2		4	7	1	1	100	0	0	0	0	0	15	15	0	1	1	0	35	35	0
441.2		4	8	0	0		0		0		0	0	0		0	0		26	26	0
		Sum	12	12	500	0	0	0	0	0	0	50	50	0	1	1	0	192	192	0
		Average	1,2	1,2	100	0	0	0	0	0	0	10	10	0	0,2	0,2	0	38,4	38,4	0
		SD	1,686548085	1,686548085	0	0	0	0	0	0	0	8,154753215	8,154753215	0	0,447213595	0,447213595	#DIV/0!	8,988882022	8,988882022	0

Slide	Row	Head	BrdU+	only BrdU	% only per all BrdU	neurod/ BrdU+	% neurod/ BrdU per all BrdU	BrdU/ HuC/D+	% HuC/D/ BrdU per all BrdU	triple+	% triple+ per all BrdU	only neurod+	only neurod+ and neurod/ BrdU+	% neurod/ BrdU+ per specific cell type	only neuroD/ HuC/D+	neurod/ HuC/D+ and triple+	% triple+ per specific cell type	only HuC/D+	HuC/D+ and HuC/D/ BrdU+	% HuC/D/ BrdU+ per specific cell type
443.2		3	3	2	66,66666667	1	33,33333333	0	0	0	0	4	5	20	0	0		38	38	0
443.2		3	4	11	11	100	0	0	0	0	0	6	6	0	1	1	0	37	37	0
443.2		3	5	10	10	100	0	0	0	0	0	8	8	0	0	0		45	45	0
443.2		3	6	6	6	100	0	0	0	0	0	4	4	0	2	2	0	55	55	0
443.2		3	7	16	16	100	0	0	0	0	0	8	8	0	0	0		63	63	0
443.2		3	8	6	6	100	0	0	0	0	0									
443.2		4	1	2	2	100	0	0	0	0	0									
443.2		4	2	3	3	100	0	0	0	0	0									
443.2		4	3	4	4	100	0	0	0	0	0									
443.2		4	4	8	8	100	0	0	0	0	0									
443.2		4	5	10	10	100	0	0	0	0	0									
443.2		4	6	10	10	100	0	0	0	0	0									
		Sum	89	88	1166,666667	1	33,33333333	0	0	0	0	30	31	20	3	3	0	238	238	0
		Average	7,416666667	7,333333333	97,22222222	0,083333333	2,777777778	0	0	0	0	6	6,2	4	0,6	0,6	0	47,6	47,6	0
		SD	4,166060562	4,271115105	9,622504486	0,288675135	9,622504486	0	0	0	0	2	1,788854382	8,94427191	0,894427191	0,894427191	0	11,21605991	11,21605991	0

Summary
29dpt

Sample	BrdU+	only BrdU	% only per all BrdU	neurod/ BrdU+	% neurod/ BrdU per all BrdU	BrdU/ HuC/D+	% HuC/D/ BrdU per all BrdU	triple+	% triple+ per all BrdU	only neurod+	only neurod+ and neurod/ BrdU+	% neurod/ BrdU+ per specific cell type	only neuroD/ HuC/D+	neurod/ HuC/D+ and triple+	% triple+ per specific cell type	only HuC/D+	HuC/D+ and HuC/D/ BrdU+	% HuC/D/ BrdU+ per specific cell type
439	1,181818182	1,181818182	100	0	0	0	0	0	0	0	0	0	0	0	0	0	0	0
440	1,75	0,833333333	70,83333333	0,833333333	27,08333333	0	0	0,083333333	2,083333333	31	32,8	5,142857143	4,4	4,6	4	53,4	53,4	0
441	1,2	1,2	100	0	0	0	0	0	0	10	10	0	0,2	0,2	0	38,4	38,4	0
443	7,416666667	7,333333333	97,22222222	0,083333333	2,777777778	0	0	0	0	6	6,2	4	0,6	0,6	0	47,6	47,6	0
Sum	11,54848485	10,54848485	368,0555556	0,916666667	29,86111111	0	0	0,083333333	2,083333333	47	49	9,142857143	5,2	5,4	4	139,4	139,4	0
Average	2,887121212	2,637121212	92,01388889	0,229166667	7,465277778	0	0	0,020833333	0,520833333	15,66666667	16,33333333	2,285714286	1,733333333	1,8	1	46,46666667	46,46666667	0
SD	3,031185856	3,135351298	14,18095684	0,404688952	13,14409252	0	0	0,041666667	1,041666667	13,42882472	14,38656781	2,680237577	2,318045153	2,433105012	2	7,563949586	7,563949586	0

Summary:

0dpt																		
Sample	BrdU+	only BrdU	% only per all BrdU	neurod/ BrdU+	% neurod/ BrdU per all BrdU	BrdU/ HuC/D+	% HuC/D/ BrdU per all BrdU	triple+	% triple+ per all BrdU	only neurod+	only neurod+ and neurod/ BrdU+	% neurod/ BrdU+ per specific cell type	only neuroD/ HuC/D+	neurod/ HuC/D+ and triple+	% triple+ per specific cell type	only HuC/D+	HuC/D+ and HuC/D/ BrdU+	% HuC/D/ BrdU+ per specific cell type
419	1,25	1,25	100	0	0	0	0	0	0	8,8	8,8	0	0,8	0,8	0	48,8	48,8	0
420	0,5	0,5	100	0	0	0	0	0	0	5,6	5,6	0	0	0	0	34,4	34,4	0
422	0,545454545	0,545454545	100	0	0	0	0	0	0	5	5	0	0,75	0,75	0	47,25	47,25	0
423	0,916666667	0,916666667	100	0	0	0	0	0	0	16	16	0	0,6	0,6	0	37,8	37,8	0
421	0,666666667	0,666666667	100	0	0	0	0	0	0	5,6	5,6	0	0,6	0,6	0	47	47	0
Sum	3,878787879	3,878787879	500	0	0	0	0	0	0	41	41	0	2,75	2,75	0	215,25	215,25	0
Average	0,803030303	0,803030303	100	0	0	0	0	0	0	8,85	8,85	0	0,5375	0,5375	0	42,0625	42,0625	0
SD	0,351600042	0,351600042	0	0	0	0	0	0	0	5,050082508	5,050082508	0	0,368272997	0,368272997	0	7,051876228	7,051876228	0

7dpt																		
Sample	BrdU+	only BrdU	% only per all BrdU	neurod/ BrdU+	% neurod/ BrdU per all BrdU	BrdU/ HuC/D+	% HuC/D/ BrdU per all BrdU	triple+	% triple+ per all BrdU	only neurod+	only neurod+ and neurod/ BrdU+	% neurod/ BrdU+ per specific cell type	only neuroD/ HuC/D+	neurod/ HuC/D+ and triple+	% triple+ per specific cell type	only HuC/D+	HuC/D+ and HuC/D/ BrdU+	% HuC/D/ BrdU+ per specific cell type
424	2,888888889	2,888888889	100	0	0	0	0	0	0	7,5	7,5	0	1	1	0	44,5	44,5	0
425	0,833333333	0,833333333	100	0	0	0	0	0	0	10,6	10,6	0	x	x	0	x	x	0
426	4	3,909090909	97,5	0,090909091	2,5	0	0	0	0	lost	lost	lost	lost	lost	lost	lost	lost	lost
427	4,583333333	4,25	93,54166667	0,5	8,541666667	0	0	0	0	9,8	10,4	4,04040404	0,6	0,6	0	40,2	40,2	0
428	0,545454545	0,545454545	100	0	0	0	0	0	0	x	x	0	x	x	0	x	x	0
Sum	12,8510101	12,42676768	491,0416667	0,590909091	11,04166667	0	0	0	0	27,9	28,5	4,04040404	1,6	1,6	0	84,7	84,7	0
Average	2,57020202	2,485353535	98,20833333	0,118181818	2,208333333	0	0	0	0	9,3	9,5	1,01010101	0,8	0,8	0	42,35	42,35	0
SD	1,824479134	1,717281636	2,824434555	0,21704248	3,702242188	0	0	0	0	1,609347694	1,734935157	2,02020202	0,282842712	0,282842712	0	3,040559159	3,040559159	0

14dpt																		
Sample	BrdU+	only BrdU	% only per all BrdU	neurod/ BrdU+	% neurod/ BrdU per all BrdU	BrdU/ HuC/D+	% HuC/D/ BrdU per all BrdU	triple+	% triple+ per all BrdU	only neurod+	only neurod+ and neurod/ BrdU+	% neurod/ BrdU+ per specific cell type	only neuroD/ HuC/D+	neurod/ HuC/D+ and triple+	% triple+ per specific cell type	only HuC/D+	HuC/D+ and HuC/D/ BrdU+	% HuC/D/ BrdU+ per specific cell type
434	1	0,909090909	83,33333333	0,090909091	16,66666667	0	0	0	0	9,25	9,5	2,083333333	0,75	0,75	0	51	51	0
435	1,545454545	1,454545455	98,21428571	0,090909091	1,785714286	0	0	0	0	8,8	9	1,25	3,6	3,6	0	47,4	47,4	0
437	4,75	4,625	98,21428571	0	0	0,125	1,785714286	0	0	0,4	0,4	0	0,4	0,4	0	33,6	33,8	0,487804878
438	2,8	1,75	74,16666667	0,7	25,83333333	0	0	0	0	17	17,8	8,787878788	6,4	6,4	0	42,2	42,2	0
436	0,916666667	0,916666667	100	0	0	0	0	0	0	x	x	0	x	x	0	x	x	0
Sum	11,01212121	9,65530303	453,9285714	0,881818182	44,28571429	0,125	1,785714286	0	0	35,45	36,7	12,12121212	11,15	11,15	0	174,2	174,4	0,487804878
Average	2,202424242	1,931060606	90,78571429	0,176363636	8,857142857	0,025	0,357142857	0	0	8,8625	9,175	2,424242424	2,7875	2,7875	0	43,55	43,6	0,097560976
SD	1,610733126	1,548432774	11,47825263	0,296229752	11,79070361	0,055901699	0,798595706	0	0	6,782007446	7,106980137	3,665543436	2,802491451	2,802491451	0	7,55314504	7,465476096	0,218152973

29dpt																		
Sample	BrdU+	only BrdU	% only per all BrdU	neurod/ BrdU+	% neurod/ BrdU per all BrdU	BrdU/ HuC/D+	% HuC/D/ BrdU per all BrdU	triple+	% triple+ per all BrdU	only neurod+	only neurod+ and neurod/ BrdU+	% neurod/ BrdU+ per specific cell type	only neuroD/ HuC/D+	neurod/ HuC/D+ and triple+	% triple+ per specific cell type	only HuC/D+	HuC/D+ and HuC/D/ BrdU+	% HuC/D/ BrdU+ per specific cell type
439	1,181818182	1,181818182	100	0	0	0	0	0	0			0			0			0
440	1,75	0,833333333	70,83333333	0,833333333	27,08333333	0	0	0,083333333	2,083333333	31	32,8	5,142857143	4,4	4,6	4	53,4	53,4	0
441	1,2	1,2	100	0	0	0	0	0	0	10	10	0	0,2	0,2	0	38,4	38,4	0
443	7,416666667	7,333333333	97,22222222	0,083333333	2,777777778	0	0	0	0	6	6,2	4	0,6	0,6	0	47,6	47,6	0
Sum	11,54848485	10,54848485	368,0555556	0,916666667	29,86111111	0	0	0,083333333	2,083333333	47	49	9,142857143	5,2	5,4	4	139,4	139,4	0
Average	2,887121212	2,637121212	92,01388889	0,229166667	7,465277778	0	0	0,020833333	0,520833333	15,66666667	16,33333333	2,285714286	1,733333333	1,8	1	46,46666667	46,46666667	0
SD	3,031185856	3,135351298	14,18095684	0,404688952	13,14409252	0	0	0,041666667	1,041666667	13,42882472	14,38656781	2,680237577	2,318045153	2,433105012	2	7,563949586	7,563949586	0

Table S7: Quantification of *nestin*:mCherry-T2A-CreER^{T2}-derived cells.

Sample	Row	Head	Nestin GFP+	HuC/D	HuC/D only	% recombined neurons
877.2	2	2	17	28	11	60,71428571
877.2	2	3	25	48	23	52,08333333
877.2	2	4	30	41	11	73,17073171
877.2	2	5	22	48	26	45,83333333
877.2	2	6	15	21	6	71,42857143
877.2	2	7	25	37	12	67,56756757
877.2	2	8	22	28	6	78,57142857
877.2	3	1	16	24	8	66,66666667
877.2	3	2	5	21	16	23,80952381
877.2	3	3	29	59	30	49,15254237
877.2	3	4	20	47	27	42,55319149
877.2	3	5	33	59	26	55,93220339
		Total	259	461	202	
		Average	21,58333333	38,41666667	16,83333333	57,29028162
		SD	7,704288456	13,96396879	8,983149208	15,59374664

Sample	Row	Head	Nestin GFP+	HuC/D	HuC/D only	% recombined neurons
878.2	2	1	26	33	7	78,78787879
878.2	2	2	20	31	11	64,51612903
878.2	2	3	28	39	11	71,79487179
878.2	2	4	28	44	16	63,63636364
878.2	2	5	28	38	10	73,68421053
878.2	2	6	26	47	21	55,31914894
878.2	2	7	26	42	16	61,9047619
878.2	3	1	35	51	16	68,62745098
878.2	3	2	24	35	11	68,57142857
878.2	3	3	11	17	6	64,70588235
878.2	3	4	23	36	13	63,88888889
878.2	3	5	15	39	24	38,46153846
		Total	290	452	162	
		Average	24,16666667	37,66666667	13,5	64,49154616
		SD	6,379417661	8,689945426	5,35129551	10,20475211

Sample	Row	Head	Nestin GFP+	HuC/D	HuC/D only	% recombined neurons
879.2	1	4	32	54	22	59,25925926
879.2	1	5	24	35	11	68,57142857
879.2	1	6	38	70	32	54,28571429
879.2	1	7	19	43	24	44,18604651
879.2	1	8	29	50	21	58
879.2	2	1	24	34	10	70,58823529
879.2	2	2	30	54	24	55,55555556
879.2	2	3	25	62	37	40,32258065
879.2	2	4	33	68	35	48,52941176
879.2	2	5	14	33	19	42,42424242
879.2	2	6	15	46	31	32,60869565
879.2	2	7	12	41	29	29,26829268
		Total	295	590	295	
		Average	24,58333333	49,16666667	24,58333333	50,29995522
		SD	8,25126253	12,81925635	8,670308093	13,09382064

Table S8: Primers used to analyze expression of *neurod* and *nestin* in *neurod*:GFP-positive cells.

Gene	Primer	Sequence	Product length
neurod	forward	5'-CGCAAGCCACACTAGACTTC-3'	177 bp
	reverse	5'-GCTGCTGTGACACTTGTCG-3'	
nestin	forward	5'-CTTCAACATCTTCAGGCCCAAG-3'	184 bp
	reverse	5'-GTGTTGGTCTGTCGATTCTCAG-3'	